Impacts of Greenhouse Gas Mitigation Policies on Agricultural Land

by

Xiaodong Wang

Master of Science
Peking University (2002)

Submitted to the Department of Urban Studies and Planning
In partial fulfillment of the requirements for the degree of

Doctor of Philosophy

in

Urban and Regional Studies

at the

MASSACHUSETTS INSTITUTE OF TECHNOLOGY

February 2008

Author ____________________
Department of Urban Studies and Planning
January 2, 2008

Certified by ____________________
Professor Karen R. Polenske
Department of Urban Studies and Planning
Dissertation Supervisor

Accepted by ____________________
Professor Eran Ben-Joseph
Chair, Ph.D. Committee
Department of Urban Studies and Planning

Impacts of Greenhouse Gas Mitigation Policies on Agricultural Land

by

Xiaodong Wang

Submitted to the Department of Urban Studies and Planning on January 2, 2008
in partial fulfillment of the requirements for the degree of
Doctor of Philosophy in Urban and Regional Studies

Abstract

Greenhouse gas (GHG) emissions are widely acknowledged to be responsible for much of the global warming in the past century. A number of approaches have been proposed to mitigate GHG emissions. Since the burning of fossil-based fuels is an important source of GHGs, the policies on GHG-mitigation encourage the replacement of fossil-based energy with biomass energy. However, a large-scale development of biomass energy may lead to changes in agricultural land use, which are important sources of GHG emissions, and therefore undermine the effectiveness of GHG-mitigation policies. In this research, I analyze the impacts of GHG-mitigation policies on five types of agricultural land (cropland, managed forestry land, pasture land, un-managed forestry land, and un-managed grassland) as well as carbon stored in such land during the 21st century.

The scholars in the MIT Joint Program of Science and Policy on Global Change use the Integrated Global Systems Model (IGSM) to simulate changes in climate in response to GHG-mitigation policies, while the researchers at the U. S. Marine Biological Laboratory (MBL) apply the Terrestrial Ecosystem Model (TEM) to simulate land productivities. Based on the predictions of land characteristics affecting land-use decisions, I develop an econometric model to predict the land use affected by climate, GHGs, and tropospheric ozone at the grid-cell scale of 0.5 * 0.5 longitude by latitude. I use the Emissions Prediction and Policy Analysis (EPPA) model to capture the regional land use driven by economic forces. Then, I develop the downscaling methods to link these two land-use effects.

I conduct this research in two scenarios: in the baseline, I assume that there are no policies to mitigate GHG emissions during the 21st century; in the policy scenario, I assume that there are specific policies to limit GHG emissions during the 21st century. I confirm the hypothesis that biomass-energy production would lead to the conversion of the five types of agricultural land, and the carbon stored in such land would decrease; the GHG-mitigation policies, leading to more production of biomass energy and conversion of agricultural land, would cause an even more severe loss of the carbon stored in agricultural land. Although the GHG-mitigation policies would generally reduce the atmospheric GHG emissions by using more energy from biomass, such endeavors would be partly counteracted by the land-use conversion as a result of large-scale production of biomass energy.

Dissertation Supervisor: Karen R. Polenske
Title: Professor, Department of Urban Studies and Planning, MIT
Dissertation Reader: John M. Reilly, Henry D. Jacoby

Acknowledgements

Dr. John M. Reilly once told me that in professional football training, players are often asked by their coaches to push heavy blocking sleds across the field in order to strengthen their muscles. Sometimes the coaches jump on the sleds so that the players have to push the weight of not only the sleds but the coaches as well. Although such training is very tiring, it would greatly help the athletes to get stronger for the future real game. Working on my dissertation is like pushing a sled in the training for my future career, and my committee members, Professor Karen R. Polenske, Dr. John M. Reilly, and Professor Henry D. Jacoby, instead of jumping on the sleds, are actually encouraging me to push the sled to the destination.

Words cannot describe how much I appreciate my academic advisor, Professor Polenske. Her heartfelt support and encouragement in the last five years have made my life at MIT much easier. What I have learned from her not only makes me prepared in the field of regional and urban economics, but also helps me become more mature for my future life journey. I express my deep gratitude to my research advisor, Dr. Reilly. Without his genuine advice, intellectual motivations, and the great "sleds" story, this dissertation would not have become a reality. I am also extremely grateful to Professor Jacoby, whose meticulous guidance and valuable suggestions are indispensable to the completion of my dissertation. I feel very fortunate to have the opportunity to work with them on this important project.

I am extremely grateful to Dr. Angelo Costa Gurgel, my best colleague and good friend at the MIT Joint Program of Science and Policy on Global Change. I cannot make it without his support and encouragement. I greatly appreciate Mr. Dave Kicklighter, Dr. Benjamin Felzer, and Mr. Tim Cronin at the U.S. Marine Biological Lab, for their support in providing me critical data on TEM simulations.

In addition, I extend my thanks to Dr. Sergey Paltsev, Mr. Weifeng Li, Mr. Hongliang Zhang, Dr. Marcus Sarofim, Dr. Andrei Sokolov, Mr. Xiaofeng Qian, Dr. Adam Schlosser, Dr. Xiang Gao, Ms. Therese Henderson, Mr. Robert Irwin, and Ms.

Valerie Karplus at MIT, and Mr. Jingcheng Liu at the U.S. Environmental Systems Research Institute for their kind help on my dissertation.

I am truly thankful to my parents and sister for their continual care and blessing.

I greatly appreciate the funding support from National Science Foundation Award BCS-0410344, Environmental Protection Agency Agreement XA-83240101, Department of Energy, Integrated Assessment Program in the Office of Biological and Environmental Research (BER) Award DE-FG02-94ER61937, and a group of corporate sponsors through the Joint Program on the Science and Policy of Global Change at MIT.

Finally, I would like to thank my wife, Ms. Feiya Huang, whose encouragement and support are always with me. Thanks to her for believing in me.

Contents

Figures

Tables

Chapter 1
Introduction

One of the most debated topics on Earth is global warming, and greenhouse gas (GHG[1]) emissions are widely acknowledged to be responsible for much of the global temperature increase observed in the past century. The Intergovernmental Panel on Climate Change (IPCC, 2007) indicated that:

Most of the observed increase in global average temperature since the mid-20th century is very likely due to the observed increase in anthropogenic GHG concentrations. Continued GHG emissions at or above current rates would cause further warming and induce many changes in the global climate system during the 21st century that would very likely be larger than those observed during the 20th century.

Some GHGs occur naturally in the atmosphere, while others result from human activities. Naturally occurring GHGs include carbon dioxide (CO_2), methane (CH_4), nitrous oxide (N_2O), water vapor (H_2O), etc., while certain human activities add to the levels of most of these naturally occurring GHGs. The most important source of CO_2 is the burning of fossil fuels (oil, natural gas, and coal), followed by the land-use changes (Jensen et al., 1996). Carbon is stored in vegetation and soil; land-use changes, such as conversion of natural forests to cultivated land, decrease the carbon stored in vegetation and speed the decomposition of soil organic carbon, leading to more CO_2 being released into the atmosphere. Methane (CH_4) is emitted during the extraction of coal, natural gas, and oil, as well as the transportation of natural gas; in addition, rice production, the decomposition of organic wastes, and

[1] GHGs are components of the atmosphere that contribute to the greenhouse effect. The earth receives energy from the sun in the form of radiation, and the earth reflects about 30% of the incoming solar radiation, while the remaining 70% is absorbed, warming the land, atmosphere and oceans. Atmospheric GHGs play important roles in trapping the energies from the sun, and therefore, warm the earth's surface (IPCC, 2001).

the raising of livestock emit methane. Nitrous oxide (N_2O) is emitted during agricultural and industrial activities, as well as combustion of solid waste and fossil fuels. Agricultural land use affects the emissions of CH_4 and N_2O significantly. Taking the United States in 2004 as an example: CH_4 emissions from enteric fermentation and manure management represented 20% and 7% of total CH_4 emissions from anthropogenic activities, respectively; agricultural soil management activities (e.g. fertilizer application) accounted for 68% of total N_2O emissions, while manure management and field burning of agricultural residues were also small sources of N_2O emissions (the U.S. Environmental Protection Agency: EPA, 2006).

GHGs that are not naturally occurring include hydrofluorocarbons (HFCs), perfluorocarbons (PFCs), chlorofluorocarbons (CFCs)[2], and sulfur hexafluoride (SF_6), which are generated in a variety of industrial processes (U.S. EPA, 2006).

Aiming at mitigating GHG emissions, most national governments have signed and ratified the Kyoto Protocol, a protocol to the United Nations Framework Convention on Climate Change (UNFCCC) with the objective of reducing GHG emissions. As of June 2007, 172 nations have ratified the Kyoto Protocol; among them, 36 countries and the European Union are required to reduce GHG emissions to the levels specified for each of them in the treaty (UNFCCC, 2007). The U.S. government,

[2] Hydrofluorocarbons (HFCs) are a group of chemical compounds, consisting of alkanes, such as methane or ethane, with one or more halogens linked, such as chlorine or fluorine, making them a type of organic halide. Perfluorocarbons (PFCs) are compounds derived from hydrocarbons by replacement of hydrogen atoms by fluorine atoms. Chlorofluorocarbons (CFCs) are compounds containing chlorine, fluorine, and carbon only, and they are widely used in industry, for example as refrigerants, propellants, and cleaning solvents (U.S. EPA, 2006).

although having not ratified this agreement yet, is also considering a number of approaches to mitigate GHG emissions.

Agricultural activities and land use are important sinks and sources of GHGs, and therefore have a significant role in the development of the policy decisions on GHG mitigation. Since the burning of conventional fossil-based fuels is an important source of GHGs, the policies on GHG-mitigation encourage the replacement of fossil-based energy with biomass energy. However, a large-scale development of biomass energy may lead to changes in agricultural land use (such as deforestation), which are important sources of GHG emissions, and therefore undermine the effectiveness of the GHG-mitigation policies. Unfortunately, such land-use effects were not included in the policy decisions on GHG mitigation. In this research, I analyze the impacts of GHG-mitigation policies on agricultural land as well as carbon stored in such land during the 21st century.

Specifically, within the framework of the MIT Integrated Global Systems Model (IGSM), I analyze the impacts of the GHG-mitigation policies on five types of agricultural land, namely, cropland, managed forestry land, pasture land, un-managed forestry land, and un-managed grassland. The impacts include land use, land rent, and the possible feedbacks on the carbon stored in the five types of agricultural land. As I just stated, biomass is gaining considerable attention as a promising way to mitigate GHG emissions; however, there is a lack of knowledge of the potentials and limitations of a worldwide large-scale development of biomass-energy production as well as the possible feedbacks in land-use effects. In this research, I include biomass in the analysis and project the future biomass-energy production as well as the resultant land-use effects. Such impacts may vary from place to place because of the differences in climate, soil, or the way the policies are adopted.

By mitigating GHG atmospheric concentrations, the GHG-mitigation policies also lead to changes in climate conditions, air temperature and precipitation for instance. In addition, such policies reduce some pollutant gases from fossil fuel burning, NOx for example, and these gases are important precursors of tropospheric ozone. In this research, I examine the combined effects of changes in climate, GHG concentrations, and tropospheric ozone levels. To the extent that land productivities are affected by climate, GHGs, and tropospheric ozone, there may be important economic consequences.

To make possible a comprehensive analysis of the impacts of GHG-mitigation policies on the five types of agricultural land, I link the impacts of economic forces at the regional scale used in a computable general equilibrium model of the world economy with the feedbacks of climate, GHGs, and tropospheric ozone at the grid-cell scale used in a biophysical model of global terrestrial ecosystems, namely, the Emissions Prediction and Policy Analysis (EPPA) model and the Terrestrial Ecosystem Model (TEM).

I then test the hypothesis that biomass-energy production would lead to the conversion of the five types of agricultural land, and the carbon stored in such land would decrease; the policies to mitigate GHG emissions, leading to more production of biomass energy and conversion of agricultural land, would cause an even more severe loss of the carbon stored in agricultural land. Although the GHG-mitigation policies would generally reduce the atmospheric GHG emissions by using more energy from biomass, such endeavors would be partly counteracted by the land-use conversion as a result of large-scale production of biomass energy. If my hypothesis is confirmed, policy makers need to take the land-use effects of biomass-energy production into consideration when developing the GHG-mitigation policies, because the capacity of the five types of agricultural land to store carbon might be diminished, and therefore, would undermine the effectiveness of GHG-mitigation endeavors.

I indicate the methodology flow of this research in Figure 1.1. As indicated, I develop an econometric land-use model based on historical data to analyze the determinants of land-use decisions at the grid-cell scale of 0.5 * 0.5 longitude by latitude. With the projections of the variables affecting land-use decisions, I use the econometric model to project gridded land use during the 21st century; from this basis I apply some downscaling methods to distribute the projected regional land use driven by economic forces during the 21st century to the grid-cell scale. Applying the downscaling methods based on the econometric land-use model, I am able to determine the impacts of economic forces as well as the feedbacks of climate, GHGs, and tropospheric ozone on the five types of agricultural land in response to the GHG-mitigation policies, and this is the most distinctive contribution of my research.

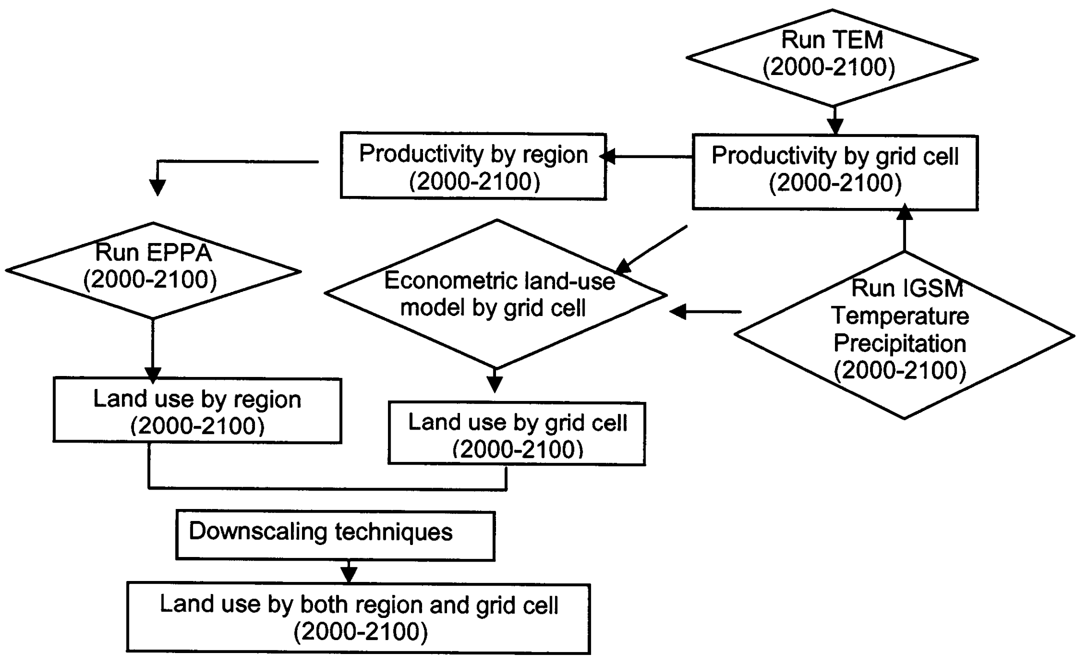

Figure 1.1: Methodology flow in this research
Source: the author.

Specifically, in Chapter 2, I review the key previous studies on the responses of agricultural plants to changes in climate, GHG concentrations, and tropospheric ozone levels, as well as the economic consequences, and I identify how my approach advances methods in this field of research.

In Chapter 3, I describe the model components as well as climate scenarios applied in this research. With the cooperation of my colleagues in the MIT Joint Program of Science and Policy on Global Change, I use the EPPA model to project the regional land-use effects driven by economic forces, and the researchers at the U. S. Marine Biological Laboratory (MBL) apply the TEM to project the gridded land productivities affected by the climate, GHGs, and tropospheric ozone. We input the data on projected gridded land productivities in the econometric land-use model to predict land-use effects as affected by climate, GHGs, and tropospheric ozone; in addition, we input the aggregated regional land productivities in the EPPA model to simulate regional land use as affected by economic forces. In this chapter, I also describe the two climate scenarios applied in this research: in the baseline, there are no policies to mitigate GHG emissions; in the policy scenario, however, there are specific policies to limit GHG emissions.

In Chapter 4, I introduce the downscaling methods I develop based on an econometric land-use model. In the econometric land-use model, based on historical data at the grid-cell scale, I determine how the spatial characteristics of land affected decisions on land use, and such spatial factors include temperature, precipitation, land productivities, and human accessibility. Then, I apply the downscaling technologies to distribute the regional land use affected by economic forces to grid cells, and the results are introduced in the next chapter.

In Chapter 5, I apply the models introduced in Chapter 3 and the techniques described in Chapter 4 to analyze the impacts of GHG-mitigation policies on the five types of agricultural land in both the baseline and GHG-mitigation policy scenarios. I conduct the study in two rounds: in the first round, I only include the impacts of economic forces; while in the second round, I also include the feedbacks of climate, GHGs, and tropospheric ozone. By analyzing the differences between the two rounds, I highlight the additional feedbacks of climate, GHGs, and tropospheric ozone. Based on the analysis in this chapter, I offer some conclusions and implications of this research in Chapter 6.

Chapter 2
Literature Review

As I stated in Chapter 1, in addition to affecting the atmospheric concentration of GHGs, the policies to mitigate GHGs would also lead to changes in climate and tropospheric ozone levels. Such changes would affect agricultural land productivities, and also lead to economic consequences. In Section 2.1, I review the past studies on responses of agricultural plants to changes in climate, GHG concentrations, and tropospheric ozone levels, and the economic consequences are reviewed in Section 2.2. Based on a review of these studies, I identify how my approach advances methods in this field of research.

2.1. Responses of agricultural plants to multiple environmental changes

The key scholars who analyzed the responses of agricultural plants to multiple changes in the environment are Kurpa and Manning (1988), Byrd and Brown (1989), Bazzaz (1990), Beyers et al. (1992), Baker et al. (1993), Rozema (1993), Wolfe and Erickson (1993), Berryman et al. (1994), Tjoelker et al. (1995), Atkinson et al. (1997), Mauzerall and Wang (2001), Percy et al. (2003), Fiscus et al. (2005), Felzer et al. (2005), Felzer et al. (2007), etc. I discuss these in detail below.

Different agricultural plants react differently to environmental changes (the Food and Agriculture Organization: FAO, 1996); therefore, I first examine the classification of agricultural plants. Based on the products formed in the initial phases of photosynthesis, agricultural plants are classified as C_3, C_4, or Crassulacean acid metabolism (CAM):

- C_3 plants include cotton, rice, wheat, barley, soybeans, sunflower, potatoes, most leguminous and woody plants, most horticultural crops, and many weeds.
- C_4 plants include maize, sorghum, sugar cane, millets, halophytes (i. e., salt-tolerant plants), and many tall tropical grasses and weed species.
- CAM plants, with an optional C_3 or C_4 pathway of photosynthesis depending on growing environments, include cassava, pineapple, opuntia, onions, castor, etc., which usually grow in arid areas (FAO, 1996).

There is general agreement that an increase of atmospheric CO_2 concentrations leads to increased productivities of plants. Rozema (1993) found that C_3 plants exhibit an increase in productivities of about 20-30% at doubled CO_2 concentrations; C_4 plants show a much less-pronounced response than the C_3 plants, increasing the productivities on average by only 5-10% at doubled CO_2 concentrations; responses, however, depend on plant species as well as soil fertility conditions (Rozema, 1993). Byrd and Brown (1989) analyzed the effects of CO_2 on the photorespiratory characteristics and leaf anatomy of selected C_3 and C_4 plants. They concluded that CO_2 concentrations during plant growth play important roles in the evolution of plants; C_4 plants are relatively insensitive to altered CO_2 levels during growth.

Wolfe and Erickson (1993) found that in general, higher CO_2 concentrations lead to improved water-use efficiency of both C_3 and C_4 plants because of reduced transpiration; this is induced by a contraction of plant stomata with the overabundance of CO_2, thereby restricting the escape of water vapor.

Many scholars have tested the responses of certain species to changed CO_2 concentrations in their experiments. Baker et al. (1993) analyzed the responses to elevated CO_2 concentrations of three crop species: rice, soybean and citrus, all of which belong to C_3 plants. They concluded that citrus has the lowest growth and photosynthetic rates, but it displays the greatest percentage increase over double-level CO_2 control treatments. In all three species, the direct effect of doubled CO_2 concentrations is always an increase in the photosynthetic rate. Berryman et al. (1994) tested the stomatal responses to doubled CO_2 concentrations of two tropical tree species: Maranthes corymbosa and Eucalyptus tetrodonta, both of which belong to C_4 plants. They concluded that stomatal conductance in the former plant is more sensitive to leaf water status under conditions of CO_2 enrichment than that of the latter. Atkinson et al. (1997) measured the dry-matter production and chloroplast components in oak seedlings and clonal cherry in doubled CO_2 concentrations, and concluded that the elevated CO_2 treatment increases the saturated-rate of photosynthesis and dry-matter production of both plants.

Bazzaz (1990) summarized the responses of natural ecosystems to the rising global CO_2 levels and concluded that plant photosynthesis is generally enhanced by CO_2 enrichment, but this enhancement may decline over time. In addition, he indicated that the adjustment of photosynthesis during plant growth is more obvious in some species than in others, and such adjustment may be influenced by resource availability.

In addition, some scholars studied the climate effects in terms of temperature and precipitation on certain species of plants. For example, Korner and Woodward (1987) studied the effects of temperature on leaf growth in five species in Austria. They found that leaf growth rates peak at midday at all elevations and such rates at 20°C in low elevation are almost twice as high as those from the highest sites, and they concluded that there is a substantial adaptive adjustment in response of leaf growth to declining mean temperature. Charles and Dukes (2007) studied the effects of warming and altered precipitation on the nutrient flows of salt marshes in the New England area in the United States. Their experimental manipulations consisted of a factorial design of warming via passive open-topped chambers, increased precipitation (double normal rainfall) and decreased precipitation via rainfall shelters, and they concluded that the nutrient flows of salt marshes in the New England area are significantly affected by changes in temperature and precipitation. Coleman and Bazzaz (1992) analyzed the effects of temperature as well as CO_2 on growth, resource acquisition and allocation of two plants: Abutilon (a C_3 plant) and Amaranthus (a C_4 plant); they concluded that elevated CO_2 and temperature treatments have significant independent effects on plant growth and resource acquisition (i.e., photosynthesis and nitrogen uptake), and the strength and direction of these affects are often dependent on plant species. The studies above are important in revealing that changes in climate and CO_2 concentrations would significantly affect plant growth in terms of stomatal conductance, dry-matter production, leaf growth, nutrient flows, resource acquisition and allocation, etc.

In recent years, many scholars have applied a biogeochemistry model – Terrestrial Ecosystem Model (TEM) to study the effects of multiple environmental changes on plant productivities in certain regions. In the TEM, plant productivities are determined by the carbon fixed by the plants. Raich et al. (1991) applied the TEM to analyze the spatial and temporal patterns of plant productivities in South America. They found that seasonal patterns of plant productivities in South America are correlated with the availability of moisture in most vegetation types, but are strongly affected by seasonal differences in cloudiness in the tropical evergreen forests. Schimel et al. (1997) applied the TEM to analyze plant productivities in North America, and indicated that plant productivities are jointly limited by the availability of water and nitrogen. Xiao et al. (1998) used the TEM to estimate plant productivities in China, and found that temperate broadleaf evergreen forests account for the highest productivity in China, while the spatial pattern of plant productivities is closely correlated to the spatial allocations of precipitation and temperature. However, these studies are limited only to certain regions. On the global level, Kicklighter et al. (1999) applied the TEM to study the differences of plant productivities over space and time and concluded that the largest differences occur during the summer months in boreal forests and during the dry seasons in tropical evergreen forests.

Different from the generally positive effects of CO_2 and resultant changes in climate in terms of temperature, precipitation, etc. on plant growth, tropospheric ozone has been found to have negative impacts on plant growth. High concentrations of tropospheric ozone have toxic effects on plant growth, and exposure to tropospheric ozone leads to photorespiratory disorders for the inhibition of plant growth (Mauzerall and Wang, 2001). Reich and Amundson (1985) found that tropospheric ozone decreases stomatal conductance, and Tjoelker et al. (1995) found a decoupling between photosynthesis and stomatal conductance as a result of long-term exposure to tropospheric ozone. While tropospheric ozone reduces stomatal conductance, it generally increase water stress by reducing root growth (McLaughlin and Downing, 1995). Beyers et al. (1992) found a reduction of 19.5% for well-watered seedlings and 11% for drought-stressed seedlings when exposed to 1.5 times ozone levels. In recent years, tropospheric ozone has been proved to affect plants through visible injury (Kurpa and Manning, 1988), photosynthesis reduction and turnover of antioxidant system (Percy et al., 2003), and growth rate decreases (Reich, 1987; Fiscus et al., 2005). These studies indicate that exposure to tropospheric ozone would affect plant growth negatively in terms of photorespiratory disorder, photosynthesis reduction, decrease in stomatal conductance, reduction in root growth rate, etc.

Different plants might react differently to tropospheric ozone concentrations. Tjoelker et al. (1995) found that shaded leaves are more sensitive than sun-lit leaves to ozone exposure in a mature stand of the shade-tolerant sugar maple. In addition, mature plants and seedlings react differently to ozone exposure, and seedlings show greater ozone sensitivity than mature plants, and this has been tested in black cherry (Fredericksen et al., 1996), sequoias (Grulke and Miller, 1994), and red spruce (Rebbeck and Jense, 1993).

Felzer et al. (2005) summarized the effects on plants of exposure to tropospheric ozone, and concluded that the damage of tropospheric ozone on crops is composed of four effects: (1) crops are inherently more sensitive to tropospheric ozone than other plants; (2) the concentrations of tropospheric ozone are higher over cropland than other agricultural land; (3) ozone damage is proportional to plant production, while fertilized crops tend to have a higher level of yield than other plants and therefore suffer more ozone damage; and (4) the damage of tropospheric ozone is more severe with applications of nitrogen fertilizer, which is widely used on crops. In addition, applying the TEM, they found that the largest damage of tropospheric ozone to agricultural plants occur in the southeastern and middle-western regions of the United States, eastern Europe, and eastern China. In 2007, Felzer et al. reviewed the experimental evidence of ozone damages on plants in both laboratory and field experiments, and concluded that exposure to ozone causes both visible and physiological damages to plants. Visible injury may or may not coincide with physiological injury, which includes reduced photosynthesis and other damages to plant functions that led to the reduction in plant growth (Felzer et al., 2007).

In summary, there have been abundant studies on the responses of agricultural plants to multiple environmental changes in terms of climate, atmospheric CO_2 concentrations, and tropospheric ozone. However, instead of being conducted at the regional or global scale, most studies were limited to specific plants in certain site areas; in addition, the further economic consequences were not included in these studies.

2.2. Economic consequences of environmental impacts on agriculture

There have been many scholars studying the economic consequences of environmental impacts on agriculture. Those focusing on global or pioneering new methods include Adams et al. (1990), Tobey et al. (1992), Reilly and Hohman (1993), Rosenzweig and Parry (1994), Mendelsohn et al. (1994), Darwin et al. (1996), Reilly et al. (2003), Izaurralde et al. (2003), Alig et al. (2003), Parry et al. (2004), and Reilly et al. (2007), which I discuss in detail below.

Adams et al. (1990) evaluated the warming effects on crop productivity based on the double-CO_2-equilibrium climate scenarios from two widely known General Circulation Models (GCMs[3]), namely, the GISS model developed by the NASA **G**oddard **I**nstitute for **S**pace **S**tudies and the GFDL model developed by the **G**eophysical **F**luid **D**ynamics **L**aboratory. They concluded that irrigated acreage would expand and regional patterns of the U.S. agriculture would shift with doubled atmospheric CO_2 concentration. Their economic results were based on impositions of climate change on the U.S. agricultural economy in 1985, while they did not consider the impacts on other parts of the world. Tobey et al. (1992) applied a

[3] General Circulation Models (GCMs) are a class of computer-driven models for weather forecasting, understanding climate and projecting climate change, where they are commonly called Global Climate Models. These computationally intensive numerical models are based on the integration of a variety of fluid dynamical, chemical, and sometimes biological equations (Edwards, 2000).

partial equilibrium model, the Static World Policy Simulation (SWOPSIM) model, to analyze the responses of global agricultural markets to global warming in three scenarios of assumed productivity increases in different regions. In this SWOPSIM model, the global agricultural market is described through a system of domestic supply and demand equations that are specified by matrices of own- and cross-price elasticities, and it encompasses all regions of the world at a considerable degree of commodity disaggregation. The SWOPSIM model applied in Tobey et al. (1992) contained 20 agricultural commodities, and covered Argentina, Australia, Brail, Canada, China, Europe, Japan, Thailand, the Union of Soviet Socialist Republics (USSR), and the United States, while the other areas were classified as "Rest of the World". Applying three experiments in which the concurrent crop-yield reductions were assumed to occur in different regions, they demonstrated that even with productivity losses that might be caused by global warming in the major grain-producing regions of the world, global warming would not seriously disrupt world agricultural markets.

Rosenzweig and Parry (1994) assessed changes in crop yield for the entire world with doubled atmospheric CO_2 concentration under three separate GCM scenarios: the GISS and GFDL models applied in Adams et al. (1990), as well as the UKMO model developed by the **U**nited **K**ingdom **M**eteorological **O**ffice. They indicated that the climate scenarios differed among these models in terms of seasonality, regionality, and overall magnitude of temperature and precipitation changes. For example, the changes between the double-CO_2 scenario and the baseline in the

1990s in global mean surface temperature and precipitation for these three models were: GISS, +4.2 °C and +11%; GFDL, + 4.0 °C and +8%; UKMO, +5.2 °C and +15%. Applying a forward-looking Computable General Equilibrium (CGE) model - the Basic Linked System (BLS), they projected the potential impacts of climate change on world food supply from 1980 to 2060. The BLS consists of a set of linked national agricultural sectors, and represents all economic factors and empirically estimated parameters. Realizing the differences among the three GCMs above, they estimated changes in crop yield for each GCM scenario for multiple sites in 23 countries with and without the yield-enhancement effects of increased ambient CO_2 levels, and concluded that doubling of the atmospheric CO_2 concentration would lead to only a small change in global crop production, while developing countries would be likely to bear the brunt of the changes.

Based on the climate scenarios from the three GCMs stated above (GISS, GFDL, and UKMO), Reilly and Hohmann (1993) applied the SWOPSIM model to investigate the costs and benefits of climate changes after taking international trade into consideration. They concluded that the adjustments in production and consumption caused by the comparative advantage in international trade will buffer the severity of the climate-change impacts on world agriculture, and therefore, result in relatively small impacts on domestic economies from a double-CO_2 climate. In addition, developing countries appear at a greater disadvantage, and the beneficial effects of CO_2 fertilization are critical in limiting the economic impacts.

As Reilly and Hohmann (1993) indicated, the SWOPSIM model is advantageous over the BLS model in that the production and price changes are summarized as welfare changes in the former model. In the SWOPSIM model, welfare measures are used to compare the benefits of avoided climate change with the costs of emissions reductions; while in the BLS model, effects of climate change are introduced as changes in the average national or regional productivity per commodity, as described in Rosenzweig and Parry (1994). However, SWOPSIM is a partial equilibrium model; it does not take into account the effects of agricultural production on resource allocations among different sectors, and it assumes that uses of resource supplies, arable land for example, will be appropriately altered to fulfill new demand and supply following a shock to the economic system. In addition, SWOPSIM is a static model, and therefore, is not applicable for projecting future impacts caused by climate change.

Different from the traditional production-function approaches, Mendelsohn et al. (1994) applied an approach to examine the impacts of climate and other variables on land values and farm revenues. Using cross-sectional data on climate, farmland prices, and other economic and geophysical data for almost 3,000 counties in the United States, they found that higher temperature in all seasons except autumn reduce average farm values, while more precipitation outside of autumn increases farm values. They applied this approach to a global-warming scenario, and found a significantly lower estimated impact of global warming on the U.S. agriculture than the traditional production-function approaches. However, they focused only on the land values and farm revenues in the United States and did not include other areas in the world. In addition, they based the climate scenarios on the conventional CO_2-doubling assumption, which took CO_2 enrichment simply as doubled instead of transient changes.

Realizing that land use and cover represent integrating elements in ecological economics, Darwin et al. (1996) developed a static CGE model, the Future Agricultural Resources Model (FARM), to capture the effects of changes in global climate, human populations, and international trade policies on tropical forests. FARM applies a number of principles to allocate the national and sub-national production of crops, pasture, and round-wood products to grid cells of 0.5 * 0.5 longitude by latitude. In the FARM, the allocation of a particular commodity is governed by a grid's land cover and population density, and such a distribution is further constrained by the plant hardiness zone (PHZ) and agro-ecological zones, AEZs, as defined by the length of growing season and thermal regime. In addition, such allocations in some geographically large countries are calibrated to or otherwise constrained at the sub-national level. Based on the FARM, Darwin et al. (1996) found that changes in global climate, human populations, and international trade policies would likely have adverse effects on the health and integrity of tropical forest ecosystems; in addition, they found forest depletion in Southeast Asia to be correlated with numerous economic indicators. Also based on the FARM, Darwin and Kennedy (2000) reported that atmospheric CO_2 has a beneficial effect on crop productivity, and this would offset some economic losses generated by climate effects of atmospheric GHG concentrations. However, the FARM they developed is a static CGE model, which was only applied to a 1995 economy. They indicated that their studies only reflected the fact that impacts between economic and ecological phenomena are complex and that adding economic and ecological details to expand the modeling capabilities is needed.

As stated, past studies used double-CO_2-equilibrium climate scenarios rather than realistic transient climate scenarios driven by gradually increased GHGs or proposed climate policies. In addition, the impacts of climate change on the environment through climate-induced changes in agricultural resource uses or the impacts of climate variability are missing. Having realized these caveats of past studies, Reilly et al. (2003) examined the impacts on U.S. agriculture of transient climate change, which were simulated for the decades of the 2030's and 2090's by two GCMs: the Canadian Center Climate (CC) model and the Hadley Centre (HC) model. They examined historical shifts in the location of crops and trends in the variability of U.S. average crop yields, and found that non-climate forces have likely dominated the north and westward movement of crops and the trend towards declining yield variability. However, this study was limited to the crops and pasture in the United States. Also based on the CC model and HC model, Alig et al. (2003) included the forestry sector in addition to crops and pasture to analyze the impacts of climate change on agricultural production, and concluded that the forestry sector has adjustment mechanisms that mitigate climate-change impacts, including interregional migration of production, substitution in consumption, and altered stand management. However, this study was also limited to the United States.

To explore the economic consequences caused by realistically proposed climate policies, Jacoby et al. (1997) explored the economic consequences of a sample climate proposal in Quantified Emissions Limitation and Reduction Objectives (QELROs). They based their research on the Emissions Prediction and Policy Analysis (EPPA) model, a computable general equilibrium (CGE) model developed by the MIT Joint Program of Science and Policy on Global Change. In this sample proposal specified in QELROs, the nations of the Organization for Economic Co-operation and Development (OECD) agreed to stabilize their CO_2 emissions at 1990 levels by 2000, bring these emissions down to 20% below 1990 levels by 2010, and stabilize them at that level thereafter. Jacoby et al. (1997) found that the burden of meeting such CO_2 emissions falls not only on the parties to the agreement but on others as well. In addition, countries without CO_2 constraints become more competitive in producing high-carbon-emitting energy sources, as well as exporting energy-intensive goods.

Reiner and Jacoby (1997) used the EPPA model to analyze the welfare implications of several proposals on carbon restrictions. They concluded that a trading regime can lead to important benefits in reducing potential conflicts within developed nations, and help avoid complicated and divisive negotiations over burden-sharing formulas. Reilly et al. (2002) investigated technological options for reducing emissions of the greenhouse gases including carbon dioxide (CO_2), methane (CH_4), nitrous oxide (N_2O), hydrofluorocarbons (HFCs), perfluorocarbons (PFCs), sulfur hexafluoride (SF_6) and credit for some carbon sinks, as specified in the Kyoto Protocol; in addition, they analyzed the economic implications of including non-CO_2 GHGs and sinks in the climate change control policy. They conducted an integrated assessment of costs using the MIT Emissions Prediction and Policy Analysis (EPPA) model combined with estimates of abatement costs for non-CO_2 GHGs and sinks. They found that including all the GHGs and sinks is actually cheaper than if only CO_2 had been included in the Kyoto Protocol and their inclusion achieves greater overall abatement. Yang et al. (2005) integrated the health effects from exposure to air pollutions into the EPPA model, and applied the model to the United States to reevaluate the benefits of air pollution regulations made by the U.S. Environmental Protection Agency (EPA). They found lower estimated benefits than the original EPA estimates, and benefits from reduced pollution exposure would be gradually realized. Although these scholars based their research on realistically proposed climate policies, none of them has taken land-use effects in response to climate policies into consideration.

In a recent study, based on the global scale, Reilly et al. (2007) examined the combined effects of changes in climate, CO_2 concentrations, and tropospheric ozone on the land productivities of crops, pasture, and managed forestry as well as the consequences for global and regional economies. They based the research on the MIT Integrated Global Systems Model (IGSM), which includes sub-models of the relevant aspects of the natural earth system coupled to a model of the human component interacting with climate processes. Compared with the past studies, this research is unique in several ways:

(1) They include the combined effects of climate, CO_2, and tropospheric ozone whereas previous work has mostly examined climate and CO_2 or climate effects only;

(2) The climate and productivity effects are from fully transient climate scenarios where gradual increases in GHGs gradually force the climate, while much previous work is based on CO_2-doubling climate scenarios;

(3) They consider effects in no-policy and policy scenarios thus making it possible to assess the "benefits" of the prescribed policy, while previous work has simply examined different climate scenarios; and

(4) They use the terrestrial biogeochemical model to simulate the relatively immediate responses of plants to climate and atmospheric changes as well as longer-term soil dynamics and its impact on land productivities; previous work, however, takes soil characteristics as unchanging.

However, the agricultural land types in the Reilly et al. (2007) study only included cropland, pasture land, and managed forestry land, while excluding the un-managed land. Such un-managed land, which could be converted to managed land, does have an economic value; however, since such land was not represented in the database of the EPPA model, it was not included in the Reilly et al. (2007) study. In addition, that research was focused on the economic responses of the 16 EPPA regions in agricultural land due to changing climate conditions, while such economic effects were not distributed to sub-regions or even finer spatial resolutions.

There are important advances represented in previous studies on the impacts of climate, GHGs, and tropospheric ozone on different agricultural land as well as the economic consequences, and my approaches in this research follow closely the state-of-the-art in both regards. However, the studies on the impacts of climate, GHGs, and tropospheric ozone were limited to specific plants in certain site areas, and the further economic consequences were not included in those studies. The studies on economic impacts, although conducted at a regional or global scale, did not include the spatial variations of impacts induced by climate, GHGs, and tropospheric ozone, as well as the spatial distribution of economic impacts.

In this research, to allow for a fairly complete assessment of the impacts of GHG-mitigation policies on agricultural land, I include both the regional impacts driven by economic forces and the feedbacks of climate, GHGs, and tropospheric ozone on agricultural land at the grid-cell scale. To make this possible, I introduce the downscaling methods to distribute the regional land use affected by economic forces to finer spatial resolutions (grid cell of 0.5*0.5 longitude by latitude) considering the spatial variations of feedbacks of climate, GHGs, and tropospheric ozone. In addition, I evaluate the combined effects on not only the managed agriculture land, but also the un-managed land, which could be converted to managed agricultural land. Therefore, in this research, I provide a fairly comprehensive assessment of impacts of GHG-mitigation policies on five types of agricultural land, including cropland, managed forestry land, pasture land, un-managed forestry land, and un-managed grassland.

Chapter 3
The Model

As I reviewed in Chapter 2, there are important advances represented in previous studies on the impacts of climate, GHGs, and tropospheric ozone on different agricultural land as well as the economic consequences, and my approaches follow closely the state-of-the-art in both regards. In this research, to make possible a comprehensive analysis of the impacts of GHG-mitigation policies on agricultural land, I link the impacts of economic forces at the regional scale used in a computable general equilibrium model of the world economy with the feedbacks of climate, GHGs, and tropospheric ozone at the grid-cell scale used in a biophysical model of global terrestrial ecosystems, namely, the Emissions Prediction and Policy Analysis (EPPA) model and the Terrestrial Ecosystem Model (TEM) within the framework of the MIT Integrated Global System Model (IGSM).

Projections of climate change have been hampered by our abilities to model the complex impacts between the human and climate systems. An important factor leading to this limitation is the significant uncertainties in climate system properties. Another difficulty lies in the "century-scale" nature of the projection: it is difficult to project emissions of GHGs and possible land-use changes over a long horizon because of the uncertainties in population growth, economic development, technological evolution, etc. (Sokolov et al., 2005). Because of these limitations, existing general circulation models (GCMs) that couple atmosphere-ocean-land components differ significantly in projections of climate change, as I stated in Chapter 2.

Considering such limitations of existing climate models, it is necessary to quantify the uncertainties in projections of climate change. The MIT Integrated Global System Model (IGSM) is designed for analyzing the global environmental changes that may result from anthropogenic causes, quantifying the uncertainties associated with the projected changes, and assessing the costs and environmental effectiveness of proposed policies to mitigate climate risk (Prinn et al., 1999; Sokolov et al., 2005). The climate system component of the IGSM is designed to provide the flexibility required to handle multiple uncertainty analyses and policy studies while representing in the best way possible the physics, chemistry, and biology components (Webster et al., 2003). Also, the earth system component of the IGSM is linked to a model of human impacts in order to include the impacts between humans and climate change into the climate projections (Sokolov et al., 2005).

Specifically, the MIT IGSM includes an economic model for analysis of GHGs and aerosol precursor emissions and mitigation proposals, a coupled atmosphere-ocean-land surface model, and models of natural ecosystems.

The major model components of the IGSM include:

- A model of human activities and emissions (the Emission Prediction and Policy Analysis or the EPPA model);

- An atmospheric dynamics, physics and chemistry model, which includes a sub-model of urban chemistry;
- An ocean model with carbon cycle and sea-ice sub-models;
- A linked set of coupled land models, namely, the Terrestrial Ecosystem Model (TEM), the Natural Emissions Model (NEM), and the Community Land Model (CLM). These models encompass the global, terrestrial water and energy budgets, and terrestrial ecosystem processes.

In order to study both the impacts of economic forces and feedbacks of climate, GHGs, and tropospheric ozone in response to GHG-mitigation policies on the five types of agricultural land (cropland, managed forestry land, pasture land, un-managed forestry land, and un-managed grassland), I base my research mainly on the EPPA model and the TEM within the MIT IGSM framework. With the cooperation from my colleagues at the MIT Joint Program of Science and Policy on Global Change, I use the EPPA model to project the regional land-use effects of GHG-mitigation policies driven by economic forces, and apply the IGSM to simulate the changes in climate caused by such policies. The researchers at the U. S. Marine Biological Laboratory (MBL) used the TEM to project the productivities of the five types of agricultural land and the carbon stored in such land. I describe the components of the EPPA model and the TEM in Sections 3.1 and 3.2, respectively, and introduce the two climate scenarios applied in this research in Section 3.3.

3.1. EPPA model

The EPPA model is the part of the MIT IGSM that represents the human systems, and it is a recursive-dynamic multi-regional Computable General Equilibrium (CGE) model of the world economy. It is designed to develop projections of economic growth and anthropogenic emissions of greenhouse-related gases and aerosols. It simulates the world economy through time to produce scenarios of GHGs, aerosols, other air pollutants and their precursors emitted by human activities (Paltsev et al., 2005). Below, I describe in detail the structure of the EPPA model and the approach to model land use in the EPPA model.

3.1.1. Structure of the EPPA model

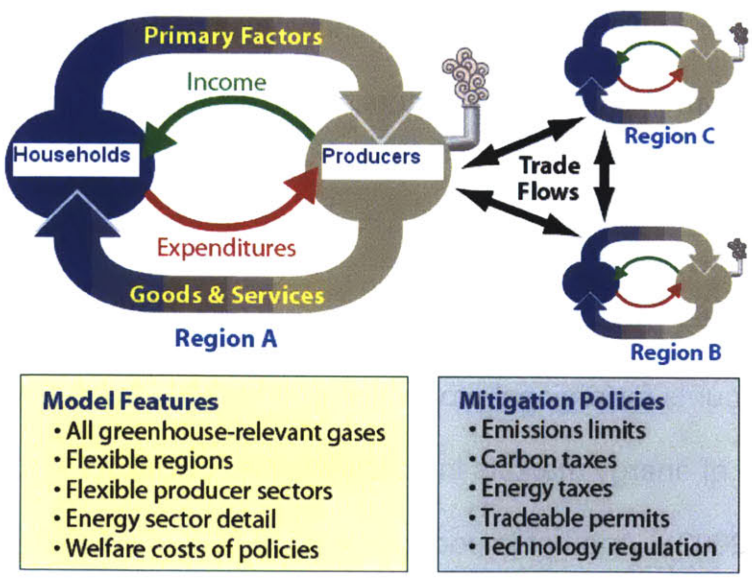

Figure 3.1: The circular flow of goods and resources in the EPPA model
Source: Paltsev et al., 2005.

As indicated in Figure 3.1, the EPPA model represents the circular flow of goods and services in the economy from producing sectors (producers) to final consumers (households), who, in turn, control the supply of capital and labor services. A reverse flow of payments corresponds to the flow of goods and services: households receive payments from the producers for the labor and capital services they provide, while they use the income they receive to pay producers for the goods and services consumed. In addition, the EPPA model simulates trade flows for all goods among regions. Some goods (crude oil for instance) are treated as perfect substitutes in global trade, while for most other goods, the EPPA model embodies the Armington convention widely used in modeling international trade (Armington, 1969). In other words, a domestically produced good is treated as a different commodity from an imported good produced by the same industry. The degree to which domestic and imported goods differ is controlled by the elasticity of substitution between them. The algorithm used to solve the EPPA model finds a solution that maximizes consumer welfare and producer profits subject to the technologies of production and consumption, consumer endowments of primary factors, and existing taxes and distortions (Paltsev et al., 2005).

The Global Trade Analysis Projection (GTAP) dataset is the main data source in the EPPA model, because it accounts for regional production and bilateral trade flows, as well as the representation of energy markets in physical units (Hertal, 1997; Dimaranan and McDougall, 2002). Another important data source in the EPPA model concerns GHGs (CO_2, CH_4, N_2O, HFCs, PFCs, and SF_6) and pollutant air emissions (SO_2, NOx, black carbon, organic carbon, NH_3, CO, etc.), which come from the U.S. Environmental Projection Agency inventory data and projections. The

GTAP data in the EPPA model are aggregated into 16 regions and 23 sectors, and the primary input factors in the EPPA model include capital, labor, energy, and land.

Table 3.1 indicates the regions, sections, and primary factors of the EPPA model applied in this research. The conventional version of the EPPA model has just one aggregate agricultural sector, which uses a single type of land as a specific factor input for agricultural production. In this research, as indicated in Table 3.1, we disaggregate the agricultural sector into three sub-sectors, namely, crops (CROP), forestry (FORS), and livestock (LIVE). Correspondingly, we model transactions among five types of land in this research: cropland, managed forestry land, pasture land, un-managed forestry land, and un-managed grassland[4]. The two types of unmanaged land usually do not have an explicit price or value, because they do not produce any kind of goods or services that are sold on the market; however, they do have economic value in terms of option values, reflecting the fact that in the future, they could be converted to managed land and provide a rental return or some other non-market returns.

[4] We define the land excluding the five types of land as "other land," including bare ground, floodplains, glaciers, lakes, cities, salt marshes, and wetlands. In this research, we assume that the "other land" would keep constant during the 21st century.

Table 3.1: Regions, sectors, and primary factors of the EPPA model in this research

Country/Region	Sectors	Primary Factors
Annex B	***Non-Energy***	***Capital***
Australia/New Zealand (ANZ)	Crops (CROP)	***Labor***
Canada (CAN)	Forestry (FORS)	***Energy***
Eastern Europe (EET)	Livestock (LIVE)	Crude oil
European Union+ (EUR)	Services (SERV)	Shale oil
Former Soviet Union (FSU)	Food Processing (FOOD)	Natural gas
Japan (JPN)	Energy Intensive Products (EINT)	Coal
United States (USA)	Other Industries Products (OTHER)	Hydro
Non-Annex B	Industrial Transportation (TRAN)	Nuclear
Africa (AFR)	Household Transportation (HTRN)	Wind and Solar
Higher Income East Asia (ASI)	***Energy***	***Land***
China (CHN)	Coal (COAL)	Cropland
Indonesia (IDZ)	Crude Oil (OIL)	Managed forestry land
India (IND)	Refined Oil (ROIL)	Pasture land
Central and South America (LAM)	Natural Gas (GAS)	Un-managed forestry land
Middle East (MES)	Electric: Fossil (ELEC)	Un-managed grassland
Mexico (MEX)	Electric: Hydro (HYDR)	
Rest of World (ROW)	Electric: Nuclear (NUCL)	
	Advanced Energy Technologies	
	Electric: Biomass (BELE)	
	Electric: Natural Gas Combined Cycle (NGCC)	
	Electric: NGCC with CO2 Capture and Storage (NGCAP)	
	Electric: Integrated Coal Gasification with CO2 Capture and Storage (IGCAP)	
	Electric: Solar and Wind (SOLW)	
	Liquid fuel from biomass (BOIL)	
	Oil from Shale (SYNO)	
	Synthetic Gas from Coal (SYNG)	

Sources: Paltsev, et al., 2005, revised by the author to indicate the adjustment of the model in this research.

Note:
1. "Higher Income East Asia" includes South Korea, Malaysia, Philippines, Singapore, Taiwan, and Thailand;
2. "Eastern Europe" includes Hungary, Poland, Bulgaria, Czech Republic, Romania, Slovakia, and Slovenia;
3. "European Union" includes the European Union (EU-15) plus countries of the European Free Trade Area (Norway, Switzerland, Iceland);
4. "Former Soviet Union" includes Russia and Ukraine, Latvia, Lithuania, Estonia, Azerbaijan, Armenia, Belarus, Georgia, Kyrgyzstan, Kazakhstan, Moldova, Tajikistan, Turkmenistan, and Uzbekistan;
5. "Rest of the World" includes all countries not included elsewhere: Turkey, and mostly Asian countries.
6. AGRI, SERV, EINT, OTHER, COAL, OIL, ROIL, and GAS sectors are aggregated from the GTAP data (Dimaranan and McDougall, 2002); TRAN and HTRN sectors are disaggregated as documented in Paltsev et al. (2004); HYDR and NUCL are disaggregated from electricity sector (FLY) of the GTAP dataset based on EIA data (2006b); BELE, NGCC, NGCAP, IGCAP, SOLW, BOIL, SYNO, and SYNG sectors are advanced technology sectors that do not exist explicitly in the GTAP dataset.

Table 3.2 indicates the sectors in need of land as the primary inputs in the EPPA model applied in this research. As shown, the sector of "Crops" uses cropland as an input; in addition, considering that biomass-energy production typically occurs in the cropland, we assume that the two sectors related to biomass, "Electric: Biomass" and "Liquid fuel from biomass", would also use cropland as an input. The "Forestry" and "Livestock" sectors use pasture land and managed forestry land, respectively.

Table 3.2: Sectors and land inputs in the EPPA model applied in this research

Sectors	**Land**
Crops (CROP)	Cropland
Forestry (FORS)	Managed forestry land
Livestock (LIVE)	Pasture land
Electric: biomass (BELE)	Cropland
Liquid fuel from biomass (BOIL)	Cropland

Source: the author.

The un-managed forestry land and grassland are not used to produce goods in the economy; however, since they can provide recreational services and conservation of natural creatures to society, we include the consumption of those recreational and conservation services in the welfare function of the un-managed land. Also, the un-managed land could be converted to agricultural production if the value of the agricultural products generated after the conversion would override the welfare generated by the un-managed land. In the next section, I describe more details on modeling land use in the EPPA model.

The base year of the EPPA model is 1997. The EPPA model simulates the economy recursively at 5-year intervals from 2000 to 2100. Production and consumption sectors in the EPPA model are represented by nested Constant

Elasticity of Substitution (CES) functions, and the model is written using the General Algebraic Modeling System (GAMS) software and solved using Mathematical Programming System for General Equilibrium analysis (MPSGE) modeling languages.

The EPPA model also disaggregates the GTAP data for transportation and existing energy-supply technologies. In addition, the EPPA model includes several alternative energy-supply technologies not in use on a large scale or available in 1997, but that could potentially be included in the future, depending on energy prices and/or climate policy conditions. Advanced technologies, such as biomass fuel, become endogenously available when they are able to compete economically with existing technologies. Several factors, such as savings, investments, energy-efficiency improvements, and productivity of labor determine the economic growth. Such economic factors, together with economic policies and depletion of resources, drive prices for inputs and hence the competitiveness of different technologies.

3.1.2. Modeling land use in the EPPA model

The effective "land quantity" of a given type can be changed through two processes: exogenous productivity growth, and land-use conversion. As I stated earlier, to identify the impacts of economic forces with the feedbacks of climate, GHGs, and tropospheric ozone in response to GHG-mitigation policies, we conduct two rounds of analysis: the first round only includes the land-use effects of economic forces, while the second round also includes the feedbacks of climate, GHGs, and tropospheric ozone. In the first round, we set up the improvement of land productivities at 1% annually, and this is in agreement with Reilly and Fuglie (1998) who estimate that the crop yield in the United States has grown by 1-3% per year historically, reflecting technological changes. This approach assures that the land rent can match historically observed trends, and we assume that all the five types of agricultural land experience the same productivity improvements. In the second round, with the feedbacks of climate, GHGs, and tropospheric ozone included, the future land productivities vary from the 1% per year increase due to environmental changes as simulated by the Terrestrial Ecosystem Model (TEM), which is described in the next section.

The area of a type of agricultural land can also be expanded by conversion from other types of agricultural land. For example, a farmer can increase the cropland area by clearing un-managed forestry land and preparing the soil to grow crops. The opposite conversion may also occur, i.e., a farmer could convert the cropland to produce forestry or pasture products. To realize such land conversion, enough investments are needed to assure that a hectare of land converted to another type is able to give a return as good as the average level of the new land type. The prices of agricultural land and its products are driven by supply and demand in the market, and will affect the land-use conversion among different agricultural land types.

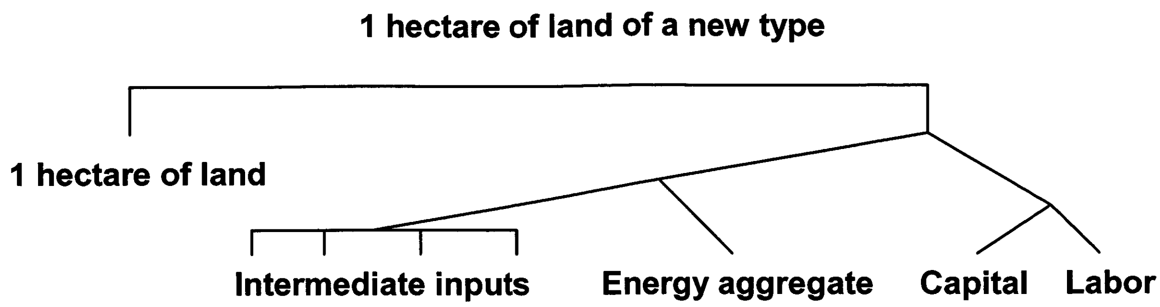

Figure 3.2: Structure of the land-conversion function in the EPPA model
Source: the author.

As indicated in Figure 3.2, the conversion among different agricultural land types is made through the land-conversion function. Specifically, a farmer could use one hectare of land with some other inputs (capital, labor, energy, and intermediate inputs) to produce one hectare of land of a new type. If the value difference between two types of land is larger than the inputs needed in the conversion, the farmers would convert the lower-value land to the higher-value land because they could benefit from such a land conversion. We assume that agricultural land can be suitable to produce any agricultural output, as long as enough investments are provided to make the land as valuable as the average level of the new agricultural land type. The investment includes the costs associated with terrain clearance, soil preparation, input of fertilizers, etc.

Table 3.3 indicates the physical area of each land type in all the EPPA regions in 1997 (Hurtt et al., 2006). Together with the GTAP land-value data of cropland, pasture land, and managed forestry land (Lee et al., 2005), we get the unit price of these three types of agricultural land, defined as the ratio of total land value over total land area. As previously noted, un-managed forestry land and grassland are also included in this research;

however, they are not included in the GTAP dataset. Therefore, we need to evaluate these two types of un-managed agricultural to be used in the EPPA model, as well as to create the demand for them.

Table 3.3: Land areas by EPPA region (1997)
Unit: Million hectare (MHa)

Region	Cropland	Managed forestry land	Pasture land	Un-managed forestry land	Un-managed grassland	Other land	Total
AFR	161	290	744	497	297	1,031	3,021
ANZ	23	39	301	191	52	22	628
ASI	47	6	0	74	7	4	138
CAN	53	35	12	333	11	575	1,019
CHN	200	53	185	185	60	256	939
EET	50	20	11	5	2	4	91
EUR	88	68	43	96	22	89	405
FSU	273	91	294	756	68	536	2,018
IDZ	26	7	5	143	1	27	208
IND	177	31	6	77	13	17	321
JPN	5	10	1	26	0	1	42
LAM	158	203	378	749	150	236	1,874
MES	14	15	183	68	96	148	523
MEX	22	46	60	52	16	9	204
ROW	119	31	150	192	100	273	864
USA	187	119	119	264	98	174	962
Globe	1,599	1,064	2,493	3,708	992	3,401	13,257

Source: Hurtt et al. (2006)
Note: 1. Details of the regional composition are provided in Table 3.1;
2. "Other land" includes bare ground, floodplains, glaciers, lakes, cities[5], salt marshes, and wetlands.

In the absence of any economic data evaluating the unit price associated with un-managed forestry land and grassland, we assume as a first approach that the price

[5] It would be interesting to indicate the urban land of different regions; however, such data are not available because the definitions of cities vary somewhat among different nations. For example, in Australia, urban areas are defined as population clusters of 1,000 or more people, and with a density of 200 or more persons per square kilometer; in Japan, urban areas are defined as contiguous areas of densely inhabited districts using census enumeration districts as units with a density requirement of 4,000 people per square kilometer. European countries, however, define urbanized areas on the basis of urban-type land use, and use satellite photos instead of census blocks to determine the boundaries of the urban area. In less developed countries such as China, in addition to land use and density requirements, a requirement that a large majority of the population is not engaged in agriculture and/or fishing is sometimes used (Demographia, 2007).

per hectare of un-managed forestry land would be the ratio of the total rent of managed forestry land over the total area of managed and un-managed forestry land in each EPPA region. We apply the same approach to the un-managed grassland. As a result, the unit price of un-managed forestry land (or grassland) is lower than that of managed forestry land (or pasture land), depending on the size of un-managed land relative to that of the managed land. In other words, in those regions with much more un-managed land than managed land, the unit price of un-managed land is assumed to be lower than in those regions with less un-managed land. We recognize that this approach is too simple to capture the value that the economic agents would attribute to unmanaged agricultural land, or the price a farmer would be willing to pay to acquire a hectare of un-managed agricultural land. Having realized this limitation, we verify if the future land-use changes predicted by the EPPA model corresponding to such rents for the first decades (before biomass production) follow the historically observed land-use trend in the database. When necessary, we adjust the un-managed land rents to assure that the future land-use changes can match the historically observed trend. Table 3.4 presents the unit prices of the five types of agricultural land by EPPA region in 1997 based on these approaches.

Table 3.4: Unit price of the five types of agricultural land by EPPA region (1997)
Unit: 1997 $/hectare

	Cropland	Managed forestry land	Pasture land	Un-managed forestry land	Un-managed grassland
AFR	45.7	2.0	2.1	0.6	0.2
ANZ	102.3	7.8	4.1	0.8	1.1
ASI	494.6	49.7	88.5	2.0	0.0
CAN	52.3	19.5	36.4	1.0	0.0
CHN	221.7	12.7	13.9	1.8	2.0
EET	115.8	15.0	91.9	7.2	20.1
EUR	405.5	9.3	131.8	3.3	12.5
FSU	30.0	3.3	4.6	0.2	1.0
IDZ	547.8	55.4	122.1	1.4	67.8
IND	212.3	15.9	447.1	3.2	0.0
JPN	1705.1	29.2	1140.1	5.8	0.0
LAM	142.1	1.5	14.3	0.2	1.7
MES	251	20.7	4.3	2.2	0.4
MEX	358.7	6.6	13.2	2.9	2.4
ROW	193.5	21.9	18.7	1.8	2.7
USA	193.2	2.5	42.8	1.4	2.5

Note: 1. Details of the regional composition are provided in Table 3.1.
2. In JPN, there is no un-managed grassland; in CAN, ASI, and IND, the un-managed grassland is aggregated to the pasture land, because the GTAP value of pasture land is too large for the pasture area in the dataset.
Source: EPPA simulation, August 2007.

After we have accounted for the unit price of different types of agricultural land in 1997, we analyze the market demand for their products and services in order to simulate the land-value changes for future years. The market of the three types of managed agricultural land (cropland, managed forestry land, and pasture land) is determined by the demand and supply of their products and services. The un-managed forestry land and grassland can provide recreational services and conservation of natural creatures to society; therefore, we include the consumption of those recreational and conservation services in the welfare function of these two types of un-managed land. In other words, the un-managed land would be consumed as recreational services and biodiversity preservation. If the benefits from consumption of more agricultural products offset the benefits from recreational services and conservation, the un-managed land would be converted to managed land.

As I stated in Chapter 1, biomass is also included in this research in terms of projections of biomass-energy production, as well as the resultant land-use effects.

Biomass energy in the EPPA model is represented through two technologies: electricity production and liquid fuel production from biomass. Biomass production uses cropland as a combination of capital, labor, and other inputs, as indicated in Figure 3.3. The biomass-fuel and biomass-electricity are considered as "backstop" technologies in the sense that they are not produced on a large scale (or not produced at all) in the initial period of the model. However, production of biomass energy could increase as soon as its relative price becomes competitive in comparison to that of conventional energy sources. Therefore, in this research, we might observe an increase in biomass-energy production.

Biomass-fuel

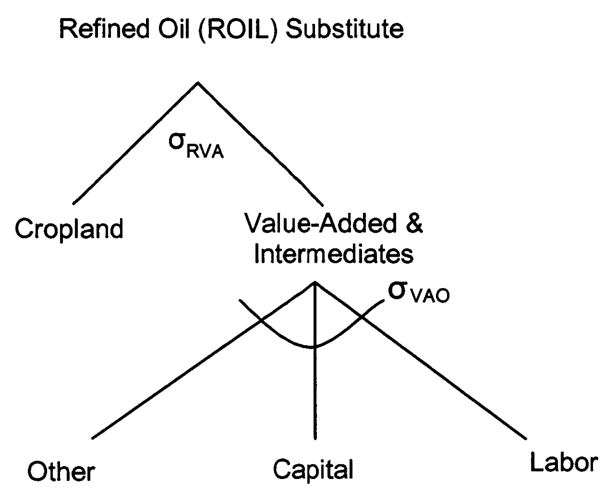

Biomass-electricity

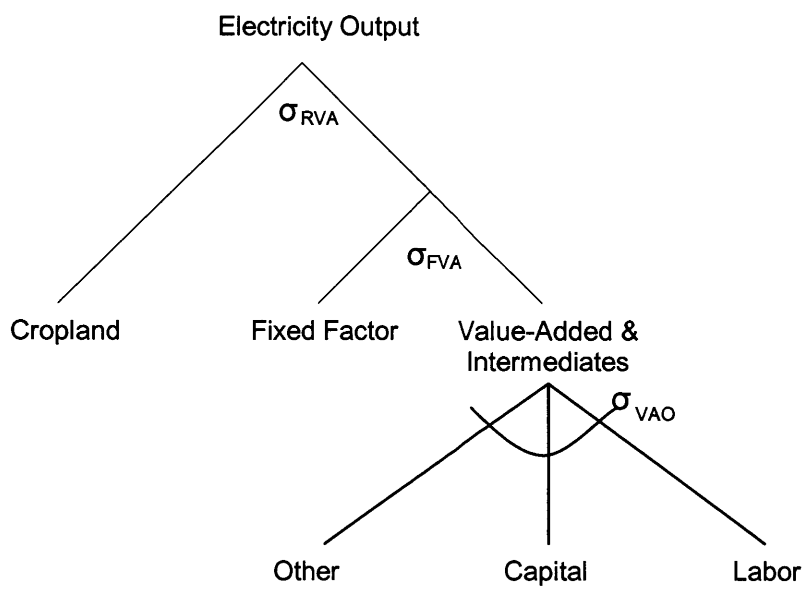

Figure 3.3: Production functions for biomass-fuel and biomass-electricity
Source: Paltsev, et al., 2005

As indicated in Figure 3.3, the production of biomass liquid fuel combines capital, labor, and intermediate inputs from the sector of "Other Industries" (OTHER), as well as cropland. Biomass electricity is produced in a similar structure, except that it has an additional "Fixed Factor," which allows the control of initial penetration of the technology (McFarland et al., 2004).

Table 3.5: Reference elasticity values in biomass-fuel and biomass-electricity technologies

σ_{RVA}	Resource (land) - Value added and intermediates	0.3	Biomass-Electricity
		0.1	Biomass-Fuel
σ_{FVA}	Fixed Factor- Value added and intermediates	0.4	Biomass-Electricity
σ_{VAO}	Labor-Capital-Other	1.0	Biomass-Fuel and Biomass-Electricity

Source: EPPA simulation, August 2007.

Because the input prices in biomass-energy production functions could change over time, the competitiveness of biomass energy over conventional energy sources also depends on the capacity to change the combination of inputs. The elasticities of substitution among different inputs, the σ_{RVA}, σ_{FVA}, and σ_{VAO} shown in Figure 3.3, are used to define the substitutability among different inputs in response to changes in their relative prices, and Table 3.5 indicates our assumed values for these elasticities applied in biomass-energy technologies.

Table 3.6: Parameters used for biomass-energy technologies

				Input Shares			
Supply Technology		Mark-up Factor		Capital	Labor	Other	Fixed Factor
Biomass-fuel		2.5-4.5		0.39	0.09	0.12	--
Biomass-electricity		1.4-2.0		0.33	0.10	0.13	0.04
Land-input shares in both technologies (regionally specific)							
AFR	ANZ	ASI	CAN	CHN	EET	EUR	FSU
0.15	0.20	0.65	0.30	0.30	0.30	0.75	0.20
IDZ	IND	JPN	LAM	MES	MEX	ROW	USA
0.55	0.30	0.90	0.16	0.65	0.80	0.35	0.40

Note: Details of the regional composition are provided in Table 3.1.
Sources: Paltsev, et al., 2005; EPPA simulation, August 2007.

The parameters used to specify the biomass-energy technologies are indicated in Table 3.6. As a consequence of regional specificities in the price and productivity of cropland, the biomass-energy technologies have regionally specified land shares. We use the GTAP land-rent data to identify the land-input shares associated with biomass-energy production, and we normalize all input shares to sum to 1.0; this approach is in agreement with Paltsev and Reilly (2007). Following a convention adopted for the addition of new technologies in the EPPA model, as described in Paltsev et al. (2005), we specify a mark-up factor to define the total cost of biomass-energy production relative to that of the conventional energy production with which the biomass competes in the base year 1997. Given the normalization of input shares among various EPPA regions, we use different mark-ups to reflect the cost differences associated with biomass-energy production among regions. For example, the mark-up for biomass-fuel in the United States is 2.5, meaning that the biomass-fuel production would be economically competitive in the United States if the price of refined oil becomes 2.5 times higher than its observed price in the reference year (1997), given input prices for both technologies as unchanged. As indicated in Table 3.6, the sum of all input shares for biomass-energy production in the United States is 1.0: taking biomass-fuel production as an example, the input shares for capital, labor, land, and others are 0.39, 0.09, 0.40, and 0.12, respectively, and they sum to 1.0. In the other regions, the shares of other inputs (excluding land) can be derived from the value in the United States by scaling them down by the land-input share.

Land requirements per dollar and per energy content of biomass production are affected by regional land availability, agricultural land productivity, and potentials for growing energy crops as well as land rent per hectare. We assume that the capacity to produce some amount of oven dry tonne (odt) of biomass per hectare (ha) per year is regionally specific. In order to be consistent with the observed levels of most efficient biomass production, as described in IPCC (2001) and Moreira (2004), we set the maximum initial odt/ha/year between 10 and 15. Taking Central and South America (LAM) as an example: in those studies (IPCC, 2001; Moreira, 2004), LAM has the highest energy potential of land-based biomass, and we set the maximum value of 15 odt/ha/year as the initial biomass productivity in LAM. This value could increase through time due to land productivity enhancements in order to reach the maximum value of 30 odt/ha/year in LAM at the end of this century. Chou et al. (1977) and Edmonds and Reilly (1985) estimated the energy potentials of land-based biomass, equivalent millions of hectares of "standard" land accounting for climate differences. In other words, their studies allow the comparison of the area of land producing biomass per year with the total available agricultural land in that region. Based on those estimates, we describe the capacity of each region in terms of odt/ha/year, which is used to describe the productivity of land producing biomass. We also compare our estimates on biomass productivities with a more recent work as described in Bot et al. (2000), and find that our estimates on biomass productivities are in agreement with their studies. In Table 3.7, we present the regional biomass productivity index, indicated as the fraction of biomass productivity of each EPPA region in that of LAM.

Table 3.7: Regional biomass productivity index
Unit: The fraction of regional biomass productivity in that of LAM

EPPA region	Biomass productivity index
AFR	0.30 - 0.40
ANZ, CAN, FSU, and MES	0.20
ASI	0.61
CHN, EET, EUR, MEX, ROW, and USA	0.50 - 0.60
IDZ	0.90
IND	0.80

Source: EPPA simulation, August 2007.

We assume that the energy input needed in the production process of biomass-energy would also come from biomass, and a 40% conversion efficiency from biomass to liquid (or electricity) energy products is assumed in this research. For example, if LAM is able to produce biomass at 15 odt/ha/year and the heating capacity of biomass is 20 gigajoule (GJ)/odt, it will correspond to 15 * 20 = 300 GJ/ha/year, leading to 300 * 40% = 120 GJ/ha/year of final liquid (or electricity) energy products.

Based on these assumptions and approaches regarding agricultural land rents, biomass-energy conversion and efficiency, and biomass productivities, we are able to calibrate the land cost in biomass-energy functions. We perform such calibrations first in the United States, and find that in 1997, 40% of the total cost to produce the expected energy from biomass is related to land, while the other 60% is distributed among other inputs as described in Figure 3.3. Then, we calculate the land costs in other EPPA regions based on the land rent/ha and land productivities of each region relative to those in the United States. For example, according to the GTAP database, land rent/ha in Central and South America (LAM) is 74% of that in the United States in 1997, meaning that we need to convert the 40% cost associated with land in the United States to 29.6% (74% * 40% = 29.6%) in LAM. In addition, as the biomass productivity in the United States is assumed to be 55% of that in LAM in 1997, the 29.6% cost associated with land in LAM becomes only 16% (29.6% * 55% = 16%).

Applying the approaches on modeling agricultural land use in the EPPA model as described above, we project regional land use driven by economic forces, indicated by $Share^{economy}_{j,\,t}$, the area share of land type **j** in year **t** in each region affected by economic forces. The **j** includes the five types of agricultural land covered in this research, namely, cropland, managed forestry land, pasture land, un-managed forestry land, and un-managed grassland, as well as the land devoted to biomass-energy production. As stated, we run the EPPA model every five years from 2000 to 2100, and therefore, the **t** would be 2000, 2005, 2010…2100. The area shares of the five types of agricultural land and the land devoted to biomass-energy production in 2000 are provided by the Hurtt land-use dataset (Hurtt et al., 2006), while those for 2005, 2010… 2100 are projected by the EPPA model. Such data are important for the downscaling methods, which are introduced in Chapter 4. In addition, the researchers at the U.S. Marine Biological Laboratory (MBL) use the Terrestrial Ecosystem Model (TEM) to simulate the impacts of climate, GHGs, and tropospheric ozone on agricultural land, and I describe such work in the next section.

3.2. TEM

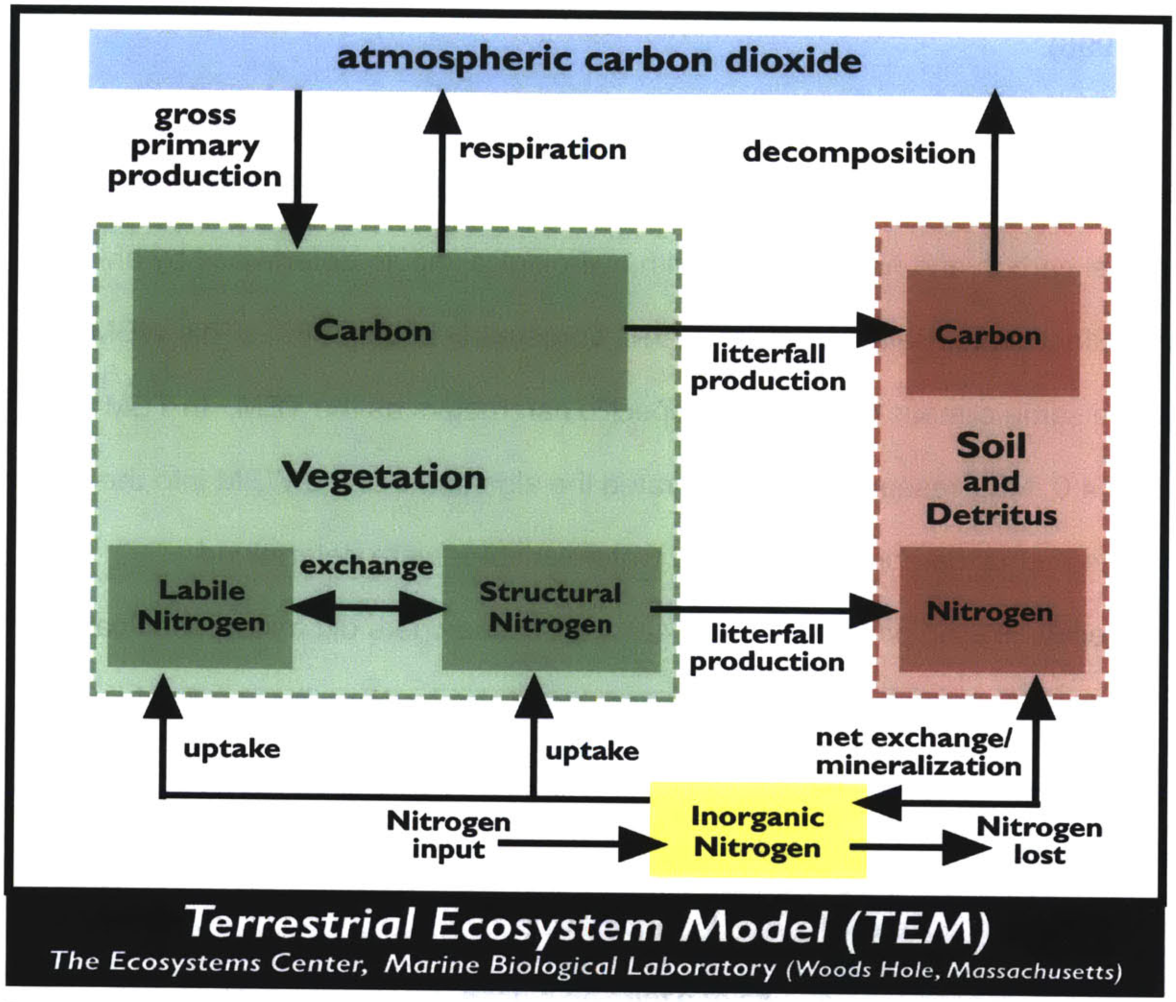

Figure 3.4: Description of the Terrestrial Ecosystem Model (TEM)
Source: The Ecosystems Center, the U.S. Marine Biological Laboratory (MBL).

The researchers in the U. S. Marine Biological Laboratory (MBL) use the TEM, as described in Figure 3.4, to document carbon and nitrogen flows among vegetation, soil, and atmosphere for terrestrial ecosystems of the globe. The TEM uses spatial information on climate, elevation, soils, vegetation and water availability as well as soil-and-vegetation-specific parameters to make estimates of carbon and nitrogen fluxes and pool sizes of terrestrial ecosystems. The TEM operates on a monthly time step and at a grid-cell spatial resolution of 0.5 * 0.5 longitude by latitude (Melillo et al., 1996).

At first, MBL researchers only used the TEM to conduct equilibrium analyses of terrestrial carbon and nitrogen flows with hydrological inputs determined by an independent Water Balance Model (WBM, Vorosmarty et al., 1989). This WBM used the same climatic data and soil-specific parameters as the TEM. In TEM Version 4.0, MBL researchers incorporated the algorithms of the WBM into the TEM so that terrestrial carbon, nitrogen and water variables were determined concurrently. Based on TEM Version 4.0, MBL researchers did minor modifications in TEM Version 4.1 to make the model capable of conducting either equilibrium or transient analyses of terrestrial carbon and nitrogen flows. TEM Version 4.2 incorporated algorithms to describe the effects of land-use changes on terrestrial carbon flows (McGuire et al., 2001); and TEM Version 4.3 further incorporated algorithms to describe the effects of ozone on plant productivities (Felzer et al., 2004). Therefore, with TEM 4.3, MBL researchers are able to examine the responses of terrestrial carbon storage and the net carbon exchange among the vegetation, soil, and atmosphere as influenced by historical climate CO_2, land use, and tropospheric ozone.

Vegetation incorporates carbon by the update of atmospheric CO_2 during photosynthesis, while soils obtain both organic carbon and nitrogen when plant tissue dies. Carbon returns to the atmosphere through autotrophic respiration (R_A)

from vegetation and heterotrophic respiration (R_H), which is associated with the decomposition of soil organic matter (Felzer et al., 2004). To simulate the productivity of the ecosystem, the TEM uses Gross Primary Productivity (GPP) to describe the total amount of carbon fixed by primary producers, mainly plants, in a given area or ecosystem. Some of the fixed carbon is used by primary producers for cellular respiration and maintenance of existing tissues, while the remaining is referred to as Net Primary Productivity (NPP). Therefore, NPP is calculated as follows: NPP = GPP - R_A (McGuire et al., 2001). Both GPP and NPP are in the units of carbon production/area/time. In terrestrial ecosystems, the mass of carbon per unit area per year (g C/m2/year) is most often used (Clark et al., 2001).

Driving variables for the TEM include ozone levels, land-surface classification, CO_2 concentrations, and climate (Melillo et al., 1993). Because there are no detailed and accurate historical surface ozone datasets for the globe, Felzer et al. (2005) developed an independent dataset (1860-1995) based on ozone distribution maps derived from the Multi-scale Atmospheric Transport and Chemistry (MATCH) model as described in Von Kuhlmann et al. (2003). They then performed two sets of simulations to examine how land management might modify the effects of ozone damage, one with and one without optimal nitrogen fertilizations. These two sets of simulations were also conducted without ozone effects. Therefore, there are a total of four model simulations designed in the TEM 4.3 to study the historical effects of ozone on terrestrial carbon sequestration. The ozone effect within TEM 4.3 is based on the AOT40 index, which is a measure of the accumulated hourly ozone levels above a threshold of 40 parts per billion (ppb). Because hourly datasets of surface ozone do not exist at the spatial extent and resolution of the TEM, MBL researchers use the MATCH model to construct global AOT40 maps for each hour. More details on these procedures are provided in Felzer et al. (2005). In this research, ozone levels in the future are influenced by potential climate policies designed to mitigate the GHG emissions, which, as I stated in the Chapter 1, would affect precursors to ozone formation.

MBL researchers have used several spatially explicit datasets of land-surface classification to estimate carbon and nitrogen stocks and fluxes for various regions of the terrestrial biosphere. Most studies are based on a global dataset of vegetations that MBL researchers created by digitizing a series of existing land-use maps and then translated the land categories into general vegetation classes. In this research, corresponding to the most-updated global land-use dataset from Hurtt et al. (2006), MBL researchers base the TEM simulation on IGSMVEG, the land-surface classifications of which are described in Table 3.8. Considering the assumption that biomass would occur only with the existence of cropland, MBL researchers treat land used for biomass-energy production the same as cropland.

Table 3.8: IGSMVEG land-surface classification

1	Bare ground
2	Needle-leaf evergreen tree temperate
3	Needle-leaf evergreen tree boreal
4	Needle-leaf deciduous tree boreal
5	Broadleaved evergreen tree tropical
6	Broadleaved evergreen tree temperate
7	Broadleaved deciduous tree tropical
8	Broadleaved deciduous tree temperate
9	Broadleaved deciduous tree boreal
10	Broadleaved evergreen shrub temperate
11	Broadleaved deciduous shrub temperate
12	Broadleaved deciduous shrub boreal
13	C_3 grass arctic
14	C_3 grass
15	C_4 grass
16	Crops
17	Wetlands (tree tropical)
18	Wetlands (no-tree tropical)
19	Wetlands (tree temperate)
20	Wetlands (no-tree temperate)
21	Wetlands (tree boreal)
22	Wetlands (no-tree boreal)
23	Mangroves
24	Coastal salt marsh
25	Inland salt marsh
26	Floodplains (tree tropical)
27	Floodplains (no-tree tropical)
28	Floodplains (tree temperate)
29	Floodplains (no-tree temperate)
30	Glaciers
31	Lakes
32	Pasture

Source: The U.S. Marine Biological Laboratory (MBL), 2007

In terms of other inputs for the TEM, MBL researchers use the CO_2 concentrations and climate variability (air temperature, precipitation, top-of-the-atmosphere and surface radiation) from the climate scenarios simulated by the MIT IGSM. For each scenario, we use emissions from the EPPA model as inputs by the two-dimensional land ocean (2D-LO) atmospheric chemistry model in the MIT IGSM, which then transports the gases across the globe and simulates the appropriate chemical reactions of the gases in the atmosphere to update climate change and atmospheric concentrations of the gases. MBL researchers use these simulations of climate conditions from the MIT IGSM, combined with the ozone levels and land-surface classification, as inputs in the TEM to project future ecosystem productivities based at the grid-cell scale of 0.5 * 0.5 longitude by latitude. In Section 3.3 follows, I describe the two climate scenarios applied in this research.

3.3. Description of scenarios

In this research, referring to the GHG-mitigation approaches described in Paltsev et al. (2007), we develop two scenarios on GHG emissions: the baseline and GHG-mitigation policy scenarios.

In the baseline scenario, we assume that there are *no* policies to mitigate GHG emissions. In this scenario, according to the projections of the EPPA model, the cumulative GHG emissions in the United States would be 114 billion metric tons (bmt) of carbon equivalent for the period of 2012-2050, and 235 bmt of carbon equivalent for the period of 2051-2100; while the corresponding global levels would be 672 bmt and 1,351 bmt, respectively (Paltsev et al., 2007).

In the GHG-mitigation policy scenario, however, we assume that there *are* policies to limit GHG emissions. A number of approaches to mitigate GHG emissions are under consideration in the United States, but the policy instrument now receiving greatest attention is a national cap-and-trade system (Paltsev et al., 2007). It specifies GHG mitigation to be achieved through 2050 for the standard six-gas basket of GHGs, including carbon dioxide (CO_2), nitrous oxide (N_2O), methane (CH_4), hydrofluorocarbons (HFC_s), perfluorocarbons (PFC_s) and sulphur hexafluoride (SF_6). We apply the case specifying reductions of GHG emissions in the United States of 50% below 1990 levels by 2050, and the other countries pursue GHG-mitigation policies as follows: Europe, Japan, Canada, Australia, and New Zealand follow an allowance path that is falling gradually from the simulated Kyoto emissions levels in 2012 to 50% below 1990 in 2050. All other countries, mainly developing ones, adopt a policy beginning in 2025 and continuing through 2034 that holds emissions to the level in year 2015, and then maintains 2000 emission levels from 2035 to 2050. Such policies are extended through 2100 by holding annual emission allowances around their 2050 level through the end of the century. The rationale behind such GHG-mitigation policies is described in Paltsev et al. (2007).

Table 3.9: Regional GHG emissions in 2050 and 2100
Unit: Million metric tons (mmt) of carbon equivalent

	2050		2100	
	Baseline	Policy	Baseline	Policy
AFR	1,626	517	1,496	499
ANZ	291	93	398	126
ASI	1,560	522	3,117	523
CAN	428	93	394	91
CHN	3,216	1,336	4,454	1,336
EET	476	152	614	194
EUR	2,071	552	1,348	355
FSU	1,485	803	1,922	803
IDZ	288	144	233	145
IND	1,623	525	2,512	526
JPN	679	201	1,026	300
LAM	1,386	539	1,414	539
MES	1,046	337	1,645	338
MEX	345	154	192	154
ROW	1,195	448	1,552	448
USA	3,604	967	5,342	937

Source: EPPA simulation, August 2007
Note: Details of the regional composition are provided in Table 3.1.

Following the implementation of these GHG-mitigation policies, based on the projection of the EPPA model, the cumulative number of GHG emissions in the United States would be 55 bmt of carbon equivalent for the period of 2012-2050 and 43 bmt of carbon equivalent for the period of 2051-2100; while the corresponding global levels would be 408 bmt and 366 bmt, respectively (Paltsev et al., 2007). In Table 3.9, we show the GHG emissions in each EPPA region in 2050 and 2100 in both the baseline and GHG-mitigation policy scenarios, which are projected by the EPPA model.

In each scenario, with the TEM simulations conducted by MBL researchers, we are able to include the impacts of climate, GHGs, and tropospheric ozone on the five types of agricultural land at a grid-cell scale. As stated, we use the EPPA model to capture the land-use effects of economic forces on a regional scale. In order to achieve a comprehensive assessment of land-use effects in response to the GHG-mitigation policies, I introduce the downscaling methods to link the regional land-use effects of economic effects with the feedbacks of climate, GHGs, and ozone at the grid-cell scale, described in the next chapter.

Chapter 4
Methods for Downscaling Land Use

As I stated in Chapter 2, the previous studies on the impacts of climate, GHGs, and tropospheric ozone on agricultural land were limited to specific plants in certain site areas, and the further economic consequences were not included; the studies on economic impacts, although being conducted at regional or global scale, did not include the spatial variations of impacts induced by climate, GHGs, and tropospheric ozone, as well as the spatial distribution of economic impacts.

To allow for a fairly complete assessment of the impacts of GHG-mitigation policies on agricultural land in this research, I include both the regional land-use effects driven by economic forces and the feedbacks of climate, GHGs, and tropospheric ozone on agricultural land at the grid-cell scale. In this chapter, I introduce the methods to distribute the regional land use affected by economic forces to finer spatial resolutions (grid cell of 0.5 * 0.5 longitude by latitude). The original motivation of the downscaling methods comes from the mixed-entropy method of You and Wood (2006). Realizing that agricultural production and land use were generally reported only on a national basis, You and Wood (2006) described an entropy-based approach on making spatially disaggregated assessments of the distribution of crop production. Using this approach, tabular crop-production statistics were blended judiciously with an array of other secondary data to assess the production of specific crops within individual "pixels," which were typically 25 - 100 square kilometers in size. The information utilized in You and Wood (2006) included crop production statistics, farming-system characteristics, satellite-derived land-cover data, biophysical-crop-suitability assessments, and population density. They indicated that although this approach was computationally intensive, it would provide reliable estimates of crop-production patterns.

In this research, because of computational feasibility and limited data availability, I use a simpler approach in the downscaling methods. Basically, based on the projections of the econometric land-use model, I develop a "prior" for the share of each of the five types of agricultural land in each grid cell, and then assign the regional land shares projected by the EPPA model to grid cells and minimize the difference between the assigned level and the "prior." Below, I describe my methods in detail.

In this research, we use the EPPA model to capture the land-use changes at the regional scale in response to economic forces, while the spatial distribution of the aggregated land use is determined by the characteristics of land that vary across different locations. In this chapter, I describe how the spatial characteristics of land impacted by climate, GHGs, and ozone affect land-use decisions, and introduce the downscaling technologies to distribute the aggregated regional land use affected by economic forces to the grid-cell scale of 0.5 * 0.5 longitude by latitude.

To explain whether land is more likely to be used for crops, pasture, or managed forestry, or left as un-managed land, I develop an econometric land-use model based on historical data to analyze the determinants of land-use decisions in each grid cell of 0.5 * 0.5 longitude by latitude. In Section 4.1, I introduce the data needed in the econometric land-use model and the sources for them; I describe the structure of the econometric model in Section 4.2, and present the regression results in Section 4.3. I assume that what I estimate from historical cross-section evidence also holds true for the future where I am explaining the aggregated regional demand for land driven by economic forces. Based on the projections of the variables affecting land-use decisions, I apply the econometric land-use model to predict the future gridded land use. Then, I apply the downscaling methods to distribute the regional land use driven by economic forces to grid cells, which are described in Section 4.4. Inputs of the downscaling methods include the regional land use driven by economic forces as projected by the EPPA model as well as the gridded land use projected by the approaches described in Section 4.3. In addition, I introduce the techniques to distribute the land devoted to biomass-energy production, which did not occur historically and therefore is not included in the econometric land-use model.

4.1. Data

As indicated by Farmer-Bowers et al. (2006), land-use changes are affected by four elements: (1) economic factors linked to agricultural production, (2) climate conditions, (3) farmers' experience of land productivities, and (4) human accessibility. The first element, economic forces causing land-use changes, is included in the EPPA model in terms of market supply and demand for agricultural products and services, while the other three elements need to be included in the econometric land-use model as factors driving land-use decisions.

Considering data availability, I use temperature and precipitation to indicate the spatial variation of climate conditions. Land productivities are indicated as the Net Primary Productivity (NPP) as summarized by Clark et al. (2001). Considering that farmers' experience is based on the historical productivities of different types of agricultural land, I use the average annual NPP of the past several years of each of the five agricultural land types in the econometric land-use model. In addition, I use the distance from the center of each grid cell to the center of the nearest city to indicate the human accessibility. By using such a proximity variable, I am able to capture the relative accessibility of land and the transportation costs of agricultural products – for example, if a piece of cropland is very far from urban markets, the price a farmer receives for crops would have to be lower than that received closer to cities to make up for the cost related to transporting the crop products to the market. Also, because of insufficient data, I am not able to include some variables possibly affecting land-use decisions, such as irrigation and slope, in the econometric land-use model in this research.

Therefore, to develop the econometric land-use model, I need the spatial data of temperature, precipitation, land productivity (indicated by NPP), and urban proximity. These variables would affect land-use decisions, indicated by the land-use composition in each grid cell of 0.5 * 0.5 longitude by latitude.

The gridded land-use data of the five types of agricultural land are provided by the Hurtt dataset (Hurtt et al., 2006). Corresponding to the land-surface classification of the Terrestrial Ecosystem Model (TEM), each grid cell includes one or more of the 32 land-cover types indicated before in Table 3.6. The agricultural land in the EPPA model applied in this research, however, includes cropland, managed forestry land, and pasture land, as well as un-managed forestry land and grassland; in addition, the other land excluding these five types of agricultural land is defined as "other land." In addition, land categories in the EPPA model are based on the regional scale. Therefore, I need to aggregate the 32 land-cover types based on the grid-cell scale in the TEM into six land categories based on the regional scale in the EPPA model.

As indicated in Table 4.1, the 32 land-surface categories in the TEM are aggregated into six land categories in the EPPA model, including five types of agricultural land (cropland, managed forestry land, pasture land, un-managed forestry land, and un-managed grassland) and "other land."

Table 4.1: Linkage of land classifications between the TEM and the EPPA model

TEM	EPPA
Crops	Cropland
Needle-leaf evergreen tree temperate	Forestry land[6] (managed and un-managed)
Needle-leaf evergreen tree boreal	
Needle-leaf deciduous tree boreal	
Broadleaved evergreen tree tropical	
Broadleaved evergreen tree temperate	
Broadleaved deciduous tree tropical	
Broadleaved deciduous tree temperate	
Broadleaved deciduous tree boreal	
Broadleaved evergreen shrub temperate	
Broadleaved deciduous shrub temperate	
Broadleaved deciduous shrub boreal	
Pasture	Pasture land
C_3 grass	Un-managed grassland
C_4 grass	
Bare ground	Other land
C_3 grass arctic	
Wetlands (tree tropical)	
Wetlands (no-tree tropical)	
Wetlands (tree temperate)	
Wetlands (no-tree temperate)	
Wetlands (tree boreal)	
Wetlands (no-tree boreal)	
Mangroves	
Coastal salt marsh	
Inland salt marsh	
Floodplains (tree tropical)	
Floodplains (no-tree tropical)	
Floodplains (tree temperate)	
Floodplains (no-tree temperate)	
Glaciers	
Lakes	

Source: the author.

[6] The Hurtt land-use dataset (Hurtt et al., 2006) distinguishes managed forestry land from un-managed forestry land.

Applying the linkage of land classifications indicated in Table 4.1, I get the aggregated regional land use of the six types of land in each EPPA region from 1970 to 2000. Considering the year 2000 as an example, I present such data in Table 4.2, and show the spatial land-use distribution of the five types of agricultural land in Figures 4.1 through 4.5. The spatial land-use distribution, indicated by the share percentage of each type of agricultural land in the total area of each grid cell, is continuous, while I divide the data into ten categories from 0 to 1 for mapping purposes.

Table 4.2: Regional summary of land categories in 2000
Unit: Thousand square kilometers

Region	Cropland	Managed forestry land	Pasture land	Un-managed forestry land	Un-managed grassland	Other land	Total
AFR	1,609	4,459	7,444	4,974	3,026	8,698	30,209
ANZ	349	723	3,924	2,266	663	202	8,128
ASI	465	78	1	744	65	25	1,379
CAN	528	741	121	3,334	111	5,135	9,969
CHN	1,995	606	1,848	1,853	621	2,472	9,394
EET	495	222	109	45	25	13	908
EUR	875	1,009	432	961	203	516	3,996
FSU	2,729	1,530	2,944	8,611	710	5,664	22,188
IDZ	256	130	49	1,428	4	208	2,076
IND	1,770	341	62	770	121	149	3,214
JPN	47	107	6	257	0	3	420
LAM	1,583	2,687	3,779	7,490	1,551	1,651	18,740
MES	137	353	1,833	680	817	1,414	5,234
MEX	219	529	596	522	155	16	2,036
ROW	1,193	472	1,497	1,920	933	2,154	8,169
USA	1,866	1,589	1,192	2,638	952	1,380	9,617
The World	16,114	15,576	25,837	38,492	9,957	29,697	135,676

Source: Hurtt et al. 2006.
Note: 1. Details of the regional composition are provided in Table 3.1.
2. "Other land" includes bare ground, floodplains, glaciers, lakes, cities, salt marshes, and wetlands.

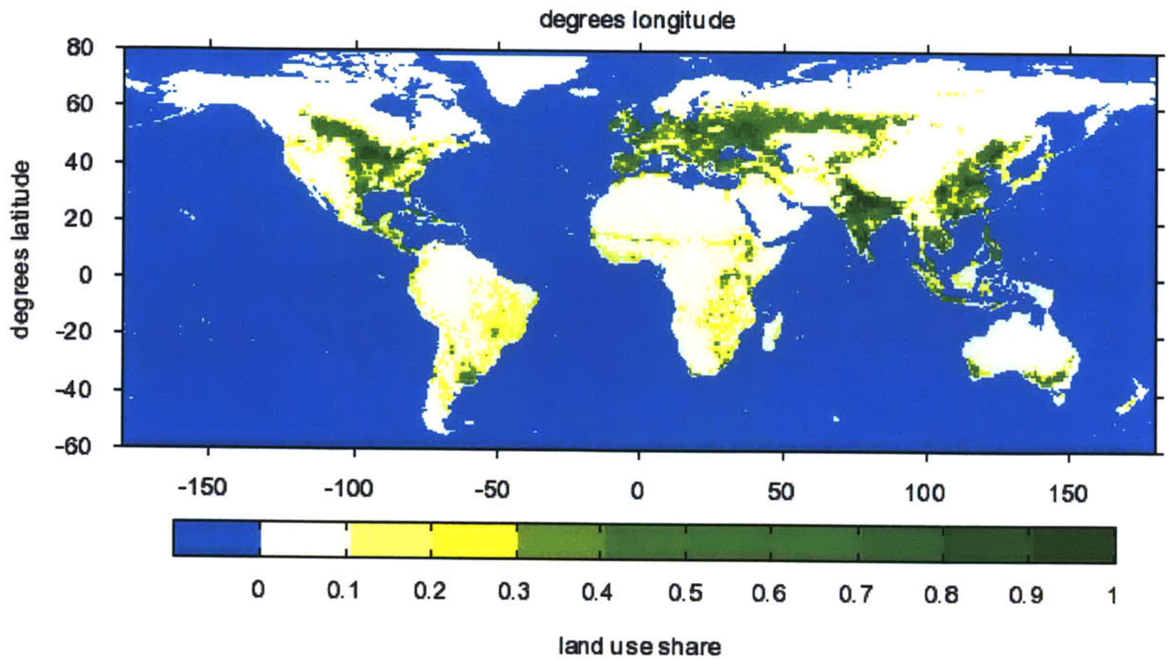

Figure 4.1: Global cropland allocation in 2000
Unit: Cropland share in each grid cell of 0.5 longitude * 0.5 latitude
Source: Hurtt et al. (2006)

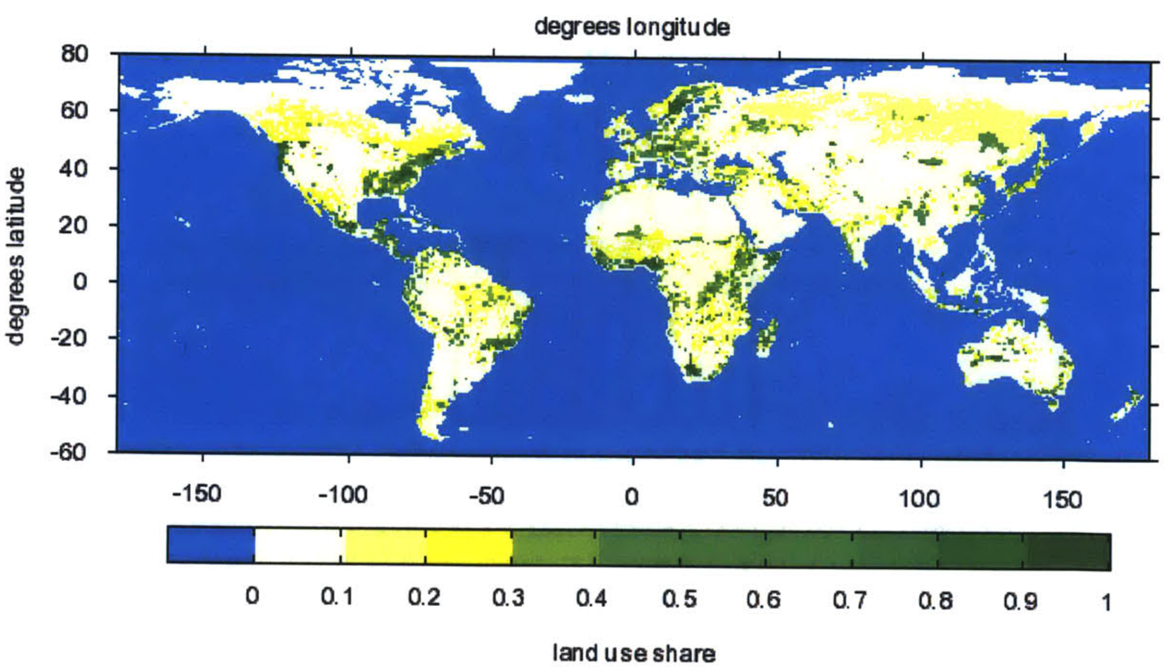

Figure 4.2: Global managed forestry land allocation in 2000
Unit: Managed forestry land share in each grid cell of 0.5 longitude * 0.5 latitude
Source: Hurtt et al. (2006)

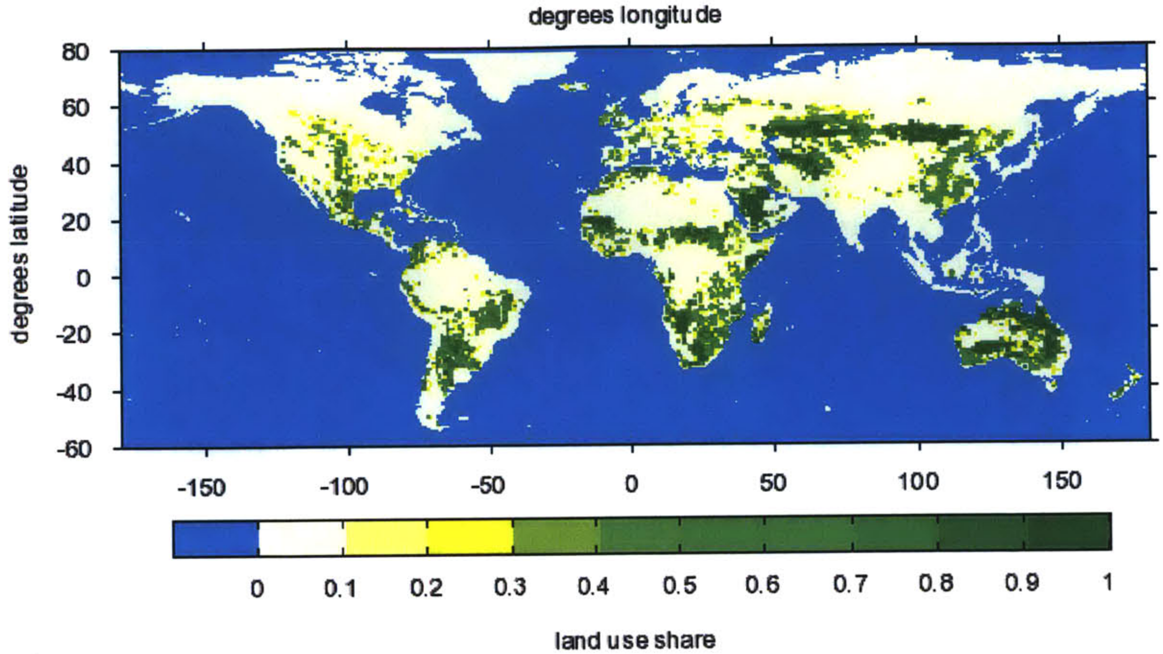

Figure 4.3: Global pasture land allocation in 2000
Unit: Pasture land share in each grid cell of 0.5 longitude * 0.5 latitude
Source: Hurtt et al. (2006)

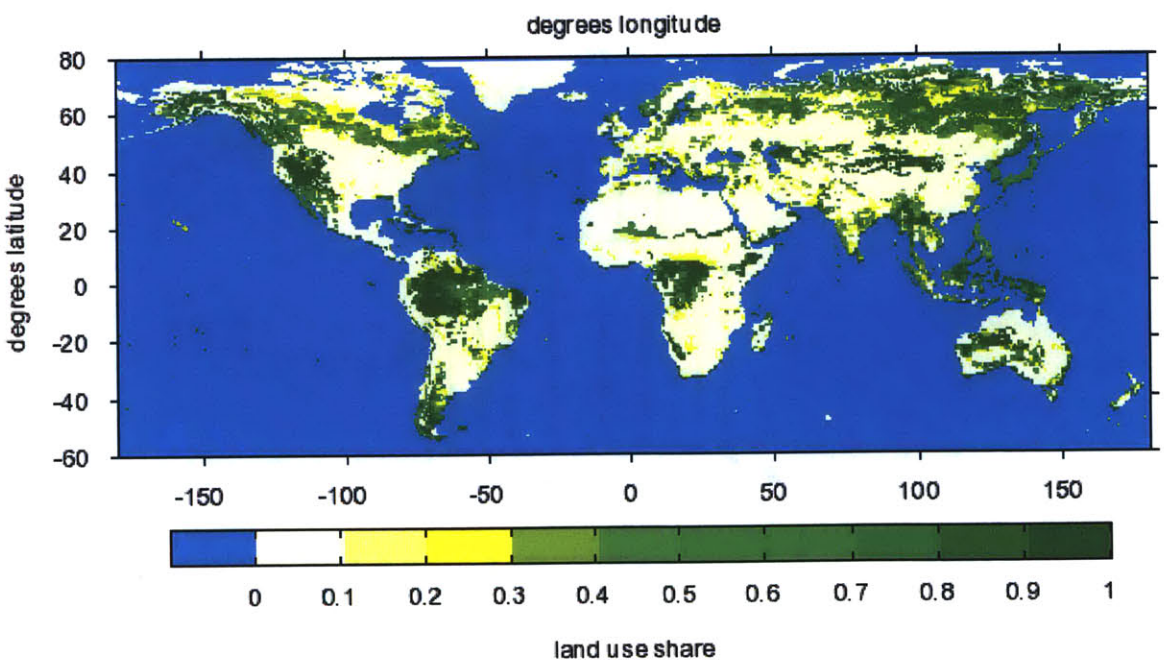

Figure 4.4: Global un-managed forestry land allocation in 2000
Unit: Un-managed forestry land share in each grid cell of 0.5 longitude * 0.5 latitude
Source: Hurtt et al. (2006)

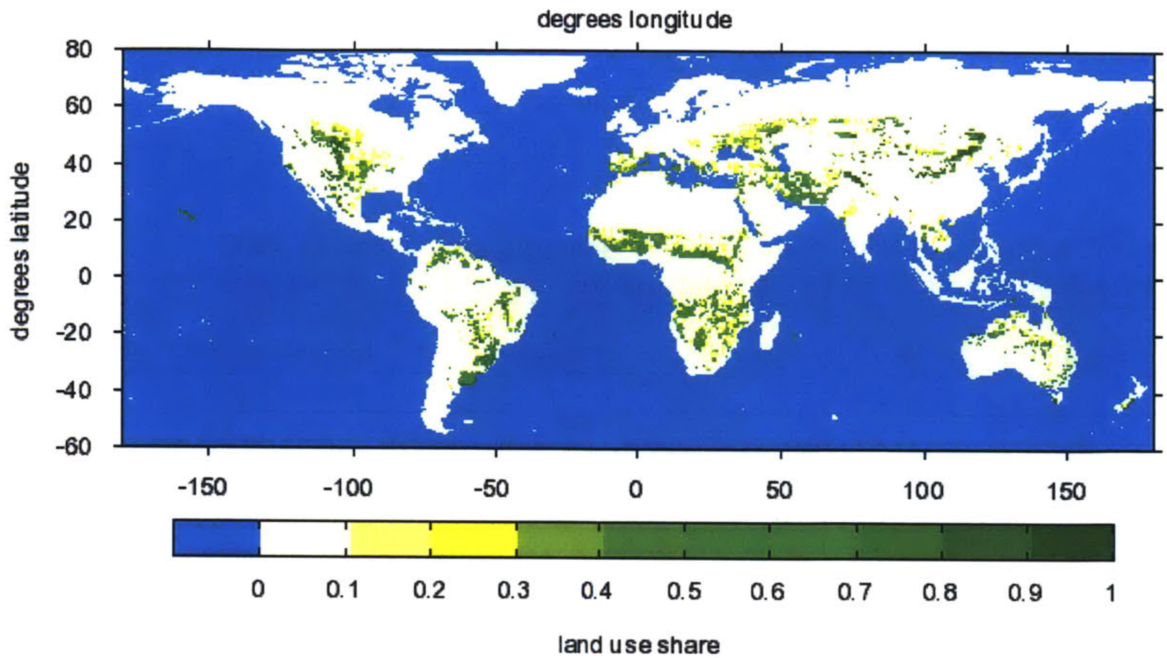

Figure 4.5: Global un-managed grassland allocation in 2000
Unit: Un-managed grassland share in each grid cell of 0.5 longitude * 0.5 latitude
Source: Hurtt et al. (2006)

As indicated in Figures 4.1 through 4.5, in 2000, main providers of cropland include the United States, Europe, China, and India. Most forestry land, both managed and un-managed, is observed in Central and South America, the United States, Africa, and Europe, while there are also large areas of un-managed forestry land in Indonesia and Russia. Pasture land and un-managed grassland are mainly found in Australia, Central and Southern Africa, Mongolia, and the Middle East.

Based on the Hurtt land-use dataset (Hurtt et al., 2006), MBL researchers simulate the historical NPP (1970-2000) at the grid-cell scale of the 32 land-cover types indicated in Table 4.1. Again using the linkage methods indicated in Table 4.1, I get the historical NPP of the five types of agricultural land on both regional and grid-cell scales. Taking the year 2000 as an example, I show the aggregated regional NPP of the five types of agricultural land in Table 4.3.

Table 4.3: Regional NPP of the five types of agricultural land in 2000
Unit: Trillion grams of carbon (equals million tons of carbon) per year

Region	Cropland	Managed forestry land	Pasture land	Un-managed forestry land	Un-managed grassland
AFR	1,647	1,019	2,351	3,313	1,036
ANZ	158	70	1,088	381	203
ASI	833	20	1	28	8
CAN	341	111	24	827	30
CHN	1,635	209	822	403	120.9
EET	294	110	44	28	8
EUR	738	342	213	445	77
FSU	1,598	203	521	1,590	166
IDZ	527	47	45	1,682	5
IND	1,522	84	30	451	25
JPN	46	69	2	204	0
LAM	2,370	1,247	2,336	6,981	1,390
MES	47	6	233	47	122
MEX	327	147	266	137	52
ROW	1,138	98	288	1,366	281
USA	1,376	703	488	669	363
The World	14,596	4,486	8,752	18,550	3,887

Source: TEM simulation, April 2007.
Note: Details of the regional composition are provided in Table 3.1.

Analysts at the Climate Research Unit (CRU) in the United Kingdom have developed a dataset of historical temperature and precipitation (1970-2000) at the grid-cell scale of 0.5 * 0.5 longitude by latitude. Using the year 2000 as an example, I show the spatial patterns of temperature and precipitation, indicated as the annual average level in each grid cell, in Figures 4.6 and 4.7, respectively. Such data are continuous but are classified into five categories for mapping purposes.

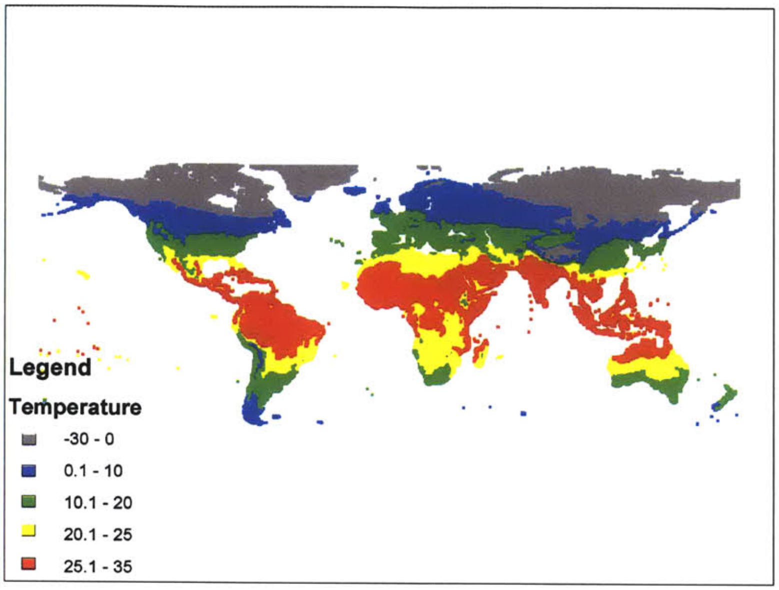

Figure 4.6: Global temperature in 2000
Unit: °C (average of the twelve months in 2000)
Source: The CRU database

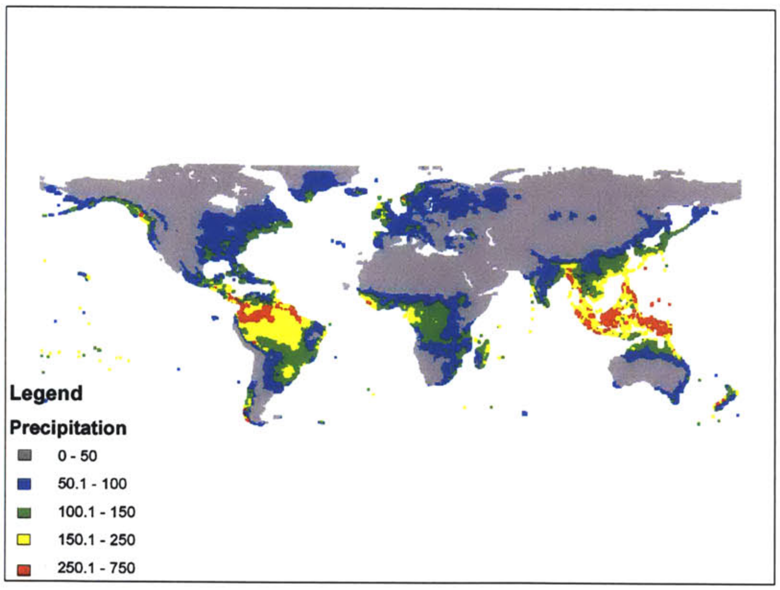

Figure 4.7: Global precipitation in 2000
Unit: Inch (average of the twelve months in 2000)
Source: The CRU Database

Scholars at the U.S. Environmental Systems Research Institute (ESRI) have created a database of global cities as of 2000. In this dataset, the city is defined as a location with a population more than 200,000. I calculate the distance from the center of each grid cell to the center of the nearest city, and indicate the results in Figure 4.8. Again, such data are continuous but are classified into five categories for mapping purposes.

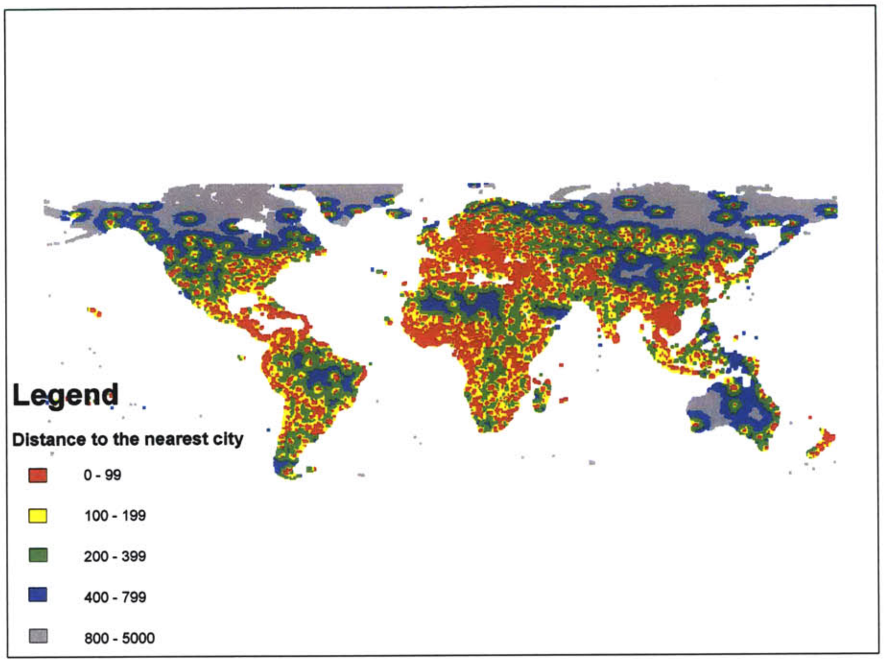

Figure 4.8: Distance from the center of each grid cell to the center of the nearest city in 2000
Unit: Kilometer
Source: Arc-GIS 9.2, the ESRI

Therefore, I obtain the following information for each grid cell: total land area, sub-area and NPP of the five types of agricultural land as well as "other land," temperature, precipitation, and distance to the nearest city. In addition, I get the aggregated regional data on land use and NPP. The regional data, as important indicators of agricultural supplies of land and products, are important inputs for the EPPA model to capture the future land-use effects in response to economic forces, while the gridded data are necessary inputs for the econometric land-use model, which is described in the next section.

4.2. Econometric land-use model

As stated earlier, I am analyzing the impacts on land-use decisions of environmental conditions (indicated by temperature and precipitation), farmers' experience (indicated by the average land productivity over the past several years), and human accessibility (indicated by the distance of the land to the nearest city).

Specifically, I use $\text{Share}_{i,j,t}$ to indicate the dependent variable: the share percentage (%) of agricultural land type **j** in grid cell **i** in the year **t**. Regarding independent variables, annual gridded productivity of each agricultural land type in the form of NPP comes from the TEM (1970-2000), and is indicated as $\text{NPP}_{i,j,t}$, the annual NPP of agricultural land type **j** in grid cell **i** in the year **t**. Therefore, such data over the past **n** years of the year **t** are indicated by Average $\text{NPP}_{i,j,t\text{-}n\sim t\text{-}1}$. Annual gridded temperature and precipitation come from the CRU (1970-2000), and are indicated as $\text{Temperature}_{i,t}$ and $\text{Precipitation}_{i,t}$, the annual temperature and precipitation in grid cell **i** in the year **t**, respectively. Concerning the distance of each grid cell to the nearest city, which is obtained from the U.S. ESRI GIS database (2000), it is indicated as $\text{Distance}_{i,t}$, the distance from the center of grid cell **i** to the center of the nearest city in the year **t**.

In the indices described above, the **j** includes cropland (**j1**), managed forestry land (**j2**), pasture land (**j3**), un-managed forestry land (**j4**), and un-managed grassland (**j5**). Concerning the "other land" (lakes and glaciers for example), I assume that such land would remain un-disturbed, and therefore constant. The **i** includes all grid cells of 0.5 * 0.5 longitude by latitude in each of the 16 EPPA regions. The **t** includes each historical year from 1970 to 2000, and the only exception occurs in Distance $_{i,\,t}$, because such data are only available in 2000. I assume that it did not change from 1970 to 2000, and would not change during the 21st century. Considering that I calculate this variable as the distance from the center of each grid cell to the *center* of the nearest city, this assumption would not significantly affect the reliability of the regressions.

Based on these data, I describe Share $_{i,\,j,\,t}$ as a function of historical average annual NPP over the past n years, temperature, precipitation, and distance from the nearest city:

$$\begin{aligned}\text{Share}_{i,j,t} = f\,(&\text{Average NPP}_{i,\,j1,\,t\text{-}n\sim t\text{-}1},\ \text{Average NPP}_{i,\,j2,\,t\text{-}n\sim t\text{-}1},\\ &\text{Average NPP}_{i,\,j3,\,t\text{-}n\sim t\text{-}1},\ \text{Average NPP}_{i,\,j4,\,t\text{-}n\sim t\text{-}1},\\ &\text{Average NPP}_{i,\,j5,\,t\text{-}n\sim t\text{-}1},\ \text{Temperature}_{i,\,t},\ \text{Precipitation}_{i,\,t},\\ &\text{Distance}_{i,\,2000})\end{aligned}$$

4.3. Regression results

Based on my descriptions of the econometric land-use model in Section 4.2, I conduct the regression for each of the five types of agricultural land based on the formula below:

$$
\begin{aligned}
\text{Share}_{i,j,2000} = {} & \beta_1{*}\text{Average NPP}_{i,j1,1995\sim1999} + \beta_2{*}(\text{Average NPP}_{i,j1,1995\sim1999})^2 \\
& + \beta_3{*}\text{Average NPP}_{i,j2,1995\sim1999} + \beta_4{*}(\text{Average NPP}_{i,j2,1995\sim1999})^2 \\
& + \beta_5{*}\text{Average NPP}_{i,j3,1995\sim1999} + \beta_6{*}(\text{Average NPP}_{i,j3,1995\sim1999})^2 \\
& + \beta_7{*}\text{Average NPP}_{i,j4,1995\sim1999} + \beta_8{*}(\text{Average NPP}_{i,j4,1995\sim1999})^2 \\
& + \beta_9{*}\text{Average NPP}_{i,j5,1995\sim1999} + \beta_{10}{*}(\text{Average NPP}_{i,j5,1995\sim1999})^2 \\
& + \beta_{11}{*}\text{Temperature}_{i,2000} + \beta_{12}{*}(\text{Temperature}_{i,2000})^2 \\
& + \beta_{13}{*}\text{ Precipitation}_{i,2000} + \beta_{14}{*}(\text{Precipitation}_{i,2000})^2 \\
& + \beta_{15}{*}\text{Distance}_{i,2000} + \alpha_0
\end{aligned}
$$

As indicated in the formula, I am using the annual average NPP of the past five years, and analyze the land-use decisions in 2000. The reason to use the average of the past several years is that the land-use decision is based on expected (average) climate impacts rather than the weather in a particular year.

Based on this formula, I develop an econometric model for each of the five types of agricultural land in each EPPA region. In Table 4.4, I explain the coefficients corresponding to the independent variables.

Table 4.4: Coefficients for independent variables in the regression

Coefficient	Independent variables
β_1	Average annual NPP (1995-1999) of the cropland
β_2	Square of average annual NPP (1995-1999) of the cropland
β_3	Average annual NPP (1995-1999) of the managed forestry land
β_4	Square of average annual NPP (1995-1999) of the managed forestry land
β_5	Average annual NPP (1995-1999) of the pasture land
β_6	Square of average annual NPP (1995-1999) of the pasture land
β_7	Average annual NPP (1995-1999) of the un-managed forestry land
β_8	Square of average annual NPP (1995-1999) of the un-managed forestry land
β_9	Average annual NPP (1995-1999) of the un-managed grassland
β_{10}	Square of average annual NPP (1995-1999) of the un-managed grassland
β_{11}	Temperature in 2000
β_{12}	Square of temperature in 2000
β_{13}	Precipitation in 2000
β_{14}	Square of precipitation in 2000
β_{15}	Distance to the nearest city in 2000
α_0	Constant

Source: the author.

Taking the United States and China as two examples, in Tables 4.5 and 4.6, I show the regression results for the five types of agricultural land, while the regression results for the other 14 EPPA regions follow.

Table 4.5: Coefficients and t statistics for the land-use regression in the United States
Unit: NPP: kilogram carbon/m^2/year; Temperature: 100°C; Precipitation: 100 inches; Distance: 1,000 kilometers

Coefficient (t-statistics)	**Cropland**	**Managed Forestry Land**	**Pasture Land**	**Un-managed Forestry Land**	**Un-managed Grassland**
β_1	**0.7** (38.0)	**-0.1** (-14.7)	**0.1** (9.2)	**-0.7** (-12.2)	**0.1** (8.6)
β_2	**-0.4** (-20.4)	**0.1** (12.4)	-	**0.5** (8.8)	**-0.2** (-15.3)
β_3	**-0.2** (-4.2)	**1.6** (32.5)	**0.2** (9.3)	**-1** (-16.4)	**0.3** (18.6)
β_4	-	**-0.7** (-17.9)	**-0.4** (-11.6)	**0.8** (11.5)	**-0.4** (-15.2)
β_5	-	**-0.3** (-4.4)	**1.4** (17.5)	**-0.3** (-10.1)	**-0.4** (-2.8)
β_6	**0.2** (4.9)	**0.1** (3.4)	**-1.5** (-15.6)	**0.4** (9.8)	**0.5** (3.1)
β_7	**-0.1** (-2.2)	**0.1** (11.1)	**-0.1** (-6.4)	**1.4** (31.5)	**-0.2** (-16.9)
β_8	**0.1** (2.2)	**-0.1** (5.9)	**0.1** (3.3)	**-1.2** (-22.2)	**0.2** (11.3)
β_9	**0.4** (3.9)	**0.3** (7.6)	**-0.2** (-9.5)	**-0.9** (-11.4)	**1.4** (27.5)
β_{10}	**-0.3** (-5.3)	**-0.3** (-10.2)	**0.1** (8.4)	**0.5** (3.3)	**-0.8** (-16.4)
β_{11}	**-0.5** (-7.2)	-	**0.4** (8.2)	**3** (11.2)	**0.7** (13.3)
β_{12}	-	-	-	-11.2 (-8.4)	-1.6 (-13.7)
β_{13}	**0.2** (8.6)	-	**-0.1** (-5.3)	**-0.9** (-13.7)	**-0.2** (-8.1)
β_{14}	**-0.1** (-6.4)	**0.1** (9.0)	**0.1** (3.3)	**0.3** (9.4)	**0.1** (5.1)
β_{15}	**-0.2** (-5.8)	-	**0.1** (4.8)	**0.1** (4.85)	-
α_0	**0.1** (15.1)	**0.1** (12.8)	**0.1** (13.2)	**0.7** (21.5)	**0.2** (17.1)
Adjusted R^2	**0.87**	**0.85**	**0.77**	**0.69**	**0.81**
Number of observations	**4,796**	**4,796**	**4,796**	**4,796**	**4,796**

Note: All correlation indices shown are significant at the 95% level where the absolute value of t is larger than 2, while those not significant at the 95% level are indicated by "-".
Source: the author.

Table 4.6: Coefficients and t statistics for the land-use regression in China
Unit: NPP: kilogram carbon/m^2/year; Temperature: 100°C; Precipitation: 100 inches; Distance: 1,000 kilometers

Coefficient (t-statistics)	**Cropland**	**Managed Forestry Land**	**Pasture Land**	**Un-managed Forestry Land**	**Un-managed Grassland**
β_1	**0.4** (32.3)	**0.2** (4.7)	**0.1** (6.9)	**-0.1** (-11.5)	**-0.4** (-6.8)
β_2	**-0.2** (-21.8)	**-0.1** (-4.6)	**-0.1** (-11.9)	**0.1** (10.2)	**0.2** (2.9)
β_3	**0.2** (2.2)	**0.4** (24.5)	**0.9** (7.6)	-	**-0.2** (-3.2)
β_4	**-0.4** (-4.6)	**-0.4** (-29.4)	**-0.7** (-11.8)	-	**0.3** (5.3)
β_5	**0.9** (5.7)	**1.3** (5.8)	**-0.3** (30.6)	**-0.4** (-12.1)	**-1** (-7.8)
β_6	**-1** (-7.1)	**-1** (-3.5)	**0.2** (-28.4)	**0.5** (10.1)	**1** (6.7)
β_7	**-0.4** (-4.7)	**-0.2** (-6.5)	**0.2** (7.1)	**2.5** (23.2)	**-0.8** (-28.7)
β_8	**0.3** (4.8)	**0.2** (4.2)	**-0.2** (-11.1)	**-1.8** (-18.8)	**0.5** (12.3)
β_9	**-0.5** (-12.7)	**-0.2** (-5.9)	-	-	**1.2** (17.6)
β_{10}	**0.4** (11.6)	**0.1** (3.4)	**0.1** (4.6)	-	**-1** (-12.2)
β_{11}	-	**0.3** (5.7)	-	-	**4.1** (14.3)
β_{12}	**1.3** (7.4)	**-5** (-5.6)	**-1.2** (-12.4)	-	**-2.1** (-5.3)
β_{13}	**0.4** (11.3)	-	**0.1** (7.0)	**-0.2** (-15.7)	**-0.9** (-3.3)
β_{14}	**-0.3** (-14.9)	**0.1** (4.4)	**-0.1** (-7.1)	**0.1** (14.9)	**0.5** (2.6)
β_{15}	**-0.3** (-11.6)	**0.1** (2.9)	**0.1** (11.4)	**0.1** (5.3)	**0.1** (4.5)
α_0	**0.1** (19.1)	**0.1** (2.4)	**0.1** (22.6)	**0.1** (20.9)	**0.5** (4.8)
Adjusted R^2	**0.88**	**0.87**	**0.76**	**0.76**	**0.84**
Number of observations	**3,873**	**3,873**	**3,873**	**3,873**	**3,873**

Note: All correlation indices shown are significant at the 95% level where the absolute value of t is larger than 2, while those not significant at the 95% level are indicated by "-".
Source: the author.

The relationship between the share a land type and its NPP indicates an issue of relative suitability of land for agricultural production: in each grid cell, the share of each land type would sum to 1.0; therefore, all land uses cannot peak at the same location, and the share of a certain land type can be increasing over some parts of the NPP ranges and decreasing over the others. It is interesting that the share of each agricultural land type is also significantly correlated with the NPPs of other agricultural land types, negatively or positively. This indicates two opposite forces: a positive sign means that the soil has the fertility to feed different plants, while a negative one indicates that different agricultural land types are competing for limited land.

Human accessibility, indicated by the distance from the nearest city, also affects agricultural land use. Taking the un-managed forestry land as an example, its share is positively correlated with its distance from the nearest city, as indicated by $\boldsymbol{\beta}_{15}$. In other words, the farther a grid cell is from populated locations, the less it would be disturbed by human beings, and the larger area of it is likely to be un-managed forestry land. The impact of distance from cities on the cropland, however, is in the opposite direction. For the cropland share in both the United States and China, the coefficient of "Distance from the nearest city" ($\boldsymbol{\beta}_{15}$) is negative, indicating that the cropland tends to be developed closer to cities, and an important reason is that the cost savings on transporting crop products to urban markets would encourage farmers to develop more cropland close to cities.

Climate conditions, indicated by temperature and precipitation, also affect agricultural land use, as indicated by the coefficients of β_{11} through β_{14}. As stated in Chapter 2, the climate exerts its impact on agricultural land productivities, which could also affect agricultural land use, as indicated in the NPP coefficients of β_1 through β_{10}, while the coefficients of temperature and precipitation in the model indicate the additional climate impacts on agricultural land use.

As stated above, farmers' experience is indicated by the historical conditions of agricultural land productivities over the past several years. I run the regression described above using the annual average NPP for the past three years, five years, and ten years. It turns out that the regression based on the five-years-NPP average has a better fit than the others in terms of higher R^2. Therefore, I use the annual average NPP over the past five years in the regression.

In contrast with earlier years, the land-use regressions in more recent years show a similar trend of independent variables' coefficients as well as significance; therefore, I base the econometric analysis on the regression results in 2000, the most updated year in the Hurtt land-use dataset.

The possible correlations among the right-hand-side variables, especially those related to the linear and squared terms of NPP, would not threaten the reliability of the regression results. The correlations among the right-hand-side variables might increase the standard deviations of the coefficient estimates. However, in such an

Ordinary Least Square (OLS) regression, as long as the standard deviations of the coefficient estimates are not too inflated to threaten the significance of the estimates, the regression results would not be biased. In my empirical results as indicated in this section, despite the possible correlations among the independent variables, the coefficient estimates are generally significant. Therefore, the regressions I apply in this research still provide unbiased estimates.

In Tables 4.7 through 4.11, I present the coefficients and t-statistics of the land-use regressions for the other 14 EPPA regions of cropland, managed forestry land, pasture land, un-managed forestry land, and un-managed grassland.

Table 4.7: Regression coefficients and t-statistics of the cropland

Unit: NPP: kilogram carbon/m^2/year; Temperature: 100°C; Precipitation: 100 inches; Distance: 1000 kilometer

	EUR	AFR	EET	FSU	CAN	LAM	ANZ	IND	IDZ	ASI	JPN	MES	MEX	ROW
β_1	**0.31** (17.5)	**0.10** (22.8)	**0.24** (13.6)	**0.14** (21.4)	**0.48** (25.7)	**0.11** (22.4)	**0.37** (26.9)	**1.46** (24.6)	**0.07** (25.6)	**0.46** (28.3)	**0.53** (12.7)	**0.05** (17.4)	**0.11** (12.8)	**0.33** (15.5)
β_2	**-0.12** (-15.1)	**-0.02** (-16.5)	**-0.18** (-4.5)	-	**-0.36** (-16.8)	**-0.04** (-15.9)	**-0.11** (-17.8)	**-0.84** (-10.4)	-	**-0.13** (-10.5)	**-0.32** (-5.3)	**-0.11** (-10.5)	**-0.02** (-9.4)	**-0.13** (-10.6)
β_3	**0.81** (7.7)	**-0.03** (-13.6)	-	**0.07** (6.9)	**-0.14** (-8.9)	**0.13** (8.2)	**-0.32** (-6.6)	-	**0.05** (6.4)	-	-	**0.40** (4.2)	**-0.26** (-3.7)	**0.50** (8.3)
β_4	**-0.94** (-5.3)	**-0.04** (-12.5)	-	**-0.13** (-5.7)	**0.36** (4.2)	**-0.15** (-3.5)	**0.29** (3.4)	**-0.27** (-6.7)	-	-	-	-	-	**-0.37** (-7.8)
β_5	**0.56** (9.4)	**0.09** (7.2)	**-0.16** (-6.2)	**0.50** (11.6)	**2.26** (16.8)	**0.06** (13.3)	**0.06** (7.6)	**0.34** (6.3)	**0.18** (2.5)	-	-	-	**0.27** (7.2)	**-0.09** (-6.4)
β_6	**-0.74** (-8.8)	**-0.08** (-10.8)	-	**-0.26** (-10.3)	**-5.80** (-17.1)	**-0.03** (-12.4)	-	**-0.20** (-5.7)	**-0.28** (-3.2)	-	-	**0.56** (3.6)	**-0.14** (-3.3)	**0.80** (6.3)
β_7	**-0.20** (-5.1)	-	**-0.21** (-6.8)	**-0.25** (-3.9)	**-0.14** (-6.8)	**-0.12** (-9.8)	**-0.04** (-7.8)	**-0.22** (-4.3)	-	**-0.20** (-3.9)	-	**-0.24** (-3.5)	**-0.26** (-4.3)	**-0.22** (-5.6)
β_8	**-0.13** (-3.5)	**-0.03** (-8.7)	**0.17** (5.1)	**0.47** (4.2)	**0.33** (9.2)	**0.06** (5.4)	-	-	-	-	-	-	**0.34** (6.1)	-
β_9	**0.22** (3.9)	-	-	**1.38** (5.8)	**1.01** (7.6)	-	**-0.09** (-6.7)	-	-	**-0.26** (-4.6)	-	**0.30** (4.6)	**-0.70** (-2.4)	**0.12** (4.3)
β_{10}	**-0.15** (-2.7)	**-0.22** (-7.1)	-	**-2.44** (-6.2)	**-0.76** (-4.8)	**-0.03** (-8.5)	-	-	-	-	-	**-1.26** (-3.7)	**1.04** (3.5)	**-0.11** (-3.2)
β_{11}	**0.70** (3.4)	**-1.01** (-4.9)	-	**0.66** (8.6)	**0.33** (7.1)	**1.16** (12.7)	-	**1.06** (4.8)	-	-	-	**-1.80** (-10.1)	-	**0.32** (7.8)
β_{12}	-	**1.50** (5.2)	**1.44** (2.6)	**0.79** (11.7)	**1.20** (4.5)	**-3.90** (-9.8)	-	-	-	**2.10** (4.4)	-	**3.60** (8.7)	-	**1.80** (9.6)
β_{13}	**-0.06** (-4.7)	**0.06** (18.1)	**-1.57** (-2.5)	**1.26** (8.9)	**-0.06** (-13.3)	**0.05** (28.2)	**-0.07** (-5.4)	-	**-0.15** (-3.8)	**0.39** (5.9)	-	**0.21** (4.8)	-	**0.11** (15.5)
β_{14}	-	**-0.04** (-19.1)	**0.75** (2.3)	**-1.10** (-5.8)	**0.01** (9.6)	**-0.01** (-13.8)	**0.03** (5.3)	-	**0.02** (3.2)	**-0.10** (-3.4)	-	**-0.35** (-4.6)	-	**-0.03** (-8.7)
β_{15}	-	**-0.07** (-12.5)	-	**-0.06** (-4.2)	**-0.03** (-3.2)	**-0.01** (12.0)	**-0.07** (-2.5)	**-0.66** (-8.6)	**-0.97** (-5.3)	**-0.68** (-5.5)	-	**-0.23** (-2.9)	-	**-0.02** (-2.3)
α_0	**0.01** (3.6)	**0.17** (5.1)	**0.38** (2.2)	**-0.26** (5.4)	**0.06** (12.5)	**-0.04** (-23.2)	**0.06** (-5.6)	**-0.01** (-9.0)	**0.36** (3.8)	**-0.19** (-5.7)	**0.01** (6.1)	**0.23** (11.9)	**0.04** (6.4)	**-0.04** (23.9)
Adjusted R^2	0.88	0.75	0.81	0.85	0.86	0.83	0.83	0.84	0.83	0.82	0.75	0.81	0.85	0.74
Number of observations	2,677	10,641	456	14,770	7,243	6,858	3,210	1,182	923	602	253	1,997	802	4,657

Note: 1. Details of the regional composition are provided in Table 3.1.

2. All the showed correlation indexes are significant at 95% level, while those not significant at 95% are indicated by "-".

Source: the author.

Table 4.8: Regression coefficients and t-statistics of the managed forestry land

Unit: NPP: kilogram carbon/m^2/year; Temperature: 100°C; Precipitation: 100 inches; Distance: 1000 kilometer

	EUR	AFR	EET	FSU	CAN	LAM	ANZ	IND	IDZ	ASI	JPN	MES	MEX	ROW
β_1	**0.06**	**-0.02**	-	**0.01**	**0.05**	**0.03**	**0.04**	**0.06**	**0.02**	**0.04**	-	-	-	**-0.02**
	(11.1)	(-5.7)		(10.2)	(9.7)	(4.9)	(7.7)	(4.2)	(12.4)	(4.8)				(-4.5)
β_2	**-0.09**	**0.01**	-	**-0.09**	**-0.07**	-	-	-	**-0.01**	**-0.02**	-	-	-	-
	(-7.3)	(4.4)		(-11.8)	(-9.5)				(-7.1)	(-5.1)				
β_3	**1.66**	**2.02**	**0.86**	**1.04**	**1.17**	**1.07**	**1.39**	**0.56**	**0.01**	-	**0.01**	**2.23**	**1.25**	**0.85**
	(17.8)	(24.5)	(15.6)	(26.1)	(23.9)	(15.4)	(19.6)	(13.6)	(21.3)		(10.9)	(15.7)	(20.1)	(12.3)
β_4	**-1.38**	**-1.89**	**-0.72**	**-0.86**	**-0.99**	**-0.88**	**-0.92**	**-0.28**	-	**0.52**	**-1.88**	**-0.01**	**-0.63**	**-0.74**
	(-13.6)	(-28.6)	(-10.7)	(-14.9)	(-27.3)	(-11.9)	(-19.1)	(-11.9)		(19.6)	(-8.9)	(-8.9)	(-11.2)	(-7.4)
β_5	**-0.29**	-	**-0.52**	**-0.05**	**-0.36**	**0.08**	**-0.43**	**-0.13**	-	-	-	**-0.22**	**0.20**	**0.06**
	(-3.7)		(-6.4)	(-5.6)	(-5.2)	(6.4)	(-8.1)	(-7.8)				(-5.1)	(8.9)	(5.1)
β_6	-	**-0.15**	**0.63**	-	**1.00**	**-0.08**	**0.37**	-	-	**0.08**	**2.73**	-	**-0.46**	**-0.17**
		(-15.0)	(7.2)		(2.9)	(-9.5)	(5.4)			(3.5)	(2.9)		(-7.1)	(-4.6)
β_7	**-0.09**	**-0.11**	**0.33**	**0.02**	**-0.07**	**-0.12**	**-0.28**	**-0.09**	**-0.32**	**0.06**	-	**-0.11**	-	-
	(-9.5)	(-23.5)	(6.9)	(13.5)	(-10.5)	(-17.2)	(-9.6)	(-4.3)	(-7.3)	(4.1)		(-3.9)		
β_8	**0.11**	-	**-0.48**	**-0.15**	**0.04**	**0.05**	**0.27**	-	**0.13**	**-0.08**	-	-	-	**-0.04**
	(7.7)		(-5.8)	(-14.1)	(6.2)	(10.6)	(7.2)		(5.9)	(-2.8)				(-5.1)
β_9	**0.17**	**-0.31**	-	**-0.08**	-	**-0.15**	**-0.19**	**-0.44**	-	**-0.16**	-	-	**-0.50**	**-0.06**
	(5.0)	(-5.2)		(-6.5)		(-8.9)	(-5.5)	(-2.9)		(-4.4)			(-5.7)	(-3.8)
β_{10}	-	**0.44**	-	**0.30**	-	**0.07**	**0.52**	**0.52**	-	**0.13**	-	**0.35**	**1.14**	**0.06**
		(8.9)		(4.3)		(6.6)	(4.6)	(3.2)		(2.3)		(2.7)	(8.3)	(3.2)
β_{11}	**-0.33**	**-4.38**	**-1.05**	**0.03**	-	**0.82**	**-2.33**	**-1.21**	-	-	-	-	-	**0.08**
	(-3.9)	(-14.2)	(-5.4)	(2.5)		(6.8)	(-3.5)	(-4.9)						(8.9)
β_{12}	-	**9.30**	**5.14**	**-0.40**	-	**-2.10**	**7.90**	**3.60**	-	-	-	-	-	**-0.09**
		(13.4)	(9.7)	(-4.9)		(-4.9)	(5.4)	(4.8)						(-8.4)
β_{13}	-	**0.02**	**1.32**	**-0.06**	**0.04**	-	-	**0.10**	**-0.02**	**0.06**	-	-	-	**-0.01**
		(3.5)	(4.8)	(-7.8)	(6.6)			(5.0)	(-2.9)	(4.9)				(-10.5)
β_{14}	-	-	**-0.70**	**0.02**	**0.01**	**-0.01**	**-0.04**	**-0.03**	-	**-0.02**	-	-	-	-
			(-4.1)	(5.2)	(3.7)	(-6.2)	(-3.3)	(-4.7)		(-5.2)				
β_{15}	**-0.06**	**-0.08**	-	**0.01**	**-0.01**	**-0.16**	-	-	**-0.26**	**-0.10**	**-0.24**	-	**-1.66**	-
	(-3.3)	(-9.7)		(2.3)	(-2.5)	(-6.9)			(-6.3)	(-6.0)	(-3.8)		(-3.6)	
α_0	**0.05**	**0.57**	**0.09**	**0.02**	**-0.01**	**-0.01**	**0.19**	**0.05**	**0.28**	**-0.02**	**0.04**	**0.02**	**0.21**	**0.02**
	(11.2)	(16.6)	(11.7)	(10.6)	(-4.6)	(-3.7)	(13.2)	(5.5)	(8.4)	(-3.4)	(12.7)	(7.6)	(12.9)	(14.6)
Adjusted R^2	0.82	0.66	0.86	0.80	0.79	0.77	0.79	0.67	0.81	0.81	0.84	0.61	0.88	0.68
Number of observations	2,677	10,641	456	14,770	7,243	6,858	3,210	1,182	923	602	253	1,997	802	4,657

Note: 1. Details of the regional composition are provided in Table 3.1.

2. All the showed correlation indexes are significant at 95% level, while those not significant at 95% are indicated by "-".

Source: the author.

Table 4.9: Regression coefficients and t-statistics of the pasture land

Unit: NPP: kilogram carbon/m^2/year; Temperature: 100°C; Precipitation: 100 inches; Distance: 1000 kilometer

	EUR	AFR	EET	FSU	CAN	LAM	ANZ	IND	IDZ	ASI	JPN	MES	MEX	ROW
β_1	**0.04** (3.2)	-	-	**0.12** (11.8)	**0.14** (18.7)	**0.11** (3.5)	**-0.27** (-12.9)	-	-	-	-	**-0.23** (-3.1)	**0.07** (10.8)	**0.23** (11.1)
β_2	-	**-0.02** (-9.9)	-	**-0.17** (-12.3)	**-0.17** (-17.6)	**-0.05** (-2.9)	**0.12** (9.1)	-	-	-	-	-	-	**-0.08** (-12.0)
β_3	-	**-0.30** (-13.3)	-	**-0.14** (-7.9)	**-0.01** (-5.1)	**-0.19** (-10.8)	**0.69** (2.8)	**0.15** (2.6)	**0.18** (3.8)	-	-	**-2.55** (-5.2)	**-0.27** (-9.4)	**-0.80** (-8.6)
β_4	**-0.17** (-4.9)	**0.29** (9.4)	-	**0.28** (8.6)	-	**0.13** (9.2)	**-1.55** (-1.6)	**-0.20** (-2.0)	**-0.19** (-4.1)	**-0.02** (-6.5)	-	**8.66** (3.9)	-	**0.91** (6.3)
β_5	**1.29** (13.2)	**2.06** (18.6)	**1.21** (17.0)	**3.30** (25.2)	**2.76** (26.3)	**1.17** (22.7)	**2.87** (22.2)	**0.36** (22.4)	**0.51** (19.2)	-	**1.87** (20.6)	**6.14** (18.1)	**1.56** (16.7)	**3.63** (16.4)
β_6	**-1.21** (-11.6)	**-1.80** (-15.7)	**-1.61** (-10.8)	**-6.08** (-24.9)	**-6.42** (-17.4)	**-0.61** (-16.6)	**-2.90** (-11.4)	**-0.10** (-13.7)	**-0.25** (-13.5)	**0.09** (15.8)	**-2.09** (-12.1)	**-12.20** (-15.8)	**-1.31** (-7.9)	**-5.80** (-14.8)
β_7	**-0.15** (-5.3)	**-0.13** (-13.8)	-	**-0.28** (-7.2)	-	**-0.08** (-9.6)	**-1.29** (-9.2)	**0.05** (7.5)	-	-	-	**-1.51** (-3.8)	**-0.25** (-5.6)	**-0.33** (-8.4)
β_8	**0.09** (3.9)	**0.08** (10.1)	-	**0.19** (5.1)	-	**0.04** (8.5)	**1.16** (7.4)	**-0.04** (-6.9)	-	-	-	**3.88** (5.2)	**0.15** (4.9)	**0.37** (8.6)
β_9	**-0.06** (-4.4)	**0.21** (11.8)	-	**-0.81** (-7.4)	**-0.08** (-8.5)	**-0.23** (-12.8)	**0.27** (10.4)	-	-	-	-	**-2.47** (-4.5)	-	**-0.32** (-8.1)
β_{10}	-	**-0.77** (-16.3)	-	**1.06** (8.9)	-	**0.10** (9.1)	**-1.63** (-7.3)	-	-	-	-	**6.83** (6.5)	-	**0.32** (7.8)
β_{11}	**0.41** (6.6)	**-0.73** (-3.5)	-	**0.45** (6.9)	-	**0.79** (4.5)	**0.09** (5.5)	-	-	-	-	-	**7.93** (6.2)	**-0.35** (-7.6)
β_{12}	**-1.50** (-5.7)	**1.68** (5.1)	-	**-2.60** (-11.7)	-	**-1.90** (-5.0)	**-2.32** (-8.3)	-	-	-	-	-	**-0.19** (-3.7)	**-0.01** (-7.2)
β_{13}	**0.19** (4.9)	**0.09** (18.8)	-	**-0.01** (-4.9)	-	**-0.08** (-4.8)	**0.01** (2.3)	**-0.09** (-3.2)	-	**-0.01** (-2.9)	-	**0.83** (7.6)	-	**-0.14** (-10.9)
β_{14}	**-0.06** (-3.9)	**-0.08** (-19.4)	-	**0.68** (11.2)	-	**0.02** (5.1)	**-0.38** (-4.8)	**0.05** (4.5)	-	**0.01** (3.7)	-	**-1.20** (-9.2)	-	**0.03** (9.9)
β_{15}	**0.11** (4.4)	**-0.25** (-7.1)	-	**-0.02** (-4.3)	-	-	-	**0.05** (2.5)	**0.20** (3.3)	-	-	**0.87** (3.2)	**0.45** (6.3)	**-0.11** (-4.7)
α_0	**-0.09** (-4.0)	**0.09** (5.1)	**0.01** (7.6)	**0.33** (23.3)	**0.01** (4.8)	**0.04** (7.5)	**-0.04** (-3.8)	**0.02** (4.4)	**-0.02** (-3.2)	**0.01** (4.6)	**0.01** (2.5)	**0.06** (3.5)	**-0.07** (-11.2)	**0.18** (22.4)
Adjusted R^2	0.78	0.74	0.91	0.88	0.84	0.87	0.81	0.86	0.87	0.80	0.85	0.73	0.81	0.82
Number of observations	2,677	10,641	456	14,770	7,243	6,858	3,210	1,182	923	602	253	1,997	802	4,657

Note: 1. Details of the regional composition are provided in Table 3.1.

2. All the showed correlation indexes are significant at 95% level, while those not significant at 95% are indicated by "-".

Source: the author.

Table 4.10: Regression coefficients and t-statistics of the un-managed forestry land

Unit: NPP: kilogram carbon/m^2/year; Temperature: 100°C; Precipitation: 100 inches; Distance: 1000 kilometer

	EUR	AFR	EET	FSU	CAN	LAM	ANZ	IND	IDZ	ASI	JPN	MES	MEX	ROW
β_1	**-0.35** (-13.6)	**-0.24** (-9.2)	-	**-0.16** (-11.3)	**-0.69** (-13.9)	**-0.38** (-17.1)	**-0.24** (-6.4)	**-0.91** (-21.0)	**-0.12** (-17.8)	**-0.56** (-11.6)	**-0.76** (-8.0)	**-0.43** (-7.1)	**-0.47** (-6.1)	**-0.07** (-15.8)
β_2	**0.18** (6.8)	**0.05** (5.7)	-	-	**0.50** (6.9)	**0.11** (10.6)	-	**0.47** (11.8)	-	**0.16** (10.9)	**0.48** (4.3)	**0.61** (5.6)	**0.09** (5.0)	**0.02** (12.2)
β_3	**-0.96** (-7.9)	**-0.45** (-12.4)	-	**1.22** (7.4)	**0.98** (11.8)	**-0.21** (-8.8)	**-1.61** (-19.2)	**-0.37** (-12.4)	**0.63** (5.8)	**0.25** (5.5)	**-0.48** (-12.5)	**2.17** (6.3)	-	**-0.25** (-6.5)
β_4	**0.71** (3.1)	**0.68** (8.2)	-	**-1.58** (-13.6)	**-0.19** (-8.5)	**0.29** (5.6)	**1.98** (12.6)	**0.43** (8.3)	**-1.08** (-9.5)	**-0.63** (-2.7)	**0.51** (11.8)	**-2.05** (-5.0)	-	-
β_5	**-0.32** (-6.1)	**-0.71** (-18.6)	-	**-2.09** (-4.6)	**-2.42** (-5.3)	**-0.98** (-16.2)	**-1.93** (-14.1)	**-0.36** (-4.6)	**-0.67** (-3.9)	-	-	**-1.37** (-5.4)	**-1.29** (-9.2)	**-0.55** (-13.9)
β_6	-	**0.48** (12.1)	-	**3.73** (13.2)	**7.72** (3.9)	**0.63** (12.1)	**2.08** (16.9)	-	**0.49** (2.7)	**-0.50** (-2.7)	**-1.51** (-7.7)	**2.34** (4.9)	**1.18** (8.6)	-
β_7	**1.13** (22.2)	**0.63** (28.1)	-	**2.66** (24.2)	**3.26** (30.4)	**0.55** (22.3)	**1.66** (18.6)	**0.84** (18.5)	**0.59** (17.2)	**0.75** (19.3)	**1.63** (8.6)	**4.43** (14.6)	**0.62** (11.8)	**1.20** (17.7)
β_8	**-0.88** (-14.9)	**-0.20** (-11.2)	**0.24** (19.2)	**-3.24** (-25.8)	**-4.24** (-23.8)	**-0.28** (-13.8)	**-1.46** (-16.9)	**-0.39** (-8.3)	-	**-0.28** (-15.4)	**-1.16** (-5.5)	**-1.63** (-8.1)	**-0.43** (-7.6)	**-0.62** (-8.9)
β_9	**-1.20** (-12.9)	**-0.21** (-7.7)	-	**0.85** (6.3)	**1.82** (7.4)	**-0.10** (-8.2)	**-1.11** (-12.7)	**-0.22** (-6.1)	-	-	-	**-2.23** (-5.6)	**-1.17** (-6.5)	**-0.63** (-4.5)
β_{10}	**0.37** (7.5)	-	-	**-2.20** (-8.8)	**-4.54** (-6.5)	**-0.05** (-4.8)	**1.36** (14.5)	-	-	**-0.41** (-8.8)	-	**4.45** (4.9)	**1.32** (5.3)	**0.22** (5.1)
β_{11}	**2.10** (19.2)	**-6.65** (-14.3)	-	**-0.77** (-9.5)	**1.20** (14.8)	**1.04** (10.6)	-	**1.33** (9.4)	**2.81** (5.9)	-	-	**-4.88** (-6.3)	-	**0.69** (19.7)
β_{12}	-	**13.40** (13.9)	-	**-2.10** (-12.4)	**3.20** (6.0)	**-1.90** (-11.2)	-	**-4.50** (-9.2)	**-6.98** (-6.1)	-	-	**10.70** (7.2)	-	-
β_{13}	-	**0.52** (6.8)	-	**-1.56** (-17.3)	**0.01** (7.7)	**0.09** (3.9)	**-6.13** (-4.4)	**0.18** (4.0)	-	**-0.48** (-5.5)	-	**1.34** (3.8)	-	**-0.06** (-3.3)
β_{14}	**0.04** (5.9)	**-0.23** (-7.9)	-	**1.30** (12.7)	-	**-0.02** (-3.0)	**0.32** (2.9)	**-0.06** (-3.5)	-	**0.12** (4.0)	-	**-2.20** (-4.2)	-	**0.02** (2.9)
β_{15}	**0.35** (4.6)	**0.10** (12.7)	-	**0.09** (14.8)	**0.02** (5.8)	**0.59** (10.0)	-	**1.06** (5.3)	**1.24** (3.5)	**1.02** (3.6)	**0.48** (4.7)	-	**0.90** (7.4)	-
α_0	**0.22** (11.5)	**0.04** (16.8)	**0.01** (3.3)	**0.62** (25.2)	**0.01** (24.7)	**0.32** (40.8)	**0.82** (37.1)	**0.20** (3.8)	**-0.52** (-5.2)	**0.88** (42.8)	**0.39** (19.5)	**0.69** (5.9)	**0.61** (3.5)	**0.15** (26.9)
Adjusted R^2	0.66	0.65	0.78	0.75	0.82	0.76	0.80	0.77	0.69	0.87	0.73	0.66	0.78	0.76
Number of observations	2,677	10,641	456	14,770	7,243	6,858	3,210	1,182	923	602	253	1,997	802	4,657

Note: 1. Details of the regional composition are provided in Table 3.1.

2. All the showed correlation indexes are significant at 95% level, while those not significant at 95% are indicated by "-".

Source: the author.

Table 4.11: Regression coefficients and t-statistics of the un-managed grassland

Unit: NPP: kilogram carbon/m^2/year; Temperature: 100°C; Precipitation: 100 inches; Distance: 1000 kilometer

	EUR	AFR	EET	FSU	CAN	LAM	ANZ	IND	IDZ	ASI	MES	MEX	ROW
β_1	-0.01	-	-	-	-	0.03	0.07	-0.16	-	-0.03	-	-	-0.06
	(-10.1)					(5.5)	(2.6)	(-2.1)		(-4.4)			(-13.5)
β_2	0.04	-	0.02	-0.01	-	-0.01	-	0.10	-	0.01	0.20	-	-
	(4.7)		(8.5)	(-6.8)		(-3.8)		(2.0)		(3.0)	(8.1)		
β_3	0.14	-	-	-	-	-0.01	0.44	-	-	0.09	-	-	0.05
	(6.8)					(-6.9)	(4.4)			(2.9)			(8.4)
β_4	-0.13	-	-	-	0.03	-	-0.43	-	-	-0.12	-	-	-
	(-5.7)				(19.5)		(-3.8)			(-4.1)			
β_5	-0.32	-0.54	-0.18	-0.30	-0.64	-0.15	-0.69	-0.04	-	-	-1.98	-0.28	-0.50
	(-6.9)	(-16.2)	(-5.4)	(-3.3)	(-16.8)	(-6.3)	(-10.8)	(-3.7)			(-5.8)	(-4.4)	(-9.8)
β_6	0.43	0.52	0.35	0.34	-	-	0.60	-	-	-	3.88	0.27	0.59
	(6.5)	(10.6)	(4.1)	(4.1)			(7.1)				(2.9)	(3.6)	(11.7)
β_7	0.05	0.14	-	-	-0.24	0.10	-	-	-	-	1.23	0.03	0.06
	(6.1)	(8.6)			(-10.1)	(4.1)					(4.3)	(4.8)	(8.4)
β_8	-0.13	-0.17	-	-	-	-0.07	-	-	-	-	-1.67	-	0.08
	(-7.3)	(-9.3)				(-5.3)					(-5.0)		(9.2)
β_9	1.55	1.62	2.73	0.88	2.10	0.69	1.88	2.49	1.29	0.99	5.88	3.33	1.81
	(13.4)	(19.5)	(11.8)	(25.1)	(47.4)	(16.7)	(17.4)	(13.4)	(16.2)	(12.8)	(10.5)	(13.3)	(19.5)
β_{10}	-0.66	-1.23	-6.01	-0.70	-3.39	-0.18	-1.57	-4.04	-0.59	-0.22	-1.33	-4.69	-1.04
	(-11.3)	(-11.2)	(-6.7)	(-17.2)	(-35.6)	(-9.8)	(-10.3)	(-18.4)	(-11.7)	(-7.3)	(-8.7)	(-8.2)	(-12.9)
β_{11}	0.21	0.01	0.02	0.01	0.01	0.01	-0.04	-3.15	-	-	7.43	-	0.14
	(13.8)	(6.4)	(2.4)	(4.2)	(7.3)	(5.2)	(-6.1)	(-13.4)			(5.6)		(8.3)
β_{12}	1.30	-	-1.80	-0.39	0.64	-0.04	0.09	7.40	-	-	-18.50	-	-0.88
	(11.6)		(-2.8)	(-5.6)	(6.5)	(-4.3)	(6.0)	(10.5)			(-6.2)		(-6.2)
β_{13}	-	0.05	-	-	-0.01	-	-0.24	-	-	0.01	-0.41	-	-0.17
		(10.1)			(-5.3)		(-3.2)			(2.8)	(-9.2)		(-14.6)
β_{14}	-	-0.02	-0.04	-	-	-	0.12	-	-	-	0.63	-	0.03
		(-8.3)	(-3.3)				(2.5)				(8.7)		(10.4)
β_{15}	-	0.07	-	0.01	-	-	0.13	0.40	-	-	0.30	-	-
		(14.1)		(5.2)			(7.4)	(2.8)			(6.4)		
α_0	0.01	0.01	0.06	0.04	0.02	-0.07	0.53	0.33	0.01	-0.01	-0.06	0.02	0.15
	(3.9)	(7.5)	(9.8)	(9.1)	(6.7)	(-12.5)	(6.8)	(12.3)	(9.5)	(-2.2)	(-2.9)	(3.7)	(28.1)
Adjusted R^2	0.73	0.81	0.75	0.84	0.77	0.80	0.87	0.76	0.80	0.83	0.87	0.73	0.73
Number of observations	2,677	10,641	456	14,770	7,243	6,858	3,210	1,182	923	602	1,997	802	4,657

Note: 1. Details of the regional composition are provided in Table 3.1.

2. All the showed correlation indexes are significant at 95% level, while those not significant at 95% are indicated by "-".

Source: the author.

Based on the projections of temperature and precipitation from the IGSM (2001-2100), the simulations of NPP from the TEM (2001-2100), I apply the econometric land-use model to project the gridded share of the five types of agricultural land in each EPPA region from 2001 to 2100.

Before I use the projected gridded land use in the downscaling methods as described in the next section, I need to satisfy two requirements:

1) $0 \leq \text{Share}_{i,j,t} \leq 1$

It indicates that the share of any land type in a grid cell cannot be negative or larger than 1. Based on this requirement, I set the negative land shares predicted by the econometric land-use model to 0, and such grid cells represent around 10 - 12% of all grid cells globally. In addition, I set the shares predicted by the econometric model as more than 1 to 1, and such grid cells represent around 7 - 10% of all grid cells globally.

2) $\sum_{j=1}^{6} \text{Share}_{i,j,t} = 1$

It indicates that the shares of all land types, including the five types of agricultural land and the "other land", in a grid cell should sum to 1. According to the econometric land-use model, when the factors affecting land-use decisions change in the future, the gridded share of each of the five types of agricultural land would also change; the share of "other land", as I stated before, is assumed to be constant during the 21^{st} century. I adjust their total to 100% according to the proportions among the five types of agricultural land.

I use an example to clarify these two requirements: suppose that in 2000, the five types of agricultural land used all the land in a grid cell. If the econometric land-use model predicts that in 2100, the share of cropland, managed forestry land, pasture land, un-managed forestry land, and un-managed grassland in this grid cell would be 101%, 10%, 10%, -3%, and 5%, respectively. According to the first requirement, I adjust their shares to 100%, 10%, 10%, 0%, and 5%. However, the sum of them would be 125%, and the second requirement is not satisfied. I conduct the following calculations to get the adjusted shares of each land category:

Cropland share = (100%/125%) * 100% = 80%

Managed forestry land share = (10%/125%) * 100% = 8%

Pasture land share = (10%/125%) * 100% = 8%

Un-managed forestry land share = (0%/125%) * 100% = 0%

Un-managed grassland share = (5%/125%) * 100% = 4%

Then, the sum of them would be 100%, and therefore, the second requirement is satisfied. The projected gridded land use of each of the five types of agricultural land after such adjustments, as well as the regional land use driven by economic forces as projected by the EPPA model, is an important input for the downscaling methods, which are described in the next section.

4.4. Downscaling methods based on the econometric land-use model

Applying the econometric land-use model described in Section 4.3, I project the gridded land use of the five types of agricultural land in each EPPA region from 2001 to 2100, and also aggregate such data to the regional scale, indicated by $Share^{climate}_{j,t}$, which is the aggregated regional share of land type **j** in the year **t** in each region affected by the climate, GHGs, and tropospheric ozone. I use such data as the aggregated "prior" indices for land use affected by the climate, GHGs, and tropospheric ozone. As stated in Section 3.1, we apply the EPPA model to project the regional land-use effects of economic forces, indicated by $Share^{economy}_{j,t}$, the share of land type **j** in the year **t** in each region affected by economic forces. The historical land-use data in 2000, the starting year for both the econometric land-use model and the EPPA model, are given by the Hurtt land-use dataset (Hurtt et al., 2006); therefore, $Share^{climate}_{j,2000}$ is equal to $Share^{economy}_{j,2000}$, while these two figures after 2000 are projected by the econometric land-use model and the EPPA model, respectively.

For land type **j** in the year **t**, if $Share^{economy}_{j,t} \neq Share^{climate}_{j,t}$, it means that the aggregated regional share of this land type affected by economic forces is not equal to that affected by climate, GHGs, and tropospheric ozone. Taking China's cropland as an example, its share in China's total land area in 2000 was 22%. If the GHG-mitigation policies specified in this research were implemented, in 2100, China's

$Share^{economy}_{cropland, 2100}$ would be 42% as projected by the EPPA model, while its $Share^{climate}_{cropland, 2100}$ would be only 25% as predicted by the econometric land-use model after aggregation. This suggests that the factors affecting the land-use decision of cropland owners, including the feedbacks of climate, GHGs, and tropospheric ozone, would favor the development of China's cropland, increasing the regional cropland share in China from 22% in 2000 to 25% in 2100. However, considering that China's cropland productivity would overall decrease mainly because of the ozone damage, such an increase from 22% to 25% in cropland share would not be enough to satisfy the demand for crop products. According to the EPPA model, affected by economic drivers, China would need 42% of its total land to develop crops in 2100 with GHG-mitigation policies implemented. Therefore, I need to implement an adjustment to fix this discrepancy of each of the five agricultural land types in each EPPA region in each year. I define an adjustment ratio as below:

$$\alpha_{j, t, adjustment} = Share^{economy}_{j, t} / Share^{climate}_{j, t} \qquad (4\text{-}1)$$

In the case of China's cropland in the policy scenario in 2100, the adjustment ratio $\alpha_{cropland, 2100, adjustment}$ is 42%/25% = 1.67.

Then, I apply this adjustment ratio to each grid cell, and get:

$$Share^{1st\ adjusted}_{i, j, t} = Share^{climate}_{i, j, t} * \alpha_{j, t, adjustment} \qquad (4\text{-}2)$$

where $\text{Share}^{\text{1st adjusted}}_{i,\,j,\,t}$ indicates the land share of category **j** in year **t** in grid cell **i** after the first adjustment.

For example, if the cropland share in a grid cell in China in 2100 was 30% as predicted by the econometric land-use model, after the first adjustment, it would be 30% * 1.67 = 50%.

Then, I sum the $\text{Share}^{\text{1st adjusted}}_{i,\,j,\,t}$ of all land types in each grid cell, and get $\text{Share}^{\text{1st adjusted}}_{i,\,t}$, indicating the sum of shares of all land types in the year **t** in grid cell **i** after the first adjustment. To make sure that the gridded shares for all land types sum to 100%, I do the second adjustment based on the proportion among different land types:

$$\text{Share}^{\text{2nd adjusted}}_{i,\,j,\,t} = \text{Share}^{\text{1st adjusted}}_{i,\,j,\,t} * 100\% / \text{Share}^{\text{1st adjusted}}_{i,\,t} \qquad (4\text{-}3)$$

where $\text{Share}^{\text{2nd adjusted}}_{i,\,j,\,t}$ indicates the share of land type **j** in the year **t** in grid cell **i** after the second adjustment.

Taking a grid cell in China as an example again, I suppose that the five types of agricultural land used all the land in this grid cell in 2000. Supposing that after the first adjustment, the share of cropland in this grid cell in 2100 was 50%, and the shares of managed forestry land, pasture land, un-managed forestry land, and un-managed grassland would be 20%, 10%, 20%, and 10%, respectively. The sum of them, $Share^{1st\ adjusted}_{i,2100}$, would be 110%. According to equation (4-3), the shares of each land type after the second adjustment would be:

Cropland: 50% * 100% / 110% = 45.4%

Managed forestry land: 20% *100%/110% = 18.2%

Pasture land: 10% * 100% / 110% = 9.1%

Un-managed forestry land: 20% * 100% / 110% = 18.2%

Un-managed grassland: 10% * 100% / 110% = 9.1%

Now, after the second adjustment, the sum of all land shares in this grid cell is 100%.

I conduct the calculations described in equations (4-1) through (4-3) until the aggregated regional level based on gridded land use equals the regional land share projected by the EPPA model, and I conduct such work for each of the five types of agricultural land in each EPPA region for 2005, 2010... 2100.

However, since there is very little land developed to biomass-energy production historically, I do not include biomass land in the econometric model. Therefore, the gridded "prior" for the five types of agricultural land obtained from the econometric model is missing for the land devoted to biomass-energy production. Before applying the downscaling methods described in equations (4-1) through (4-3), I need to find the gridded "prior" for the land devoted to biomass-energy production. As stated before, considering that biomass typically occurs on cropland, I assume that biomass-energy production would only occur in grid cells with the existence of enough cropland. Based on this assumption, in those regions projected by the EPPA model to produce biomass energy, I assign the regional share of land devoted to biomass-energy production as the biomass "prior" of those grid cells where the cropland share is no less than 5% of total gridded land. I aggregate the gridded biomass "prior" to the regional scale, and use such data as the $\text{Share}^{\text{climate}}_{\text{biomass, t}}$. Then, I follow the downscaling methods described in equations (4-1) through (4-3) to distribute the regional land projected by the EPPA model, including the five types of agricultural land and the land devoted to biomass-energy production, to grid cells in 2005, 2010...2100.

In summary, applying the downscaling methods based on the econometric land-use model, in both the baseline and GHG-mitigation policy scenarios, I distribute the regional land use driven by economic forces to grid cells, and such distributions are based on gridded land-use projections affected by climate, GHGs, and tropospheric ozone. Therefore, I am making a fairly comprehensive assessment of land-use effects in response to the policies on GHG mitigation by including both the impacts of economic forces and the feedbacks of climate, GHGs, and tropospheric ozone.

Chapter 5
Results and Analysis

In this chapter, based on the models and approaches described in Chapter 3, and the econometric land-use model and downscaling methods described in Chapter 4, I present the impacts of GHG-mitigation policies on the five types of agricultural land, namely, cropland, managed forestry land, pasture land, un-managed forestry land, and un-managed grassland, as well as the biomass-energy production and the resultant land-use effects.

To identify the impacts of economic forces with the feedbacks of climate, GHGs, and tropospheric ozone, we apply the models and techniques in two rounds: in the first round discussed in Section 5.1, only the land-use effects of economic forces in response to GHG-mitigation policies are considered; while in the second round discussed in Section 5.2, the feedbacks of climate, GHGs, and tropospheric ozone caused by the GHG-mitigation policies are also included. As I stated in Chapter 1, my most distinctive contribution is that, by applying the downscaling methods, I am able to also include the feedbacks of climate, GHGs, and tropospheric ozone in the land-use effects. To highlight the distinctive findings of my research, in addition to introducing the results of round two in Section 5.2, I emphasize the differences of the two rounds in terms of land use, land rent, and carbon stored in the five types of agricultural land.

5.1. Impacts of GHG-mitigation policies on agricultural land (round one)

As just stated, only the impacts driven by economic forces in response to the GHG-mitigation policies are considered in this round. Therefore, based on the econometric land-use model described in Chapter 4, the gridded land use for each of the five types of agricultural land affected by climate, GHGs, and tropospheric ozone would keep constant at the year 2000 level. In other words, the gridded land use in 2000 is taken as the "prior" in the downscaling methods.

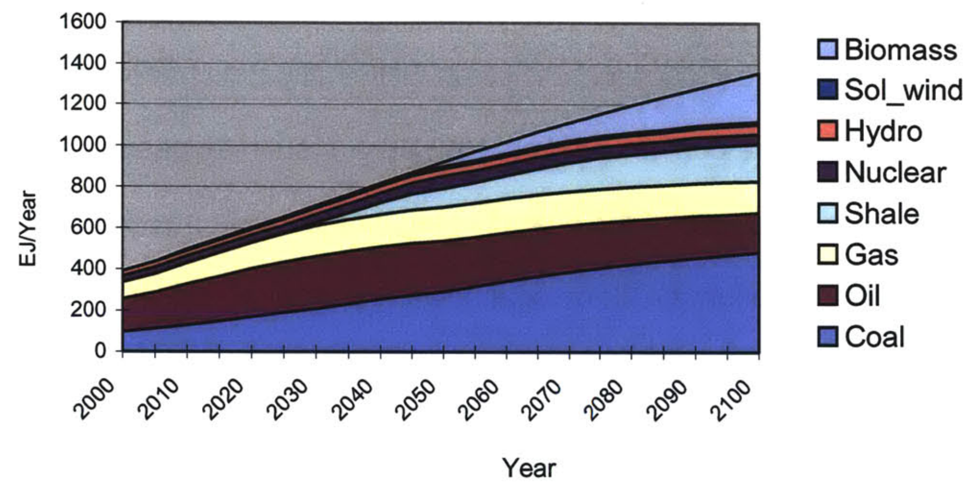

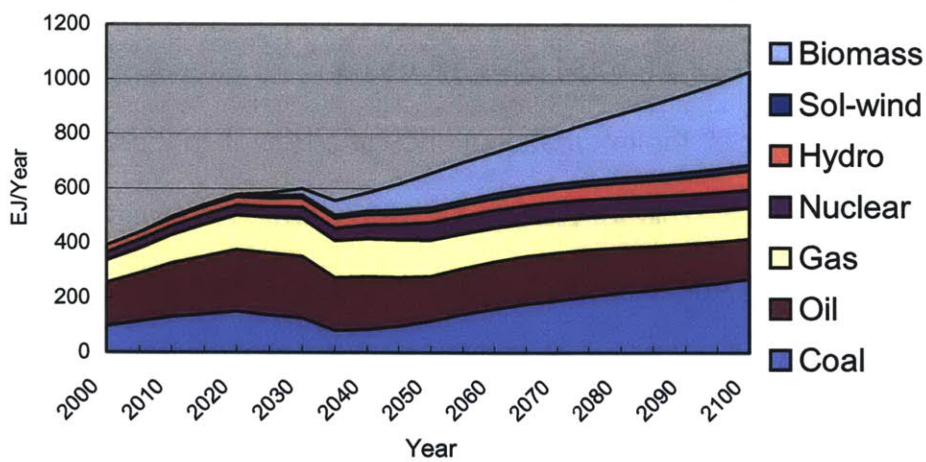

Figure 5.1: Global primary energy demand in round one: top - baseline; bottom - policy case
Unit: Exajoule (EJ) / year
Source: EPPA simulation, August 2007.

Figure 5.1 indicates the global primary energy demand in both the baseline and GHG-mitigation policy scenarios. If GHG-mitigation policies were implemented, the world would need less energy than in the baseline considering that the mandatory mitigation on GHGs would limit the use of conventional energy sources such as coal and oil. As stated in the scenario descriptions in Chapter 3, in 2025, the GHG-mitigation policies would be implemented in both developed and developing countries, and this would lead to the decrease of demand for conventional energy sources beginning from 2025, as indicated in the policy case in Figure 5.1. In 2035, when the proposed policies on GHG mitigation become even stricter, the demand for the conventional energy sources such as gas and oil would be less than before. Because of the projected technological improvement of Carbon Capture and Sequestration (CCS) on coal power generation, which indicates the technological change toward low- or no-carbon emitting technologies (McFarland et al., 2004), the demand for coal would increase in the policy case. In addition, we would need significant energy to be produced from biomass in both scenarios. The increasing price of oil would drive the demand for biomass-fuel on a large scale: in the EPPA model, the international price of crude oil in 2100 is projected to be around three times higher than that in 1997[7], which is around $25/barrel (Energy Information Administration, 1997). Compared with the baseline, when there are limitations on GHG emissions, we would need more biomass. As shown in Figure 5.1, compared with the baseline, the world demand

[7] We use the EPPA model to predict the long-term, not short-term, of oil price, and therefore, do not include the possible spike in oil price; in addition, the oil price in the EPPA model is indicated in real terms, and the nominal oil price in 2100 should be higher than the real one. I compared the oil-price predictions of the EPPA model with those of International Energy Outlook (2007), and found that they are similar.

for biomass-energy is initiated earlier in the policy case in 2025, the year at which the policies would be applied to all regions. Biomass energy would account for around 18% of global primary energy demand in the baseline in 2100, while that figure for the policy scenario reaches 34%. The larger share of biomass energy in the policy scenario than in the baseline is mainly due to the substitution of biomass fuel for conventional fossil-based fuel, because the former is the only alternative to the latter in the EPPA model.

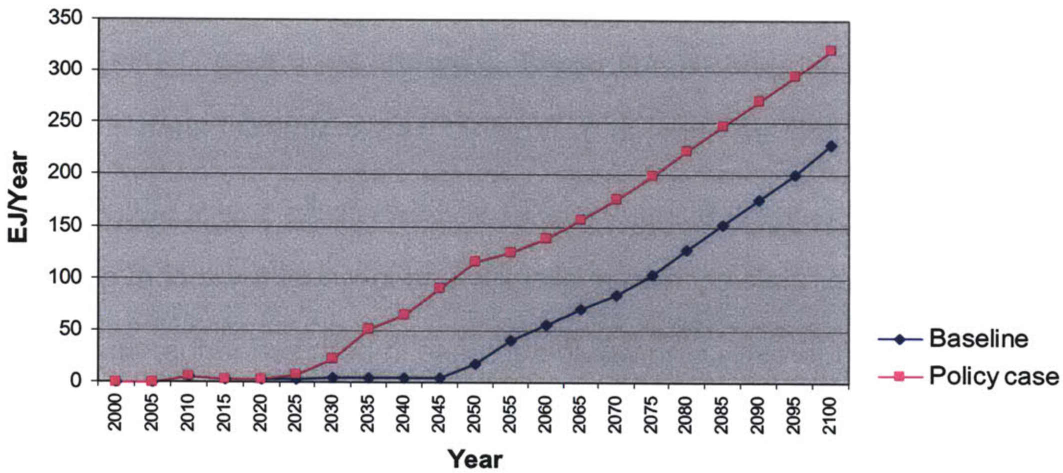

Figure 5.2: Global production of biomass energy in round one
Unit: Exajoule (EJ) / year
Source: EPPA simulation, August 2007.

Figure 5.2 indicates the global production of biomass energy in both scenarios. In the policy scenario, the expansion of biomass energy would start in 2025, which is much earlier than in the baseline, and global production of biomass energy would reach around 340 EJ in 2100. Because the biomass-energy production would mainly be driven by the increasing oil price, most of the biomass energy would come from biomass-fuel production, while biomass electricity would represent only less than 1% of total biomass-energy production.

Based on the land-use modeling techniques described in Chapter 3, we use the EPPA model to project the land use of the five types of agricultural land as well as biomass in both the baseline and policy scenarios, as indicated in Figure 5.3. The increasing demand for biomass energy would boost the value of land producing biomass energy; this would increase the land-use conversion from cropland to biomass, as well as that from other types of agricultural land to cropland. As a result, all the five types of agricultural land would give space to biomass-energy production. As I stated, land requirements per dollar and per energy content of biomass-energy production are affected by regional land availability, land productivities, and potentials for growing energy crops as well as land rent per hectare. Because of the relatively high availability and low cost to be converted to other land, un-managed forestry land would decrease in both scenarios. In the policy case which needs more land to be devoted to biomass-energy production, un-managed forestry land would experience a more severe loss than in the baseline.

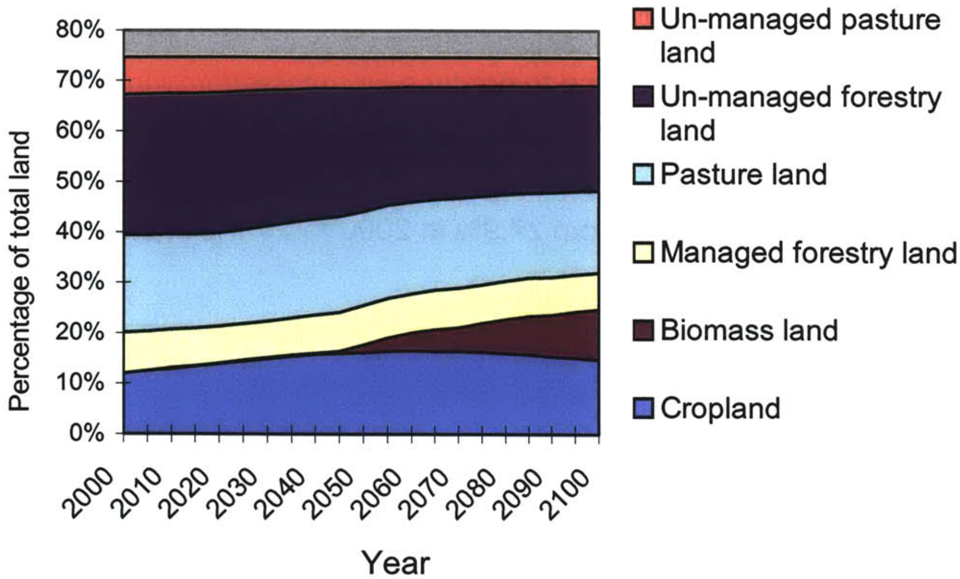

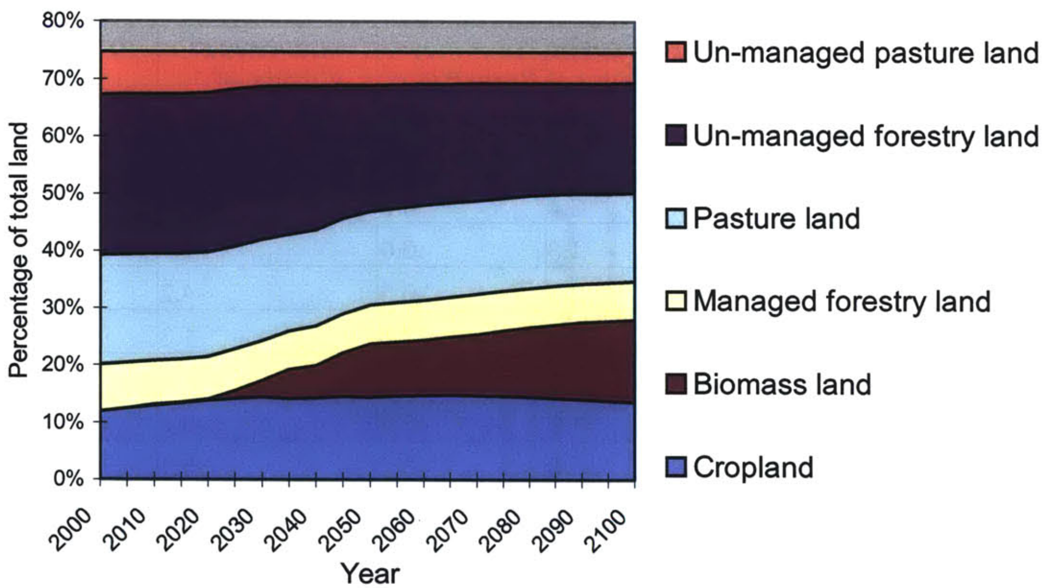

Figure 5.3: Predicted agricultural land use in round one[8]
(top – baseline; bottom - policy scenario)
Source: EPPA simulation, August 2007.

[8] The land excluding these six types of land is "other land", as indicated in gray in both graphs.

As projected by the EPPA model, although biomass-energy was not developed in 2000, the world would need 9.9% of global land to produce biomass-energy in the baseline and 14.4% in the policy case in 2100. The percentage of un-managed forestry land in global land would decrease from 27.9% in 2000 to 20.7% in the baseline, and 19.2% in the policy scenario, respectively.

Tables 5.1 and 5.2 show the regional land-use changes in the two climate scenarios, indicated by the percentages of the five types of agricultural land and biomass land in total regional land in 2100 in comparison with those in 2000 for each EPPA region.

Table 5.1: Regional land-use changes (2100 in comparison with 2000) in the baseline in round one

Unit: % in total regional land

Region	Cropland	Biomass land	Managed forestry land	Pasture land	Un-managed forestry land	Un-managed grassland
AFR	4.0	17.5	-3.3	-8.0	-5.2	-5.0
ANZ	0.1	0.1	2.4	-0.7	-2.4	0.5
ASI	13.5	2.3	3.4	0.0	-18.3	-0.9
CAN	-1.7	2.4	1.3	0.0	-1.1	-1.0
CHN	9.9	0.0	2.1	-6.5	-4.2	-1.4
EET	-1.2	0.8	-2.4	1.5	1.3	0.0
EUR	-4.8	5.2	-1.3	2.4	-2.4	0.9
FSU	7.0	0.0	1.9	0.2	-8.8	-0.2
IDZ	8.8	24.6	1.8	-0.1	-35.1	0.0
IND	4.7	0.5	-1.2	0.8	-5.1	0.4
JPN	-2.6	2.6	1.9	0.1	-2.0	0.0
LAM	2.2	25.6	-3.5	-5.5	-18.7	0.0
MES	2.4	0.3	2.5	2.7	-2.5	-5.4
MEX	14.5	10.0	-3.8	-13.6	-5.0	-2.0
ROW	0.5	3.0	0.8	-0.4	-3.9	0.0
USA	-6.6	18.5	-4.8	-0.7	-2.5	-4.0

Source: EPPA simulation, August 2007.

Note: Details of the regional composition are provided in Table 3.1.

Table 5.2: Regional land-use changes (2100 in comparison with 2000) in the policy scenario in round one

Unit: % in total regional land

Region	Cropland	Biomass land	Managed forestry land	Pasture land	Un-managed forestry land	Un-managed grassland
AFR	2.2	20.6	-3.6	-10.1	-3.4	-5.6
ANZ	1.1	4.0	2.8	-5.0	-2.8	0.0
ASI	2.6	7.4	2.4	0.0	-11.6	-0.8
CAN	-2.5	2.9	1.4	0.0	-1.3	-1.1
CHN	9.2	0.2	1.9	-6.0	-3.9	-1.3
EET	-1.2	0.6	-2.1	1.5	1.3	0.0
EUR	-5.8	17.5	-4.4	0.5	-7.8	0.0
FSU	6.6	5.6	2.1	-0.5	-13.5	-0.2
IDZ	4.1	31.9	1.0	-0.2	-36.9	0.1
IND	1.2	1.9	-0.4	0.9	-3.7	0.3
JPN	-2.3	2.3	1.9	0.1	-1.9	0.0
LAM	0.8	27.8	-4.2	-2.6	-21.8	0.0
MES	1.0	0.2	1.7	3.7	-1.7	-4.9
MEX	12.4	19.3	-7.5	-15.6	-5.8	-2.8
ROW	-0.8	12.0	-0.1	-1.4	-9.8	0.0
USA	-8.6	32.8	-7.4	-3.3	-6.8	-6.8

Source: EPPA simulation, August 2007.

Note: Details of the regional composition are provided in Table 3.1.

As indicated in Tables 5.1 and 5.2, biomass-energy production would occur mainly in the United States (baseline: +18.5%; policy case: +32.8%), Central and South America (baseline: +25.6%; policy case: +27.8%), Africa (baseline: +17.5%; policy case: +20.6%), and Indonesia (baseline: +24.6%; policy case: +31.9%). The regional disparity in land use is affected by two factors: first, in some regions like the United States, there is abundant available un-managed land to be converted to cropland, therefore leading to the occurrence of biomass-production on a large scale considering the assumption that biomass would occur in cropland; second, biomass is more productive in tropical areas. However, some regions with abundant un-managed land and in tropical areas, such as China and India, devote very little land to biomass-energy production. An important reason is that in these regions, the demand for food would be very high considering their population; as a result, these regions would specialize in the production of crop products and livestock. In addition, international trade is included in the EPPA model, and this further drives the specialization of different agricultural products in various regions.

To distribute such regional land-use changes affected by economic forces to finer spatial resolutions, I apply the downscaling methods described in Chapter 4 and get the gridded land use of the five types of agricultural land and biomass from 2005 to 2100 (the historical land-use data in 2000 are given in the Hurtt dataset). Figures 5.4 through 5.9 present the global gridded land-use maps in both scenarios of cropland, biomass land, managed forestry land, pasture land, un-managed forestry land, and un-managed grassland in 2100. Such gridded land-use data, indicated by the shares of each land category in the total area of each grid cell, are continuous, while I classify them into ten categories from 0 to 1 for mapping purposes.

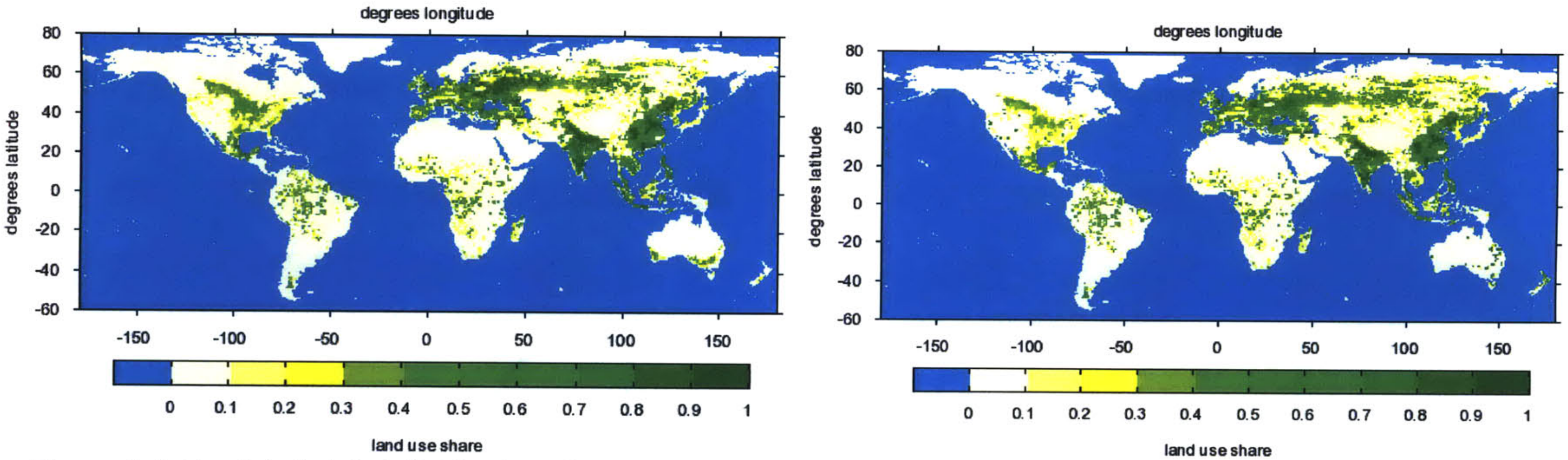

Figure 5.4: Predicted global distribution of cropland in 2100 in round one: left – baseline; right – policy scenario
Source: the author.

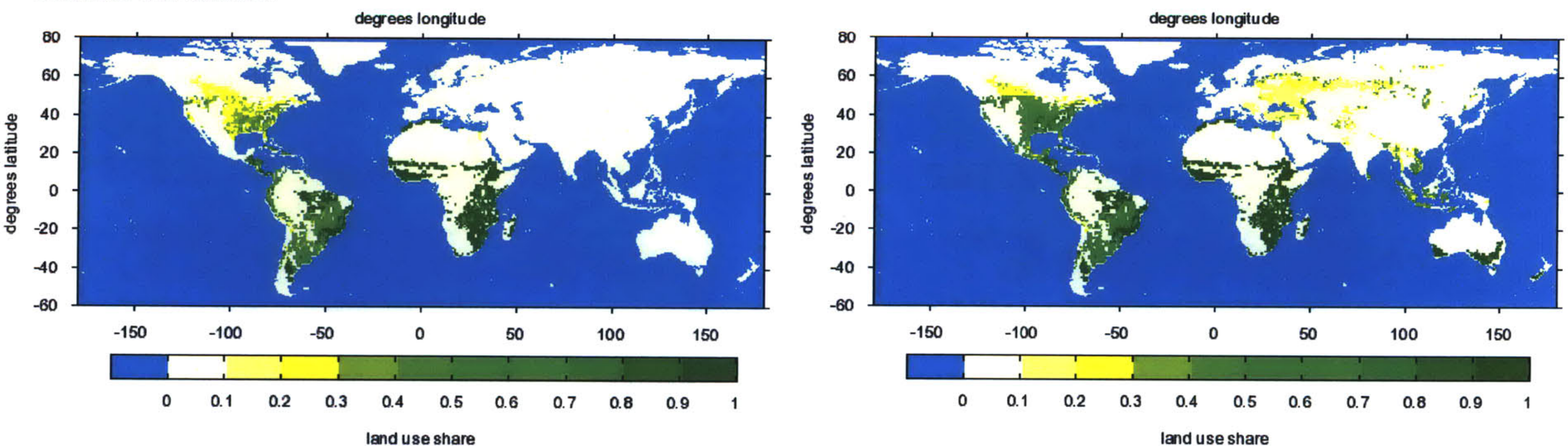

Figure 5.5: Predicted global distribution of biomass land in 2100 in round one: left – baseline; right – policy scenario
Source: the author.

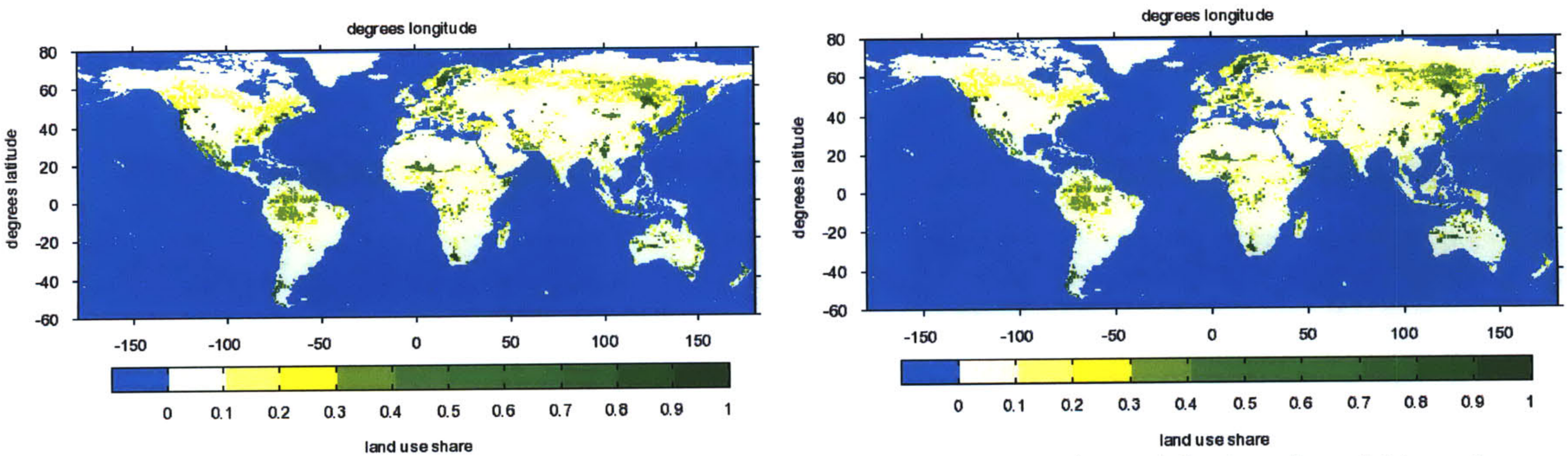

Figure 5.6: Predicted global distribution of managed forestry land in 2100 in round one: left – baseline; right – policy scenario
Source: the author.

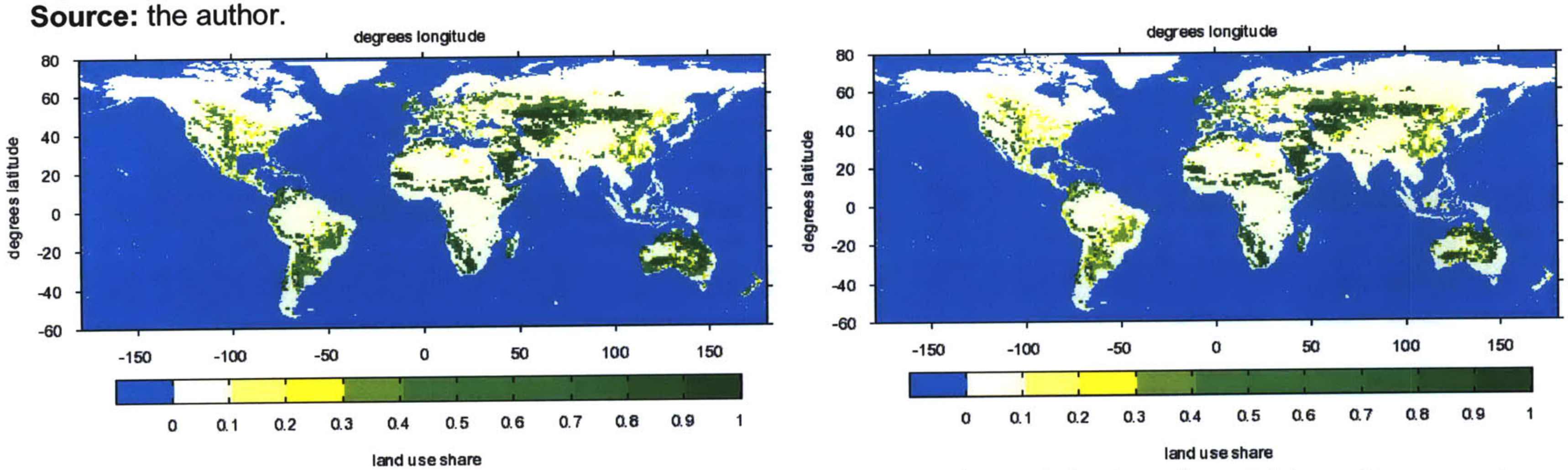

Figure 5.7: Predicted global distribution of pasture land in 2100 in round one: left – baseline; right – policy scenario
Source: the author.

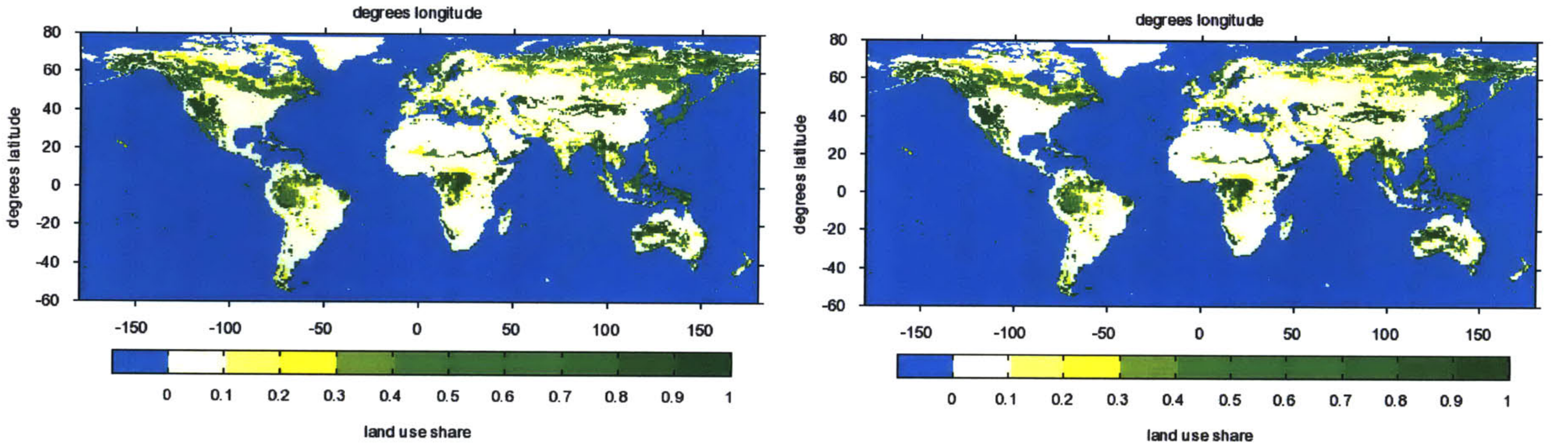

Figure 5.8: Predicted global distribution of un-managed forestry land in 2100 in round one: left – baseline; right – policy scenario
Source: the author.

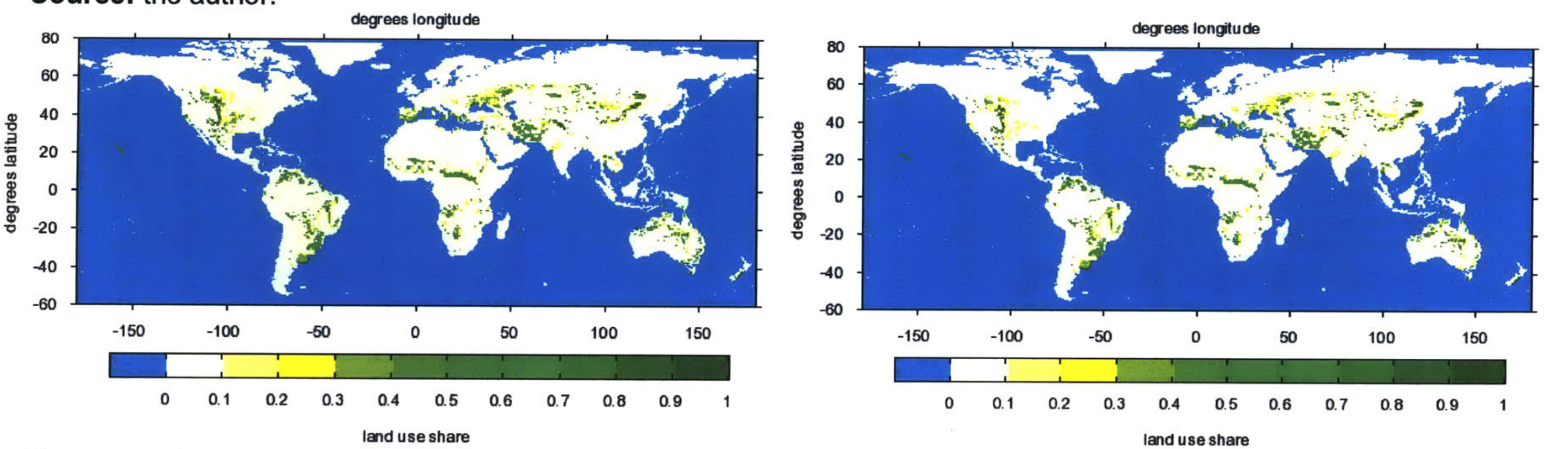

Figure 5.9: Predicted global distribution of un-managed grassland in 2100 in round one: left – baseline; right – policy scenario
Source: the author.

As stated before, we assign biomass land only to those grid cells where the cropland share is not less than 5%. Therefore, in those biomass-production regions, we may observe that the biomass would replace cropland, which would further be pushed to other types of agricultural land, especially the un-managed forestry land. As we can observe in the four main providers of biomass energy (the United States, Central and South America, Africa, and Indonesia), in comparison with 2000 as indicated in Figures 4.1 through 4.5, cropland and un-managed forestry land are much less in the Rocky Mountain and eastern areas in the United States, Amazon rain forest areas in Central and South America, Congo rain forests in Africa, and Indonesia. In those regions without large-scale biomass-energy production, China and India for example, cropland would expand in responses to the increasing demand for food. In comparison with the baseline, in the policy case in which there would be more biomass-energy production, such trends would be more obvious in terms of biomass replacement of cropland and un-managed forestry land, as well as the cropland expansion in China and India.

Therefore, on a global scale, the policies to mitigate GHG emissions would increase biomass-energy production at the expense of the five types of agricultural land, especially un-managed forestry land. In comparison with the baseline, in those regions where large-scale biomass-energy production is developed, more un-managed forestry land would be cleared to make space for biomass if the GHG-mitigation policies were implemented. In those regions with very little biomass-energy production, China and India for example, the land-use effects caused by higher demand for biomass energy in the policy case would not occur, and therefore, the land-use distributions would be similar in the two climate scenarios.

I show the land-rent effects in the baseline and policy scenarios in Tables 5.3 and 5.4. In addition to the absolute land rent in 2100, I indicate the land-rent ratio, indicated as the land rent in 2100 over that in 2000, in the parentheses.

Table 5.3: Regional rent of the five types of agricultural land in 2100 in round one - baseline

Unit: $ per hectare

	Cropland	Managed forestry land	Pasture land	Un-managed forestry land	Un-managed grassland
AFR	73.1 (1.6)	41.0 (20.5)	41.0 (19.5)	33.0 (55.0)	28.9 (144.3)
ANZ	92.1 (0.9)	49.9 (6.4)	12.7 (3.1)	13.1 (16.4)	13.5 (12.3)
ASI	791.4 (1.6)	387.7 (7.8)	407.1 (4.6)	152.6 (76.3)	0.0 (1.0)
CAN	78.5 (1.5)	87.8 (4.5)	54.6 (1.5)	11.5 (11.5)	0.0 (1.0)
CHN	776.0 (3.5)	308.6 (24.3)	312.8 (22.5)	247.0 (137.2)	261.6 (130.8)
EET	301.1 (2.6)	273.0 (18.2)	349.2 (3.8)	318.3 (9.5)	303.5 (15.1)
EUR	405.5 (1.0)	81.8 (8.8)	197.7 (1.5)	40.6 (12.3)	92.5 (7.4)
FSU	57.0 (1.9)	28.4 (8.6)	31.7 (6.9)	10.7 (53.4)	25.0 (25.0)
IDZ	986.0 (1.8)	687.0 (12.4)	805.9 (6.6)	321.2 (229.4)	745.8 (11.0)
IND	849.2 (4.0)	451.6 (28.4)	760.1 (1.7)	338.6 (105.8)	0.0 (1.0)
JPN	1364.1 (0.8)	230.7 (7.9)	1596.1 (1.4)	68.4 (11.8)	0.0 (1.0)
LAM	198.9 (1.4)	61.4 (40.9)	58.6 (4.1)	50.7 (253.4)	57.6 (33.9)
MES	276.1 (1.1)	184.2 (8.9)	49.0 (11.4)	67.8 (30.8)	38.6 (96.6)
MEX	287.0 (0.8)	103.0 (15.6)	100.3 (7.6)	77.7 (26.8)	79.2 (33.0)
ROW	329.0 (1.7)	177.4 (8.1)	177.7 (9.5)	76.1 (42.3)	97.5 (36.1)
USA	251.2 (1.3)	52.5 (21.0)	68.5 (1.6)	29.8 (21.3)	54.0 (21.6)

Source: EPPA simulation, September 2007.

Note: 1. Details of the regional composition are provided in Table 3.1.

2. The number in the parentheses indicates the land-rent ratio, calculated as the land rent in 2100 over that in 2000.

Table 5.4: Regional rent of the five types of agricultural land in 2100 in round one - policy scenario

Unit: $ per hectare

	Cropland	Managed forestry land	Pasture land	Un-managed forestry land	Un-managed grassland
AFR	64.0 (1.4)	36.2 (18.1)	36.1 (17.2)	28.0 (46.7)	25.1 (125.3)
ANZ	92.1 (0.9)	49.9 (6.4)	15.6 (3.8)	12.8 (16.0)	14.4 (13.1)
ASI	840.8 (1.7)	442.3 (8.9)	460.2 (5.2)	212.0 (106.0)	0.0 (1.0)
CAN	99.4 (1.9)	85.8 (4.4)	54.6 (1.5)	10.3 (10.3)	0.0 (1.0)
CHN	753.8 (3.4)	276.9 (21.8)	280.8 (20.2)	215.1 (119.5)	226.4 (113.2)
EET	289.5 (2.5)	262.5 (17.5)	340.0 (3.7)	308.2 (9.2)	295.5 (14.7)
EUR	486.6 (1.2)	139.5 (15.0)	250.4 (1.9)	98.0 (29.7)	118.8 (9.5)
FSU	69.0 (2.3)	35.0 (10.6)	39.1 (8.5)	15.0 (74.8)	25.1 (25.1)
IDZ	1040.8 (1.9)	759.0 (13.7)	732.6 (6.0)	392.0 (280.0)	813.6 (12.0)
IND	679.4 (3.2)	298.9 (18.8)	581.2 (1.3)	194.6 (60.8)	0.0 (1.0)
JPN	1364.1 (0.8)	233.6 (8.0)	1596.1 (1.4)	66.1 (11.4)	0.0 (1.0)
LAM	198.9 (1.4)	61.5 (41.0)	58.6 (4.1)	50.8 (254.0)	46.9 (27.6)
MES	276.1 (1.1)	153.2 (7.4)	28.8 (6.7)	31.5 (14.3)	17.7 (44.3)
MEX	358.7 (1.0)	144.5 (21.9)	141.2 (10.7)	120.1 (41.4)	122.2 (50.9)
ROW	329.0 (1.7)	188.3 (8.6)	188.9 (10.1)	86.0 (47.8)	108.0 (40.0)
USA	328.4 (1.7)	117.8 (47.1)	115.6 (2.7)	94.6 (67.6)	121.0 (48.4)

Source: EPPA simulation, September 2007.

Note: 1. Details of the regional composition are provided in Table 3.1.
2. The number in the parentheses indicates the land-rent ratio, calculated as the land rent in 2100 over that in 2000.

As just stated, the large-scale development of biomass-energy production drives the decrease of un-managed forestry land; therefore, as indicated in Tables 5.3 through 5.4, we observe a big increase in the land rent of un-managed forestry in those biomass-producing regions. In addition, the rent of un-managed forestry land would also be affected by its availability within the region. As a result, in Indonesia (IDZ) where large-scale biomass-energy production would be developed and little un-managed forestry land would remain in 2100, we observe the highest increase in the rent of un-managed forestry land, reaching $321.2/hectare in the baseline and $392.0/hectare in the policy scenario in 2100, which would be 229.4 and 280 times that in 2000, respectively. In Central and South America (LAM) where some un-managed forestry land would still remain, we observe the second highest increase in the rent of un-managed forestry land, reaching $50.7/hectare in the baseline and $50.8/hectare in the policy scenario, both of which would be more than 250 times higher than the rent in 2000. Also because of these two drivers in terms of biomass-energy production and availability of un-managed forestry land, the un-managed forestry land rent in the United States and Africa as well as other biomass-production regions would increase.

In comparison with the baseline, the un-managed forestry land rent would be generally even higher in the policy scenario because of the larger scale of biomass-energy production: taking the United States (USA) as an example, the un-managed forestry land rent in the policy case in 2100 is $94.6/hectare, 67.6 times that in 2000; while that in the baseline is $29.8/hectare, which is only 21.3 times that in 2000. The rent of un-managed grassland would also increase because some of it would be cleared for biomass-energy production after first being converted to cropland; however, the rent of un-managed grassland would not increase as much as that of un-managed forestry land, because the loss of the former is not as severe as that of the latter. In those regions without large-scale biomass-energy production but with cropland expansion, China (CHN) and India (IND) for example, the rent of un-managed land would also increase because the cropland would be expanded at the expense of un-managed land.

The availability of un-managed land, which has the potential to be converted to cropland and biomass land, would also affect the cropland rent. In those regions with abundant un-managed land, the cropland rent would not increase a lot, such as the United States (baseline: $251.2/hectare in 2100, 1.3 times that in 2000; policy case: $328.4/hectare in 2100, 1.7 times that in 2000) and Europe (baseline: $405.5/hectare in 2100, the same as that in 2000; policy case: $486.6/hectare in 2100, 1.2 times that in 2000). However, in those regions with little un-managed land, the cropland rent would experience a big increase, as we would observe in China ($776.0/hectare in the baseline and $753.8/hectare in the policy scenario, which would be 3.5 and 3.4 times that in 2000, respectively) and India ($849.2/hectare in the baseline and $679.4/hectare in the policy scenario, which would be 4.0 and 3.2 times that in 2000, respectively).

It has been commonly acknowledged that forestry is a great reservoir for carbon storage. Then, we may be concerned about a question: if we cut a lot of natural forest for the production of crops and biomass-energy, would the carbon stored in agricultural land be reduced? To answer this question, MBL researchers apply the TEM to simulate the carbon stored in the five types of agricultural land in both the baseline and GHG-mitigation policy scenarios. Because we assume that biomass would only occur in the cropland, MBL researchers treat the biomass land the same as cropland in the carbon-storage projection.

Table 5.5: Projected carbon stored in the five types of agricultural land in round one
Unit: Billion metric tons (bmt)

Year	Baseline scenario	GHG-mitigation policy scenario
2000	573.4	573.4
2010	560.6	560.9
2020	555.6	555.2
2030	541.4	537.7
2040	519.7	486.6
2050	489.2	433.7
2060	454.3	417.3
2070	442.1	404.9
2080	427.9	392.5
2090	419.3	387.8
2100	411.9	384.6

Source: TEM simulation, August 2007.

As indicated in Table 5.5, in the baseline scenario, the carbon stored in the five types of agricultural land would change from 573.4 billion metric tons (bmt) in 2000 to 411.9 bmt in 2100; such figures in the GHG-mitigation policy scenario would be 573.4 bmt and 384.6 bmt, respectively. Therefore, in the baseline, the five types of agricultural land would lose 161.5 bmt of carbon, equaling to 7.6% of the total anthropogenic GHG emissions globally during the 21st century. In contrast with the baseline, if the GHG-mitigation policies were implemented, more un-managed forestry land would be cleared to grow biomass energy, and therefore, the five types of agricultural land would experience a more severe loss of carbon storage, which are projected to be 188.8 bmt of carbon, equaling to 23% of the total anthropogenic GHG emissions globally during the 21^{st} century.

In summary, taking only the land-use effects driven by economic forces into consideration, during the 21^{st} century, biomass-energy production would be developed on a large scale globally, which would lead to the conversion of the five types of agricultural land and the decrease of carbon stored in such land. The implementation of GHG-mitigation policies, leading to more production of biomass energy and conversion of agricultural land, would cause an even more severe loss of the carbon stored in agricultural land. Therefore, my hypothesis about the biomass-energy production and agricultural carbon storage of these two scenarios is confirmed in this round.

However, as I stated, only the land-use effects of economic forces are included in this round. In the next round, we also include the feedbacks of climate, GHGs, and tropospheric ozone, and highlight the differences between the two rounds in terms of land use, land rent, and carbon storage.

5.2. Impacts of GHG-mitigation policies on agricultural land (round two)

In this round, in additional to the land-use effects of economic forces, we also include the feedbacks of climate, GHGs, and tropospheric ozone. Therefore, the differences of impacts on the five types of agricultural land in response to GHG-mitigation policies between the two rounds are caused by the inclusion of such feedbacks, and we highlight such differences in this section.

In this round, the productivity of the five types of agricultural land, indicated by NPP, would be affected by the climate, GHGs, and tropospheric ozone. Figures 5.10 and 5.11 indicate the NPP changes of the five types of agricultural land globally in both the baseline and policy scenarios from 2000 to 2100.

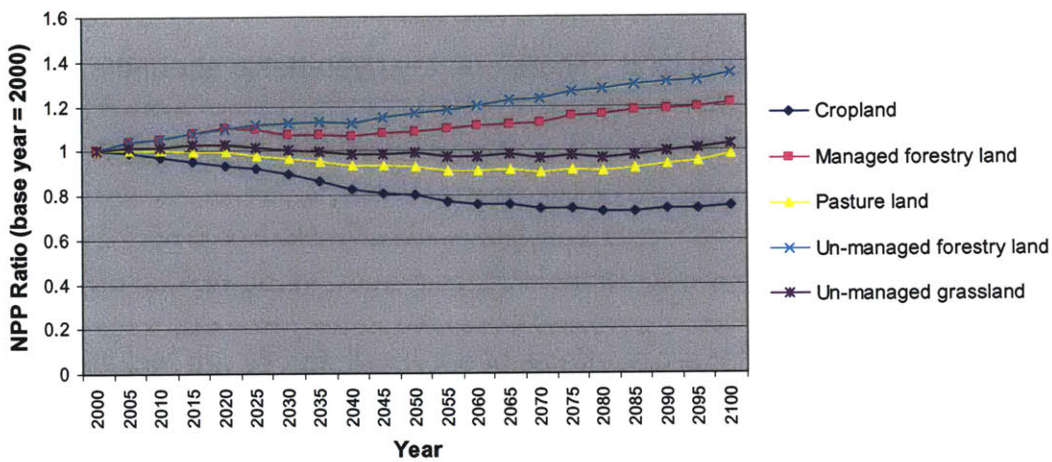

Figure 5.10: Projection of agricultural productivities in the baseline scenario
Source: TEM simulation, August 2007
Note: NPP ratio = NPP in year t / NPP in 2000

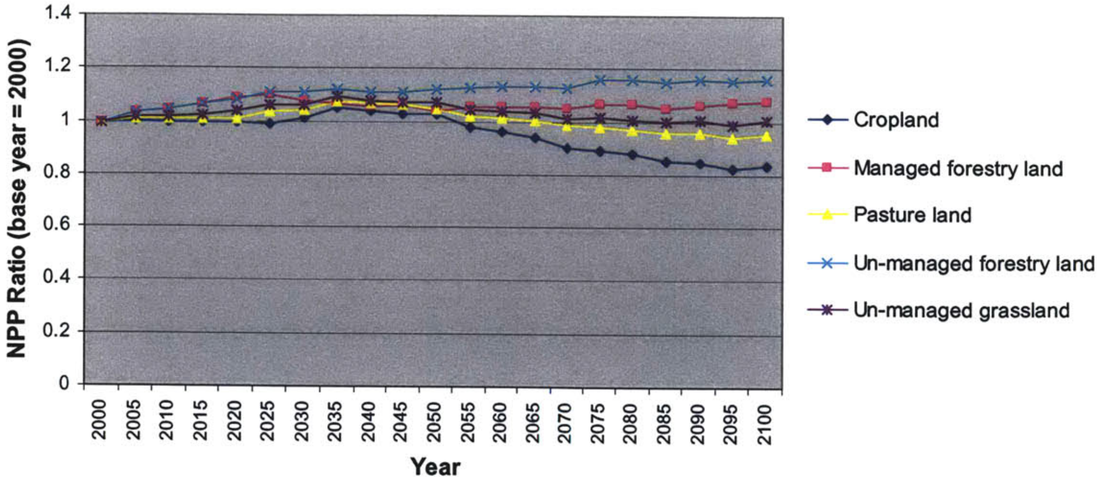

Figure 5.11: Projection of agricultural productivities in the policy scenario
Source: TEM simulation, August 2007
Note: NPP ratio = NPP in year t / NPP in 2000

As stated in Chapter 2, an increase of atmospheric CO_2 would generally increase the productivity of agricultural land; the tropospheric ozone, which would be affected by the changes in atmospheric GHG concentrations, has generally a negative impact on the productivity of agricultural land, especially that of cropland (Felzer et al., 2005). In addition, changes in atmospheric GHG concentrations would also lead to changes in climate, temperature and precipitation for example. Agricultural NPP shown in Figures 5.10 and 5.11 indicate the combined effects of climate, GHG concentrations, and ozone levels on the five types of agricultural land in the two climate scenarios.

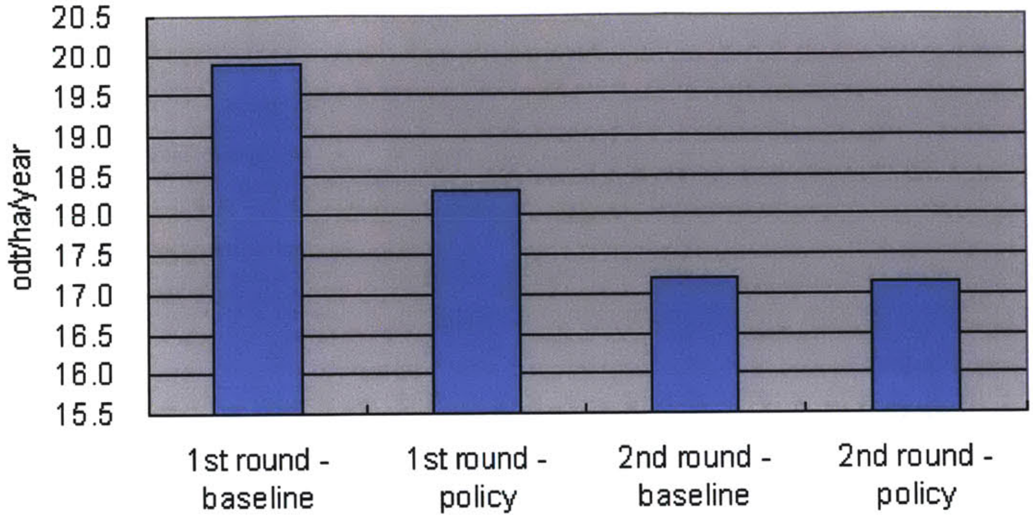

Figure 5.12: Productivity of land devoted to biomass-energy production in 2100
Unit: Oven dry tonne (odt) / hectare (ha) / year
Source: EPPA simulation, August 2007

Figure 5.12 indicates the productivity of land devoted to biomass-energy production in 2100. As stated in Section 5.1, the world would need significant energy from biomass production in both scenarios, while the mandatory limitations on GHG emissions in the policy case would lead to a higher demand for biomass energy than in the baseline. Land requirements per dollar and per energy content of biomass-energy production are affected by regional land availability, agricultural land productivities, and potentials for growing energy crops as well as land rent per hectare. In comparison with the first round in which the productivities of the five types of agricultural land are assumed to increase by 1% annually, the cropland productivity in this round would be generally lower. In this research, we assume that biomass-energy production would occur in cropland, and therefore the productivity of land devoted to biomass-energy production would also be generally lower than that in the first round, as indicated in Figure 5.12.

Compared with the first round, the demands for biomass energy and crop products in this round would be similar, while the productivity of land for crops and biomass energy would be lower. Therefore, we would need more cropland and biomass land in both the baseline and policy scenarios in this round than in the first round. Tables 5.6 and 5.7 indicate the differences between the two rounds on projected global land use in both scenarios.

Table 5.6: Differences between round one and round two on predicted global land use in the baseline

Unit: % of each land type in total global land

Year	Cropland	Biomass land	Managed forestry land	Pasture land	Un-managed forestry land	Un-managed grassland
2000	0.0	0.0	0.0	0.0	0.0	0.0
2010	1.3	0.1	2.2	0.5	-0.2	-0.6
2020	3.2	-0.1	2.0	1.1	-1.8	-0.9
2030	4.7	-0.1	2.3	1.5	-3.9	-1.1
2040	6.3	0.6	2.2	2.1	-6.6	-1.1
2050	7.1	1.2	1.8	1.9	-7.3	-1.3
2060	7.7	1.0	1.4	1.3	-6.7	-1.4
2070	8.3	1.4	1.1	0.9	-6.8	-1.5
2080	8.4	2.0	1.0	0.5	-6.8	-1.6
2090	8.0	2.9	1.0	-0.4	-6.6	-1.6
2100	7.7	3.5	1.0	-0.9	-6.2	-1.7

Source: EPPA simulation, August 2007

Table 5.7: Differences between round one and round two on predicted global land use in the policy scenario

Unit: % of each land type in total global land

Year	Cropland	Biomass land	Managed forestry land	Pasture land	Un-managed forestry land	Un-managed grassland
2000	0.0	0.0	0.0	0.0	0.0	0.0
2010	1.1	0.2	2.2	0.6	-0.2	-0.5
2020	3.6	0.0	2.1	1.2	-1.7	-0.5
2030	4.3	1.0	2.2	1.4	-5.2	-0.4
2040	4.5	2.7	2.3	1.6	-6.9	-0.8
2050	4.9	2.5	2.1	1.3	-6.3	-1.1
2060	5.7	2.8	1.7	0.8	-6.5	-0.9
2070	6.5	3.0	1.5	0.3	-6.7	-1.2
2080	6.7	3.6	1.3	-0.4	-6.5	-1.3
2090	6.7	4.7	1.2	-1.1	-6.7	-1.3
2100	6.9	4.8	1.1	-1.5	-6.5	-1.4

Source: EPPA simulation, August 2007

As indicated in Tables 5.6 and 5.7, after including the feedbacks of climate, GHGs, and tropospheric ozone in this round, the world would need more land developed for the production of crops and biomass energy in both scenarios than in the first round. In addition, the un-managed forestry land would generally experience an increase in NPP, and therefore, we would need less land for un-managed forestry. As a result, there would be more un-managed forestry land being converted to cropland and biomass land in this round. In terms of managed forestry land, pasture land, and un-managed grassland in this round, they would be similar to those in the first round because of their relative constant NPP. In both scenarios, we notice that the loss of un-managed forestry land in the latter half of the 21st century would not be as severe as that from 2000 to 2050, and this is induced by the NPP changes of cropland: in comparison with 2000-2050, the cropland NPP from 2050 to 2100 would not decrease so severely in both scenarios; therefore, the cropland area would not expand so greatly, and the loss of un-managed forestry land from 2050 to 2100 would not be as severe as that in the former half of the 21st century.

In addition, compared with the baseline, if the GHG-mitigation policies were implemented, we would need more land for biomass-energy production, and un-managed forestry land would experience a more severe loss.

Figure 5.13 indicates the projected global land use for the five types of agricultural land as well as the land devoted to biomass-energy production after including the feedbacks of climate, GHGs, and tropospheric ozone in this round.

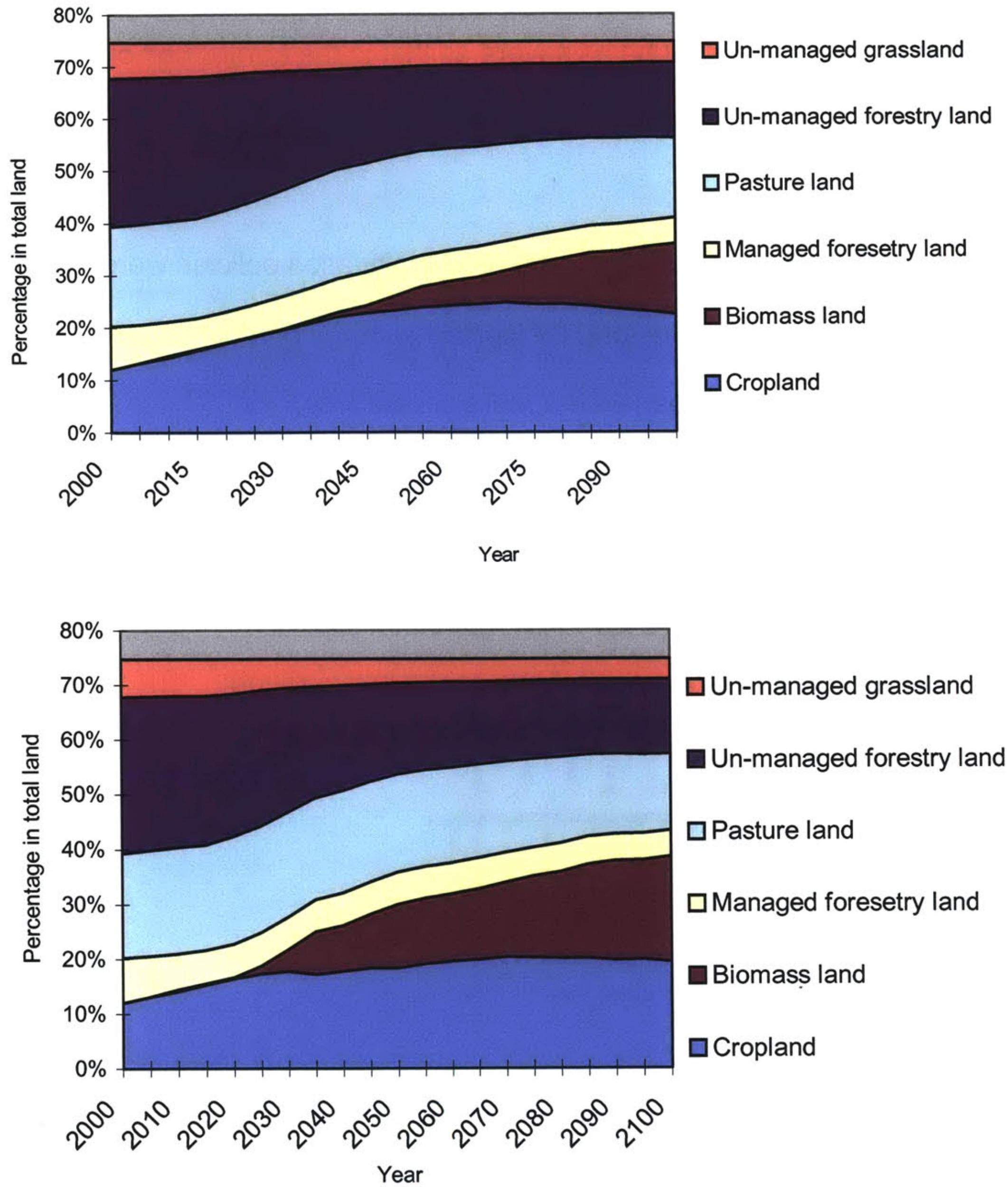

Figure 5.13: Predicted global agricultural land use in round two[9]
(top – baseline; bottom – policy scenario)
Source: EPPA simulation, August 2007

In this round, although no land was developed for biomass-energy production in 2000, we would need 13.4% (baseline) and 19.1% (policy scenario) of global land

[9] The land excluding these six types of land is "other land", as indicated in gray in both graphs.

devoted to biomass-energy production in 2100. However, the cropland percentage in global land would increase from 12% in 2000 to 22.5% (baseline) and 19.5% (policy scenario) in 2100, while the percentage of un-managed forestry land in global land would decrease from 27.9% in 2000 to 14.5% (baseline) and 13.7% (policy scenario), respectively.

To understand the regional differences of land-use effects, we present the regional NPP changes of the five types of agricultural land from 2000 to 2100 in both the baseline and policy scenarios in Tables 5.8 and 5.9.

Table 5.8: Changes in NPP (2100 in comparison with 2000) in the baseline
Unit: Percentage change (%)

Baseline	Cropland	Managed forestry land	Pasture land	Un-managed forestry land	Un-managed grassland
AFR	-13	8	13	17	3
ANZ	41	36	47	48	35
ASI	8	4	6	11	-4
CAN	-42	41	-4	42	-7
CHN	-54	6	-41	24	0
EET	-41	32	-38	66	-8
EUR	-48	41	-41	41	-12
FSU	-45	42	15	36	-10
IDZ	-38	0	-6	14	-5
IND	-26	11	-7	23	3
JPN	-69	31	-58	32	0
LAM	-5	-5	14	15	1
MES	2	21	40	57	16
MEX	-10	24	32	51	22
ROW	-16	32	9	18	5
USA	-38	15	-8	47	0

Note: Details of the regional composition are provided in Table 3.1.
Source: TEM simulation, August 2007

Table 5.9: Changes in NPP (2100 in comparison with 2000) in the policy scenario
Unit: Percentage change (%)

Policy scenario	Cropland	Managed forestry land	Pasture land	Un-managed forestry land	Un-managed grassland
AFR	5	-3	6	7	3
ANZ	31	13	21	17	24
ASI	11	0	3	9	-1
CAN	-26	20	20	-10	-20
CHN	-46	-3	11	-28	-5
EET	-41	17	31	-28	5
EUR	-42	18	20	-30	-7
FSU	-40	18	13	0	-13
IDZ	-8	-7	5	6	6
IND	-15	2	12	-6	5
JPN	-59	16	18	-39	0
LAM	9	-14	5	10	4
MES	0	16	33	15	2
MEX	5	12	31	20	7
ROW	-9	10	8	-7	1
USA	-30	8	24	-5	3

Note: Details of the regional composition are provided in Table 3.1.
Source: TEM simulation, August 2007

As indicated in Tables 5.8 and 5.9, the cropland NPP in 2100 would be lower than that in 2000 in most regions. The largest decrease in cropland NPP would occur in Canada, China, Europe, Japan, and the United States. An important reason is that tropospheric ozone levels are highest in these mid-latitude temperate areas where the largest emissions occur, and these regions would experience a more severe loss in the cropland NPP than the other regions. However, in some regions without high tropospheric ozone levels, Australia and the Middle East for example, the cropland NPP would be better off during the 21st century; an important reason is that these regions would not be affected as much as elsewhere by ozone damage, while the combined effects of climate conditions in response to GHG policies would increase the cropland NPP. As I stated in Chapter 2, the ozone damage on agricultural land other than cropland is not as severe as that on cropland; therefore, as indicated in Tables 5.8 and 5.9, we would not observe a severe NPP decrease in pasture land, un-managed grassland, managed and un-managed forestry land, especially the latter two.

In comparison with the baseline, in those regions experiencing severe ozone damage, the cropland NPP would be higher if the GHG-mitigation policies were implemented because of the diminishing ozone damage. However, in other areas without high tropospheric ozone levels, the cropland NPP would be lower in the policy scenario than in the baseline. The NPPs of forestry land and pasture land, both managed and un-managed, are affected by changes in climate in response to different climate policies, and such effects vary among different regions, considering the spatial disparity of soil quality, environmental conditions, and the way the policies would be adopted.

The impacts of climate, GHGs, and tropospheric ozone on agricultural land productivities among different regions would affect the land use of each land type in each region. In Table 5.10, we present the regional land-use changes of the five types of agricultural land as well as biomass in the baseline, indicated by the differences between the shares of each land type in total regional land in 2100 with those in 2000, while the figures in the policy scenario are shown in Table 5.11. To highlight the regional land-use effects after including the feedbacks of climate, GHGs, and tropospheric ozone, in addition to showing the figures of this round in

Tables 5.10 and 5.11, we show in the parentheses the differences between the two rounds.

Table 5.10: Regional land-use changes (2100 in comparison with 2000) in the baseline in round two

Unit: % of total regional land

Region	Cropland	Biomass	Managed forestry land	Pasture land	Un-managed forestry land	Un-managed grassland
AFR	7.1 (3.1)	23.8 (6.3)	-7.2 (-3.9)	-9.6 (-1.6)	-7.7 (-2.5)	-6.4 (-1.4)
ANZ	3.1 (3.0)	3.7 (3.6)	6.3 (3.9)	-6.8 (-6.1)	-6.2 (-3.8)	-0.3 (-0.8)
ASI	15.2 (1.7)	21.3 (19.0)	1.0 (-2.4)	0.0 (0.0)	-36.3 (-18.0)	-1.1 (-0.2)
CAN	0.8 (2.5)	0.4 (-2.0)	4.6 (3.3)	2.1 (2.1)	-5.7 (-4.6)	-1.1 (-0.1)
CHN	25.2 (15.3)	0.0 (0.0)	-0.9 (-3.0)	-8.5 (-2.0)	-12.0 (-7.8)	-3.6 (-2.2)
EET	4.0 (5.2)	0.0 (-0.8)	-7.8 (-5.4)	4.7 (3.2)	0.0 (-1.3)	-0.8 (-0.8)
EUR	12.2 (17.0)	0.0 (-5.2)	-10.7 (-9.4)	10.1 (7.7)	-11.3 (-8.9)	-0.2 (-1.1)
FSU	21.5 (14.5)	0.0 (0.0)	-0.3 (-2.2)	2.7 (2.5)	-23.5 (-14.7)	-0.5 (-0.3)
IDZ	22.4 (13.6)	19.5 (-5.1)	3.7 (1.9)	0.7 (0.8)	-46.3 (-11.2)	0.0 (0.0)
IND	17.8 (13.1)	0.6 (0.1)	-6.2 (-5.0)	2.5 (1.7)	-14.5 (-9.4)	-0.2 (-0.6)
JPN	8.0 (10.6)	0.0 (-2.6)	6.6 (4.7)	3.5 (3.4)	-18.0 (-16.0)	0.0 (0.0)
LAM	6.1 (3.9)	36.7 (11.1)	-7.1 (-3.6)	-5.5 (0.0)	-28.1 (-9.4)	-1.7 (-1.7)
MES	5.0 (2.6)	7.5 (7.2)	4.0 (1.5)	-2.4 (-5.1)	-4.0 (-1.5)	-10.1 (-4.7)
MEX	25.9 (11.4)	18.7 (8.7)	-10.0 (-6.2)	-17.1 (-3.5)	-13.5 (-8.5)	-3.9 (-1.9)
ROW	11.8 (11.3)	5.8 (2.8)	-0.2 (-1.0)	-6.3 (-5.9)	-3.3 (0.6)	-7.8 (-7.8)
USA	2.2 (8.8)	18.9 (0.4)	-10.0 (-5.2)	-0.8 (-0.1)	-5.5 (-3.0)	-4.7 (-0.7)

Source: EPPA simulation, August 2007

Note: 1. Details of the regional composition are provided in Table 3.1.

2. The figure in the parentheses indicates the difference between the two rounds.

Table 5.11: Regional land-use changes (2100 in comparison with 2000) in the policy scenario in round two

Unit: % of total regional land

Region	Cropland	Biomass	Managed forestry land	Pasture land	Un-managed forestry land	Un-managed grassland
AFR	4.4 (2.2)	27.2 (6.6)	-7.1 (-3.5)	-10.2 (-0.1)	-7.7 (-4.3)	-6.6 (-1.0)
ANZ	3.1 (2.0)	16.2 (12.2)	6.0 (3.2)	-17.1 (-12.1)	-6.4 (-3.6)	-1.8 (-1.8)
ASI	0.7 (-1.9)	38.9 (31.5)	0.1 (-2.3)	0.0 (0.0)	-37.9 (-26.3)	0.0 (0.8)
CAN	7.7 (10.2)	1.0 (-1.9)	0.7 (-0.7)	3.3 (3.3)	-11.7 (-10.4)	-1.1 (0.0)
CHN	23.1 (13.9)	0.0 (-0.2)	-0.4 (-2.3)	-8.4 (-2.4)	-11.0 (-7.1)	-3.3 (-2.0)
EET	4.0 (5.2)	0.0 (-0.6)	-7.1 (-5.0)	3.5 (2.0)	-0.1 (-1.4)	-0.3 (-0.3)
EUR	8.4 (14.2)	12.8 (-4.7)	-12.8 (-8.4)	5.6 (5.1)	-13.3 (-5.5)	-0.6 (-0.6)
FSU	18.7 (12.1)	3.9 (-1.7)	0.1 (-2.0)	2.4 (2.9)	-24.6 (-11.1)	-0.5 (-0.3)
IDZ	7.0 (2.9)	42.1 (10.2)	1.3 (0.3)	-0.1 (0.1)	-50.2 (-13.3)	0.0 (-0.1)
IND	14.9 (13.7)	0.6 (-1.3)	-5.4 (-5.0)	2.7 (1.8)	-12.8 (-9.1)	-0.1 (-0.4)
JPN	6.9 (9.2)	0.0 (-2.3)	7.7 (5.8)	2.7 (2.6)	-17.3 (-15.4)	0.0 (0.0)
LAM	3.9 (3.1)	38.2 (10.4)	-6.9 (-2.7)	-5.5 (-2.9)	-28.5 (-6.7)	-1.6 (-1.6)
MES	5.0 (4.0)	7.5 (7.3)	4.0 (2.3)	-2.4 (-6.1)	-4.0 (-2.3)	-10.1 (-5.2)
MEX	18.7 (6.3)	33.6 (14.3)	-13.1 (-5.6)	-19.6 (-4.0)	-15.1 (-9.3)	-4.5 (-1.7)
ROW	2.8 (3.6)	17.5 (5.5)	-1.6 (-1.5)	-9.8 (-8.4)	-5.7 (4.1)	-3.2 (-3.2)
USA	-3.7 (4.9)	32.9 (0.1)	-12.0 (-4.6)	-4.0 (-0.7)	-7.4 (-0.6)	-6.0 (0.8)

Source: EPPA simulation, August 2007

Note: 1. Details of the regional composition are provided in Table 3.1.

2. The figure in the parentheses indicates the difference between the two rounds.

In this round, the main providers of biomass energy, including Central and South America (LAM), the United States (USA), Africa (AFR), and Indonesia (IDZ), would generally develop more land for biomass-energy production than in the first round. Taking LAM as an example, no land was devoted to biomass-energy production in 2000, while in 2100, 36.7% (baseline) and 38.2% (policy scenario) of total regional land in LAM would be developed to produce biomass energy, which would be 11.1% (baseline) and 10.4% (policy scenario) higher than those in the first round. Some other regions which are projected to produce very little biomass energy in the first round, including Australia and New Zealand (ANZ), higher income east Asia (ASI), Mexico (MEX), etc., would devote significant amount of land to biomass-energy production in this round. Using ASI as an example, the land devoted to biomass-energy production in 2100 in the first round would be 2.3% (baseline) and 7.4% (policy scenario) of total regional land, while such figures in this round would increase to 21.3% and 38.9%, respectively. As a result, the un-managed forestry land in the regions producing biomass energy would experience a more severe loss than in the first round. Taking LAM for instance, in comparison with 2000, its un-managed forestry land in 2100 would experience a loss of 18.7% (baseline) and 21.8% (policy scenario) of total regional land in the first round, and such figures would increase to 28.1% (baseline) and 28.5% (policy scenario) in this round. Therefore, after including the feedbacks of climate, GHGs, and tropospheric ozone, there would be more land devoted to biomass-energy production, and the un-managed forestry land would experience a more severe loss than in the first round.

As stated, the diminishing productivity of cropland would increase cropland areas to satisfy the demand for food, especially in those regions that are main providers of crop products while also being affected by the ozone damage. China is an example for such cases: in the first round, in comparison with 2000, its cropland in

2100 would experience an increase of 9.9% (baseline) and 9.2% (policy scenario) of total regional land; after including the feedbacks of climate, GHGs, and tropospheric ozone in this round, such figures would increase to 25.2% (baseline) and 23.1% (policy case).

I apply the downscaling methods described in Chapter 4 to distribute such regional land-use effects to grid cells from 2001 to 2100. Figures 5.14 through 5.19 indicate the global gridded land-use maps of the five types of agricultural land as well as the biomass land in both scenarios in 2100, indicated as the share of each land type in the total land area of the grid cell. Again, the data are continuous, while I classify them into ten categories for mapping purposes.

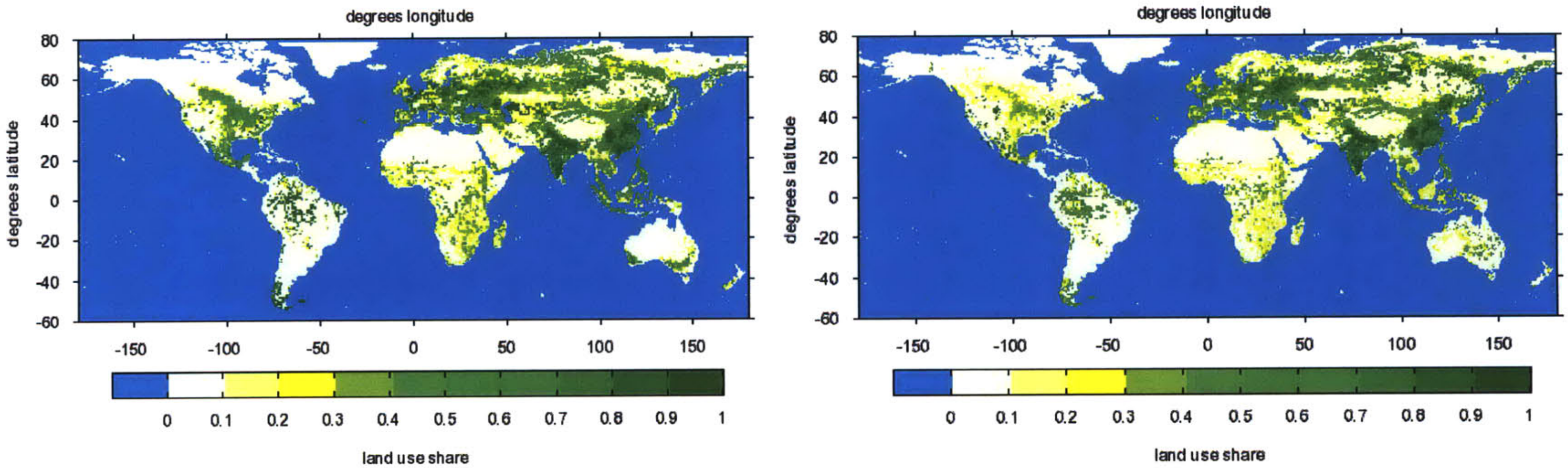

Figure 5.14: Predicted global distribution of cropland in 2100 in round two: left – baseline; right – policy scenario
Source: the author.

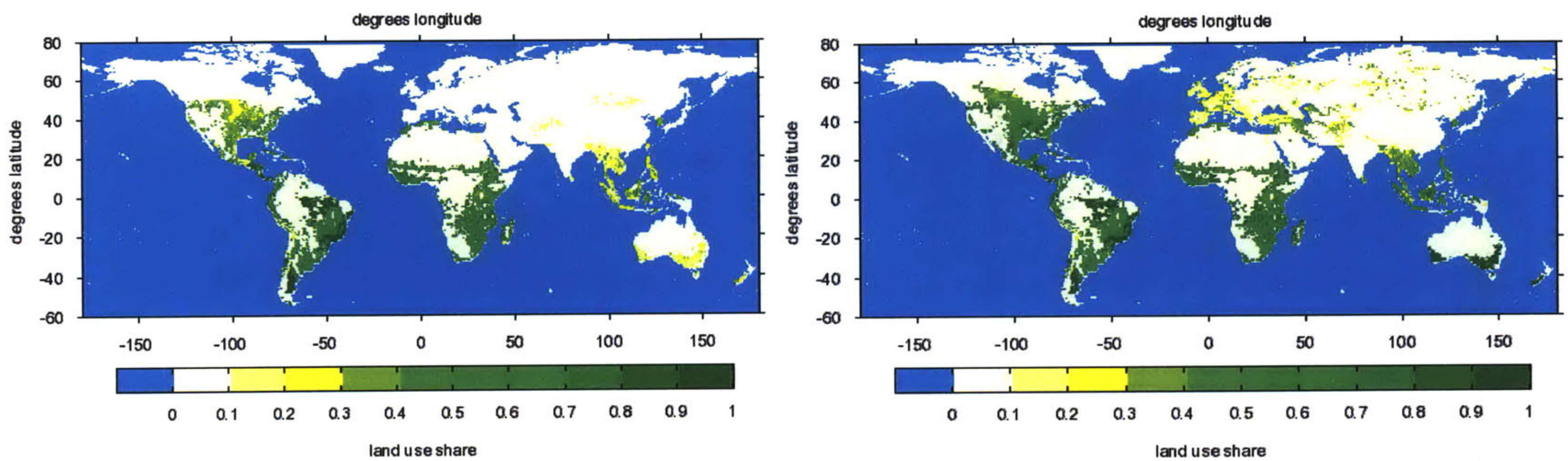

Figure 5.15: Predicted global distribution of biomass land in 2100 in round two: left – baseline; right – policy scenario
Source: the author.

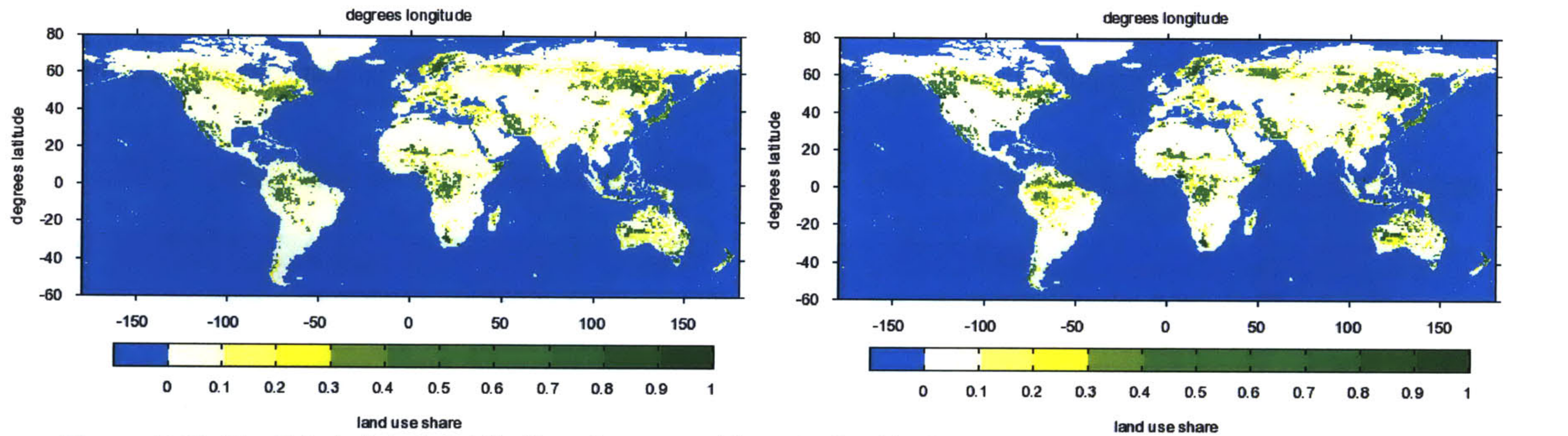

Figure 5.16: Predicted global distribution of managed forestry land in 2100 in round two: left – baseline; right – policy scenario
Source: the author.

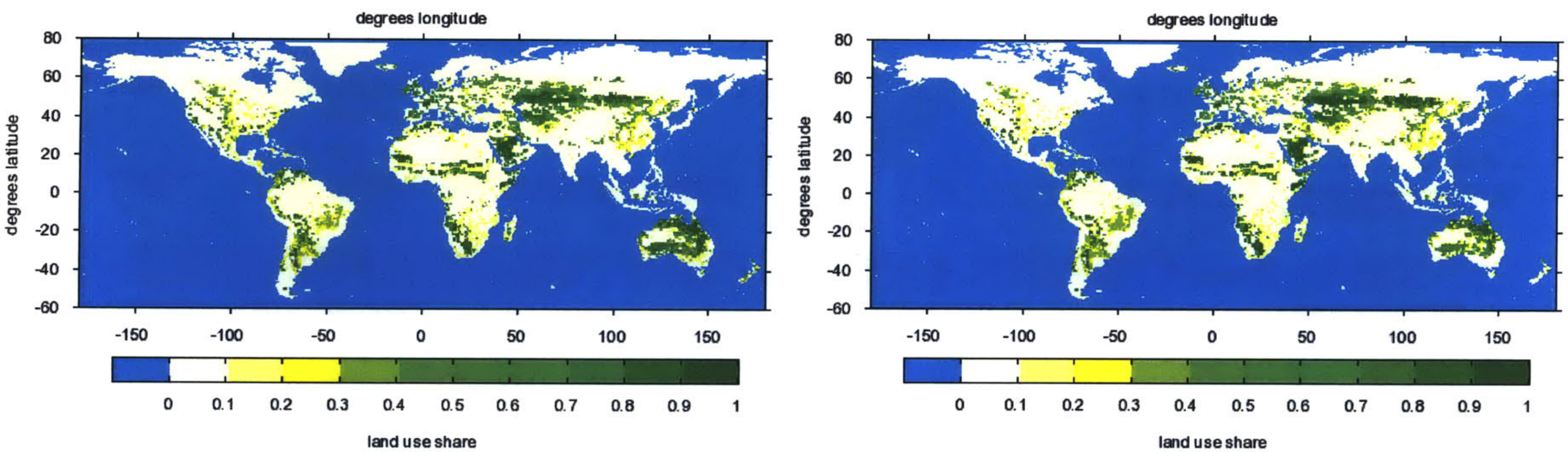

Figure 5.17: Predicted global distribution of pasture land in 2100 in round two: left – baseline; right – policy scenario
Source: the author.

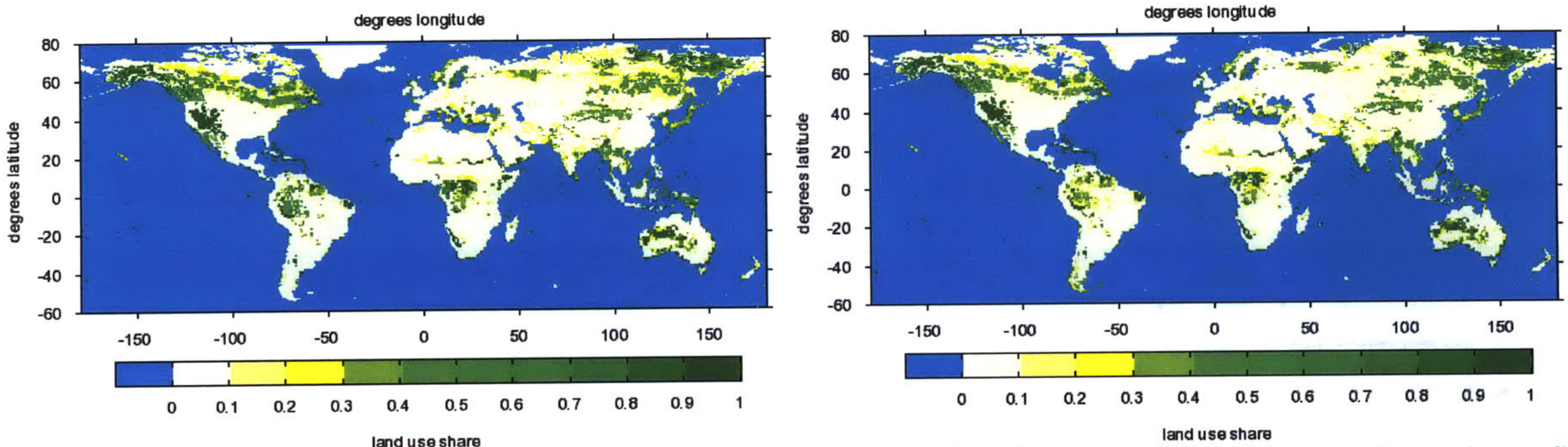

Figure 5.18: Predicted global distribution of un-managed forestry land in 2100 in round two: left – baseline; right – policy scenario
Source: the author.

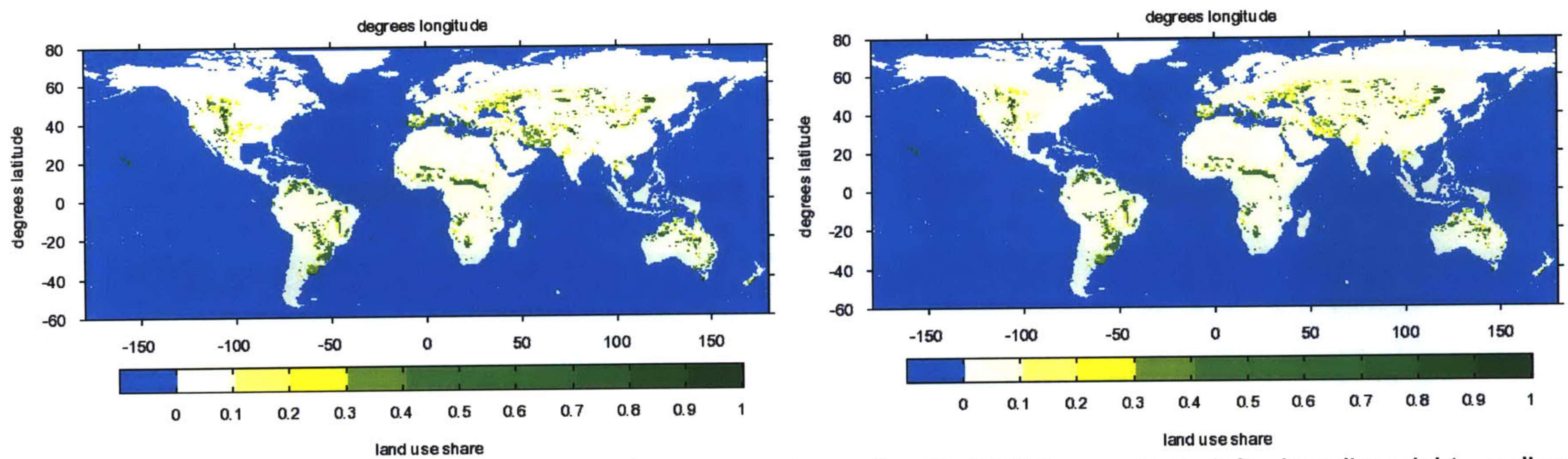

Figure 5.19: Predicted global distribution of un-managed grassland in 2100 in round two: left – baseline; right – policy scenario
Source: the author.

As just stated, in comparison with the first round, we would observe more cropland and biomass land as well as less land for the other types of agricultural land, especially un-managed forestry land. We compare the gridded land use described in Figures 5.14 through 5.19 with those in round one as shown in Figures 5.4 through 5.9, and notice that the increased cropland would mainly be developed in the northern hemisphere, Canada and Russia for example. An important reason is that the temperature in these high-latitude areas is very low and not suitable for crop growth before 2000, and such conditions would not be improved during the 21st century in the first round because the temperature is assumed to be constant. When we also include the feedbacks of climate, GHGs, and tropospheric ozone in this round, the temperature would increase, and these areas might be more suitable than before to develop cropland. We assume that biomass would occur in the grid cells with the existence of cropland, and therefore, we would also observe more land devoted to biomass-energy production in these regions. Taking the Former Soviet Union (FSU) as an example, in the first round, its cropland would be 19.3% (baseline) and 18.9% (policy case) in 2100; in the second round, such figures would increase to 33.8% and 31%, respectively. The cropland in those regions that are main providers of crop products, China and India for example, cropland would expand more than in the first round.

Similar to the first round, in the locations of large-scale production of biomass energy, we would observe the decrease of cropland and un-managed forestry land, as indicated in eastern United States, Amazon rain forest areas, southern

Africa, Indonesia, etc. Such trends are more obvious in the policy scenario because there would be more land devoted to biomass-energy production.

Tables 5.12 and 5.13 indicate the projected land rent of the five types of agricultural land in each EPPA region in 2100. In addition to the absolute land rent in 2100, we indicate the land-rent ratio, indicated by the land rent in 2100 over that in 2000, in the parentheses.

Table 5.12: Regional rent of the five types of agricultural land in 2100 in round two - baseline

Unit: $ per hectare

	Cropland	Managed forestry land	Pasture land	Un-managed forestry land	Un-managed grassland
AFR	59.4 (1.3)	61.0 (30.5)	38.0 (18.1)	36.0 (60.0)	33.1 (165.4)
ANZ	30.7 (0.3)	25.0 (3.2)	9.4 (2.3)	8.5 (10.6)	8.5 (7.7)
ASI	692.4 (1.4)	750.5 (15.1)	593.0 (6.7)	498.4 (249.2)	0.0 (1.0)
CAN	68.0 (1.3)	37.1 (1.9)	36.4 (1.0)	8.0 (8.0)	0.0 (1.0)
CHN	1662.8 (7.5)	635.0 (50.0)	1009.1 (72.6)	472.1 (262.3)	605.8 (302.9)
EET	567.4 (4.9)	255.0 (17.0)	533.0 (5.8)	180.9 (5.4)	351.8 (17.5)
EUR	405.5 (1.0)	102.3 (11.0)	224.1 (1.7)	61.4 (18.6)	106.3 (8.5)
FSU	63.0 (2.1)	29.4 (8.9)	22.1 (4.8)	17.6 (87.8)	30.3 (30.3)
IDZ	1095.6 (2.0)	1074.8 (19.4)	671.6 (5.5)	441.6 (315.4)	637.3 (9.4)
IND	1188.9 (5.6)	745.7 (46.9)	894.2 (2.0)	572.2 (178.8)	0.0 (1.0)
JPN	2557.7 (1.5)	140.2 (4.8)	1482.1 (1.3)	87.6 (15.1)	0.0 (1.0)
LAM	127.9 (0.9)	112.4 (74.9)	67.2 (4.7)	59.9 (300.1)	62.1 (36.5)
MES	125.5 (0.5)	169.7 (8.2)	35.3 (8.2)	42.0 (19.1)	33.8 (84.4)
MEX	215.2 (0.6)	124.1 (18.8)	99.0 (7.5)	84.4 (29.1)	102.0 (42.5)
ROW	251.6 (1.3)	177.4 (8.1)	144.0 (7.7)	115.2 (64.0)	117.5 (43.5)
USA	231.8 (1.2)	91.3 (36.5)	85.6 (2.0)	49.7 (35.5)	79.0 (31.6)

Source: EPPA simulation, September 2007.

Note: 1. Details of the regional composition are provided in Table 3.1.
2. The number in the parentheses indicates the land-rent ratio, calculated as the land rent in 2100 over that in 2000.

Table 5.13: Regional rent of the five types of agricultural land in 2100 in round two - policy scenario
Unit: $ per hectare

	Cropland	Managed forestry land	Pasture land	Un-managed forestry land	Un-managed grassland
AFR	41.1 (0.9)	52.6 (26.3)	31.1 (14.8)	30.1 (50.1)	25.1 (125.3)
ANZ	40.9 (0.4)	33.5 (4.3)	20.1 (4.9)	12.2 (15.3)	15.4 (14.0)
ASI	791.4 (1.6)	919.5 (18.5)	672.6 (7.6)	651.6 (325.8)	0.0 (1.0)
CAN	62.8 (1.2)	56.6 (2.9)	47.3 (1.3)	15.3 (15.3)	0.0 (1.0)
CHN	1285.9 (5.8)	613.4 (48.3)	742.3 (53.4)	468.7 (260.4)	563.6 (281.8)
EET	567.4 (4.9)	288.0 (19.2)	468.7 (5.1)	251.3 (7.5)	263.3 (13.1)
EUR	446.1 (1.1)	184.1 (19.8)	263.6 (2.0)	112.5 (34.1)	140.0 (11.2)
FSU	72.0 (2.4)	46.2 (14.0)	33.1 (7.2)	28.3 (141.6)	35.5 (35.5)
IDZ	1040.8 (1.9)	1739.6 (31.4)	818.1 (6.7)	753.8 (538.4)	833.9 (12.3)
IND	764.3 (3.6)	572.4 (36.0)	625.9 (1.4)	430.7 (134.6)	0.0 (1.0)
JPN	1875.6 (1.1)	163.5 (5.6)	1140.1 (1.0)	99.8 (17.2)	0.0 (1.0)
LAM	99.5 (0.7)	104.0 (69.3)	58.6 (4.1)	65.4 (327.1)	47.8 (28.1)
MES	125.5 (0.5)	115.9 (5.6)	37.4 (8.7)	27.9 (12.7)	33.1 (82.8)
MEX	251.1 (0.7)	199.3 (30.2)	155.8 (11.8)	143.0 (49.3)	172.1 (71.7)
ROW	232.2 (1.2)	234.3 (10.7)	183.3 (9.8)	141.1 (78.4)	136.4 (50.5)
USA	309.1 (1.6)	176.0 (70.4)	149.8 (3.5)	110.5 (78.9)	138.3 (55.3)

Source: EPPA simulation, September 2007.
Note: 1. Details of the regional composition are provided in Table 3.1.
2. The number in the parentheses indicates the land-rent ratio, calculated as the land rent in 2100 over that in 2000.

As indicated in Tables 5.12 and 5.13, we observe a big increase in the rent of un-managed forestry land in those biomass-producing regions because the supply of un-managed forestry land would be scarce during the 21st century to give space to biomass-energy production. Also considering that the rent of un-managed forestry land is affected by its availability within the region, we would observe the highest increase of un-managed forestry land in Indonesia (IDZ), reaching $441.6/hectare in the baseline and $753.8/hectare in the policy scenario in 2100, which would be 315.4 and 538.4 times that in 2000, respectively. We would observe the second highest increase in un-managed forestry land rent in Central and South America (LAM), reaching $59.9/hectare in the baseline and $65.4/hectare in the policy scenario, both of which would be more than 300 times higher than the rent in 2000. In the United States (USA) and Africa (AFR), where the biomass-energy production would be developed in a large scale but abundant un-managed forestry land would be available, the rent of un-managed forestry land would increase, but not as high as those observed in IDZ.

If the GHG-mitigation policies were implemented, more un-managed forestry land would be converted to biomass-energy production, and this would lead to a generally higher rent of un-managed forestry land than in the baseline. Taking the United States as an example, the rent of un-managed forestry land in the baseline in 2100 would be $49.5/hectare, 35.5 times that in 2000; while that in the policy scenario would be $110.5, 78.9 times that in 2000. Because of the high demand for biomass energy, some un-managed grassland would also be converted to produce biomass energy, leading to the increase of un-managed grassland rent. In those regions without biomass-energy production but with large-scale cropland expansion, China (CHN) and India (IND) for example, the rent of un-managed land would increase because the cropland would be expanded at the expense of un-managed land. Taking China as an example, its un-managed forestry land rent in 2100 would reach $472.1/hectare (baseline) and $468.7/hectare (policy scenario), which would be 262.3 and 260.4 times that in 2000, respectively.

As I stated in the first round, the availability of un-managed land would also affect the rent of cropland. In those regions with abundant un-managed land, the rent of cropland would not increase a lot, such as the United States (baseline: $231.8/hectare in 2100, 1.2 times that in 2000; policy case: $309.1/hectare in 2100, 1.6 times that in 2000). However, in those regions with few supplies of un-managed land, the rent of cropland would increase a lot: taking China as an example, its cropland rent in 2100 would be $1662.8/hectare in the baseline and $1285.9/hectare in the policy scenario, which would be 7.5 and 5.8 times that in 2000, respectively.

To highlight the land-rent effects caused by the feedbacks of climate, GHGs, and tropospheric ozone, we indicate in Tables 5.14 and 5.15 the differences between the two rounds in terms of regional land rent of the five types of agricultural land in the two climate scenarios in 2100.

Table 5.14: Differences between round one and round two on regional land rent in 2100 in the baseline

Unit: $ per hectare

	Cropland	Managed forestry land	Pasture land	Un-managed forestry land	Un-managed grassland
AFR	-13.7	20.0	-3.0	3.0	4.2
ANZ	-61.4	-24.9	-3.3	-4.6	-5.0
ASI	-99.0	362.8	185.9	345.8	0.0
CAN	-10.5	-50.7	-18.2	-3.5	0.0
CHN	886.8	326.4	696.3	225.1	344.2
EET	266.3	-18.0	183.8	-137.4	48.3
EUR	0.0	20.5	26.4	20.8	13.8
FSU	6.0	1.0	-9.6	6.9	5.3
IDZ	109.6	387.8	-134.3	120.4	-108.5
IND	339.7	294.1	134.1	233.6	0.0
JPN	1193.6	-90.5	-114.0	19.2	0.0
LAM	-71.0	51.0	8.6	9.2	4.5
MES	-150.6	-14.5	-13.7	-25.8	-4.8
MEX	-71.8	21.1	-1.3	6.7	22.8
ROW	-77.4	0.0	-33.7	39.1	20.0
USA	-19.4	38.8	17.1	19.9	25.0

Source: EPPA simulation, September 2007

Note: Details of the regional composition are provided in Table 3.1.

Table 5.15: Differences between round one and round two on regional land rent in 2100 in the policy scenario

Unit: $ per hectare

	Cropland	Managed forestry land	Pasture land	Un-managed forestry land	Un-managed grassland
AFR	-22.9	16.4	-5	2.1	0.0
ANZ	-51.2	-16.4	4.5	-0.6	1.0
ASI	-49.4	477.2	212.4	439.6	0.0
CAN	-36.6	-29.2	-7.3	5.0	0.0
CHN	532.1	336.5	461.5	253.6	337.2
EET	277.9	25.5	128.7	-56.9	-32.2
EUR	-40.5	44.6	13.2	14.5	21.2
FSU	3.0	11.2	-6	13.3	10.4
IDZ	0.0	980.6	85.5	361.8	20.3
IND	84.9	273.5	44.7	236.1	0.0
JPN	511.5	-70.1	-456	33.7	0.0
LAM	-99.4	42.5	0.0	14.6	0.9
MES	-150.6	-37.3	8.6	-3.6	15.4
MEX	-107.6	54.8	14.6	22.9	49.9
ROW	-96.8	46	-5.6	55.1	28.4
USA	-19.3	58.2	34.2	15.9	17.3

Source: EPPA simulation, September 2007

Note: Details of the regional composition are provided in Table 3.1.

In comparison with the first round, when we include the feedbacks of climate, GHGs, and tropospheric ozone in this round, in those regions with large-scale biomass-energy production, more un-managed forestry land would need to be converted to biomass-energy production than in the first round, leading to an even higher increase in the rent of un-managed forestry land. Taking Central and South America (LAM) as an example, the inclusion of the feedbacks of climate, GHGs, and tropospheric ozone would lead to an additional rent increase of un-managed forestry land of $9.2/hectare in the baseline and $14.6/hectare in the policy scenario. Higher income East Asia (ASI: +$345.8/hectare in the baseline and

+$439.6/hectare in the policy scenario) and Indonesia (IDZ: +$120.4/hectare in the baseline and +$361.8/hectare in the policy scenario) are two other examples in this aspect. The increase of un-managed forestry land rent in ASI and IDZ would be sharper than that in LAM, because the availability of un-managed forestry land in the former two regions would be much less than that in LAM.

The availability of un-managed land would also affect the cropland rent. After including the feedbacks of climate, GHGs, and tropospheric ozone, the demand for cropland would be higher than in the first round, leading to the increase of cropland rent, especially in those regions with large-scale crop production but with few supplies of un-managed land. In addition, the rent of un-managed land in those regions would also increase. Taking China as an example, the inclusion of the feedbacks of climate, GHGs, and tropospheric ozone would lead to an additional increase of cropland rent of $886.8/hectare in the baseline and $532.1/hectare in the policy scenario. Such figures would be $225.1/hectare (baseline) and $253.6/hectare (policy scenario) for un-managed forestry land, and $344.2/hectare (baseline) and $337.2/hectare (policy scenario) for un-managed grassland in China, respectively.

Based on the projected global agricultural land use during the 21st century, MBL researchers apply the TEM to simulate the carbon stored in the five types of agricultural land during the 21st century. To highlight the feedbacks of climate, GHGs, and tropospheric ozone, I indicate in Tables 5.16 and 5.17 the projected carbon stored in the five types of agricultural land globally in both rounds, as well as the differences between the two rounds.

Table 5.16: Carbon stored in the five types of agricultural land in the baseline
Unit: Billions of metric tons (bmt)

Year	1st round	2nd round	Difference
2000	573.4	573.4	0.0
2010	560.6	531.5	-29.1
2020	555.6	501.7	-53.9
2030	541.4	453.7	-87.7
2040	519.7	384.2	-135.5
2050	489.2	347.1	-142.1
2060	454.3	329.7	-124.6
2070	442.1	322.3	-119.8
2080	427.9	316.5	-111.4
2090	419.3	318.1	-101.2
2100	411.9	321.7	-90.1
Carbon storage loss (2100-2000)	-161.6	-251.7	-90.1

Source: TEM simulation, August 2007.

Table 5.17: Carbon stored in the five types of agricultural land in the policy scenario
Unit: Billions of metric tons (bmt)

Year	1st round	2nd round	Difference
2000	573.4	573.4	0.0
2010	560.9	532.7	-28.2
2020	555.2	504.3	-50.9
2030	537.7	441.6	-96.1
2040	486.6	372.4	-114.2
2050	433.7	325.1	-108.6
2060	417.3	307.3	-110.0
2070	404.9	289.3	-115.6
2080	392.5	281.7	-110.8
2090	387.8	277.4	-110.4
2100	384.6	274.8	-109.8
Carbon storage loss (2100-2000)	-188.8	-298.6	-109.8

Source: TEM simulation, August 2007.

As indicated in Table 5.16, in the baseline, the carbon stored in the five types of agricultural land in 2000 was 573.4 bmt, and such a figure in 2100 would be 411.9 bmt in the first round and 321.7 bmt in the second round. In other words, in the baseline, the carbon stored in the five types of agricultural land would experience a loss of 161.6 bmt in the first round and 251.7 bmt in the second round. The difference between the two rounds, which would amount to 90.1 bmt, is the additional carbon-storage loss caused by the feedbacks of climate, GHGs, and tropospheric ozone.

If the GHG-mitigation policies were implemented during the 21st century, as indicated in Table 5.17, the carbon stored in the five types of agricultural land would experience a loss of 188.8 bmt in the first round and 298.6 bmt in the second round. In other words, the inclusion of feedbacks of climate, GHGs, and tropospheric ozone would lead to an additional carbon-storage loss in the five types of agricultural land of 109.8 bmt during the 21st century.

Therefore, after we include the feedbacks of climate, GHGs, and tropospheric ozone as well as the impacts of economic forces in this round, in the baseline, the carbon stored in the five types of agricultural land would experience a loss of 251.7 bmt, equaling to 12% of the total anthropogenic GHG emissions globally during the 21st century. The implementation of GHG-mitigation policies would increase such a loss to 298.6 bmt, which equals to 36.8% of the total anthropogenic GHG emissions globally during the 21st century.

As I stated, in comparison with the baseline, the implementation of GHG-mitigation policies would lead to a larger-scale production of biomass energy, which would reduce the GHG emissions by replacing the conventional fossil-based energy sources. However, the large-scale production of biomass energy would lead to the conversion of the five types of agricultural land, and therefore, result in the carbon-storage loss in agricultural land, which would increase the atmospheric GHG concentrations. According to the EPPA predictions, in the first round, in comparison with the baseline, the reduction in GHG emissions in the policy scenario by using more biomass energy would be 125 bmt (carbon equivalent); however, the land-use conversion as a result of larger-scale production of biomass energy would increase the atmospheric GHG emissions by 28 bmt (carbon equivalent) during the 21st century. In the second round, such figures would be 136 bmt and 47 bmt, respectively. In other words, although the GHG-mitigation policies would generally reduce the atmospheric GHG emissions by using more energy from biomass, part of the endeavors would be counteracted by the land-use conversion as a result of large-scale production of biomass energy.

In summary, when we also include the feedbacks of climate, GHGs, and tropospheric ozone in this round, in comparison with the first round, the productivity of cropland and biomass land would decrease in most regions, while that for managed and un-managed forestry land would generally increase. In comparison with the first round, more land would need to be devoted to the production of crops and biomass energy through the sacrifice of other types of agricultural land, especially un-managed forestry land. In addition to affecting the rent of the five types of agricultural land, such land-use conversion would result in a significant loss of carbon stored in the five types of agricultural land. In both rounds, in comparison with the baseline, the implementation of GHG-mitigation policies would lead to more biomass-energy production, more land-use conversion, and a more severe carbon-storage loss; as a result, the GHG-mitigation endeavors of such policies would be partly counteracted. Therefore, my hypothesis on biomass-energy production, land-use conversion, and carbon storage in the five types of agricultural land of the two climate scenarios is confirmed again.

Chapter 6
Conclusions and Implications

In this chapter, based on the two rounds of analysis in Chapter 5, I offer some conclusions and implications of this research.

Conclusions

In this research, I conduct a comprehensive impact assessment of GHG-mitigation policies on the five types of agricultural land during the 21st century: cropland, managed forestry land, pasture land, un-managed forestry land, and un-managed grassland. In addition, I include biomass-energy production as well as the resultant land-use effects. I develop the downscaling methods based on the econometric land-use model to link the impacts driven by economic forces at the regional scale with the feedbacks of climate, GHGs, and tropospheric ozone at the grid-cell scale. Applying these approaches in two climate scenarios with and without GHG mitigation, I analyze the impacts of GHG policies on land use, land rent, and resultant carbon storage loss in the five types of agricultural land. To identify the impacts of economic forces with the feedbacks of climate, GHGs, and tropospheric ozone, I conduct the study in two rounds: in the first round, only the impacts of economic forces are included, while in the second round, the feedbacks of climate, GHGs, and tropospheric ozone are also included.

My research indicates that when considering the impacts of economic forces only, 9.9% of global land would be devoted to biomass-energy production in 2100, and the carbon stored in the five types of agricultural land would experience a loss of

161.6 billion metric tons (bmt) during the 21st century. If the GHG-mitigation policies were implemented, such figures would increase to 14.4% and 188.8 bmt, respectively. When the feedbacks of climate, GHGs, and tropospheric ozone are also included, such figures would increase to 13.4% and 251.7 bmt in the baseline, and 19.1% and 298.6 bmt in the policy scenario, respectively. In other words, with the inclusion of the feedbacks of climate, GHGs, and tropospheric ozone in this research, there would be an additional 3.5% (baseline) and 4.7% (policy scenario) of global land devoted to biomass-energy production, leading to an additional carbon-storage loss of 90.1 bmt (baseline) and 109.8 bmt (policy scenario).

From these two rounds of analysis, the conclusion follows that biomass-energy production would be developed on a large scale at the expense of the conversion of the five types of agricultural land, especially un-managed forestry land. As a result, the carbon stored in such land would experience a significant loss during the 21st century. In comparison with the baseline without any GHG mitigation, the foremost policies to mitigate GHG emissions globally would lead to more biomass-energy production, more land-use conversion, and therefore, a more severe carbon-storage loss. When the feedbacks of climate, GHGs, and tropospheric ozone are included in addition to the impacts of economic forces, there would be more land devoted to biomass-energy production; therefore, we would observe an even more severe loss of carbon stored in the five types of agricultural land.

I confirm the hypothesis that biomass-energy production would lead to the conversion of the five types of agricultural land, and the carbon stored in such land would decrease; the policies to mitigate GHG emissions, leading to more production of biomass energy and conversion of agricultural land, would cause an even more severe loss of the carbon stored in agricultural land. Although the GHG-mitigation policies would generally reduce the atmospheric GHG emissions by using more energy from biomass, such endeavors would be partly counteracted by the land-use conversion as a result of large-scale production of biomass energy.

From this research, we should realize that the policy makers should take the land-use effects of biomass-energy production into consideration when developing the GHG-mitigation policies, because the capacity of agricultural land to store carbon might be diminished, and thereby undermine the effectiveness of GHG-mitigation endeavors.

Implications

There are several implications for studies assessing the GHG-mitigation policies on agricultural land:

(1) We have been connecting the EPPA model and the TEM with a "once-through" process. In other words, we run the EPPA model for 100 years from 2000 to 2100, while MBL researchers run the TEM for the same period separately. As I have indicated in my research, the land-use changes would cause a significant loss of carbon stored in agricultural land, and therefore, lead to an increase of

atmospheric concentration of GHGs such as CO_2, which would further affect land use through the additional feedbacks of climate, GHGs, and tropospheric ozone. However, I did not include such additional impacts on land use in this research. In the future, as indicated in Figure 6.1, we would link the EPPA model and the TEM throughout the 21st century.

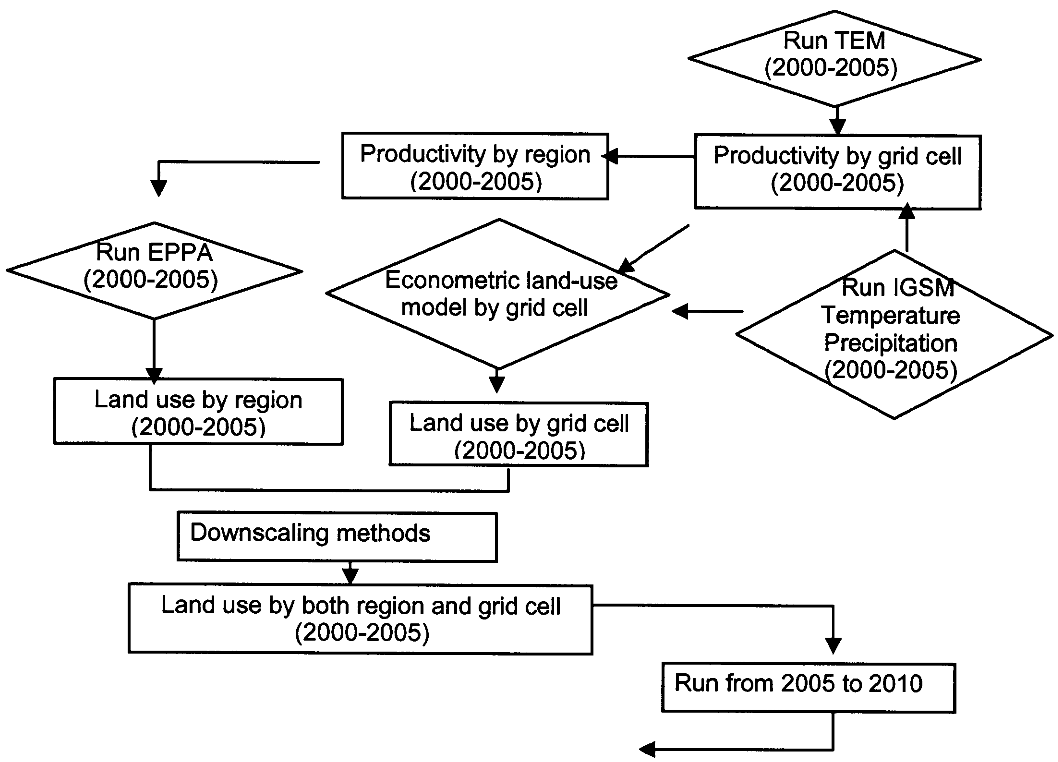

Figure 6.1: Impact linkage between the EPPA model and the TEM
Source: the author.

(2) Five types of agricultural land are included in this research: cropland, managed forestry land, pasture land, un-managed forestry land, and un-managed grassland. As I noted in Chapter 2, different agricultural plants react differently to climate in terms of growth and photosynthesis rate, resource acquisition, etc. In the future, a

more detailed subdivision of agricultural land would be helpful for understanding the impacts on agricultural land of changes in climate caused by GHG policies. For example, we could conduct the research based on the classification of agricultural land growing cotton, rice, wheat, barley, soybeans, maize, sorghum, sugar cane, onions, etc.

(3) In the econometric land-use model, I describe agricultural land use as a function of land productivities, temperature, precipitation, and human accessibility. Some other factors, such as irrigation and land slope, might also affect agricultural land use. However, because of insufficient data, I did not include such information in the econometric model. In addition, the historical data on land use, climate, and human accessibility from 2001 to 2007 are not available. If and when such data become available, we will be able to increase the accuracy of the econometric land-use model, and therefore improve the downscaling methods to distribute regional economic effects to finer spatial resolutions.

To re-emphasize the fundamental rationale for the possible future research in this area: on a matter so crucial for humanity's future, we must do our utmost to discern whether proposed GHG-mitigation policies are likely to make our future better or worse.

References

Adams, R. M., C. Rosenzweig, R. M. Peart, J. T. Richie, B. A. McCarl, J. D. Glyer, R. B. Curry, J. W. Jones, K. J. Boote, and L. H. Allen. 1990. "Global climate change and U.S. agriculture." *Nature*, Vol. 345, pp: 219-224.

Alig, R. J., D. M. Adams, and B. A. McCarl. 2003. "Projecting impacts of global climate change on the U.S. forest and agriculture sectors and carbon budgets." *Forest Ecology and Management*, Vol. 169, pp: 3-14.

Armington, P. S. 1969. *A Theory of Demand for Products Distinguished by Place of Production*. International Monetary Fund Staff Papers, Vol. 16, pp: 159-176.

Atkinson, C. J., J. M. Taylor, D. Wilkins, R. T. Besford. 1997. "Effect of elevated CO2 on chloroplast components, gas exchange and growth of oak and cherry." *Tree Physiology*, Vol. 17, pp: 319-325.

Baker, J. T., and L. H. Allen. 1993. "Contrasting crop species responses to CO_2 and temperature: rice, soybean and citrus." Vegetation, Vol. 104, pp: 239-260.

Bazzaz, F. A. 1990. "The responses of natural ecosystems to the rising global CO_2 levels." *Annual Review of Ecological System*, Vol. 21, pp: 187-196.

Berryman, C. A., D. Eamus, and G. A. Duff. 1994. "Stomatal responses to a range of variables in two tropical tree species grown with CO_2 enrichment." Journal of Experimental Botany, Vol. 45, pp: 539-546.

Beyers, J. L. G. H. Riechers, and P. J. Temple. 1992. "Effects of long-term ozone exposure and drought on the photosynthetic capacity of ponderosa pine." *New Phytologist*, Vol. 122, pp: 81-90.

Byrd, G. T., and R. H. Brown. 1989. "Influence of CO_2 and O_2 during growth on photorespiratory characteristics and leaf anatomy." *Plant Physiology*, Vol. 90, pp: 1022-1028.

Charles, H., and J. Dukes. 2007. "Effects of warming and altered precipitation on plant and nutrient dynamics of New England salt marshes." ESA/SER Joint Meeting, August 5 – August 10, 2007. San Jose, California.

Clark, D A, S. Brown. D. W. Kicklighter, J. Q. Chambers, J. R. Thomlinson, J. Ni. 2001. "Measuring net primary production in forests: Concepts and field methods." *Ecological Applications*, Vol. 11, pp: 356-370.

Coleman, J. S., and F. A. Bazzaz. 1992. "Effects of CO_2 and temperature on growth and resource use of Co-occurring C_3 and C_4 annuals." *Ecological Society of America*, Vol. 73 (4), pp: 1244-1259.

Darwin, R., M. Tsigas, J. Lewandrowski, and A. Raneses. 1996. "Land use and cover in ecological economics." *Ecological Economics*, Vol. 17, pp: 157-181.

Darwin, R., and D. Kennedy. 2000. "Economic effects of CO_2 fertilization of crops: transforming changes in yield into changes in supply." *Environmental Modeling and Assessment*, Vol. 5 (3), pp: 157-168.

Demographia. 2007. *World Urban Areas: All Identified World Urbanized Areas 500,000+ and Others – Population and Density.*
URL: http://www.demographia.com/db-worldua.pdf

Dimaranan, B., and R. McDougall. 2002. "Global trade, assistance and production: the GTAP5 data base." Center for Global Trade Analysis, Purdue University, West Lafayette, Indiana.

Edwards, Paul N. 2000. "A Brief History of Atmospheric General Circulation Modeling." *General Circulation Model Development*, edited by David A. Randall, pp. 67-90. San Diego, CA: Academic Press.

Energy Information Administration, 2007.
URL: http://www.eia.doe.gov/emeu/international/oilprice.html

FAO (Food and Agriculture Organization). 1996. "Direct and indirect effects of changing hydrological, pedological and plant physiological processes." *Global Climate Change and Agricultural Production*. John Wiley & Sons Ltd., London.

FAO (Food and Agriculture Organization). 2002. *World Agriculture: Towards 2015/2030 Summary Report.* Food and Agriculture Organization of the United Nations, Rome, pp.75.

FAO (Food and Agriculture Organization). 2003. *World Agriculture: Towards 2015/2030 An FAO Perspective*, Earthscan Publishing Ltd., London.

Farmar-Bowers, Quentin, Jim Crosthwaite, Julia Callaghan, Carole Hollier, and Andrew Straker. 2006. *Matching opportunities to motivations: ideas for biodiversity and NRM policy based on understanding the drivers of land use change that matter to farmers.* The Drivers of Land Use Change (DLUC) Project Report, pp: 6-7.

Felzer, B., T. Cronin, J. Melillo, J. Reilly, X. Wang, and D. Kicklighter. 2007. "Impact of ozone on trees and crops." *CRAS Geoscience*, forthcoming.

Felzer, B., J. Reilly, J. M. Melillo, D. W. Kicklighter, C. Wang, R. Prinn, M. Sarofim, Q. Zhuang. 2004. *Past and future effects of ozone on net primary productivity and carbon sequestration using a global biogeochemical model.* Joint Program Report No. 103. MIT, Cambridge, Massachusetts.

Felzer, B., J. Reilly, J. M. Melillo, D. W. Kicklighter, M. Sarofim, C. Wang, R. Prinn, and Q. Zhuang. 2005. "Future effects of ozone on carbon sequestration and climate change policy using a global biogeochemical model." *Climate Change*, Vol. 73, pp: 345-373.

Fiscus, E. L., L. B. Fitzgarrald, and K. O. BUrkey. 2005. "Crop responses to ozone: uptake, modes of action, carbon assimilation and partitioning." *Plant, Cell and Environment*, Vol. 28, pp: 997-1011.

Fredericksen, T. S., J. M. Skelly, K. C. Steiner, T. E. Kolb, and K. B. Kouterick. 1996. "Size-mediated foliar response to ozone in black cherry trees." *Environmental Pollution*, Vol. 91, pp: 53-63.

Grulke, N. E., and P. R. Miller. 1994. "Changes in gas exchange characteristics during the lifespan of giant sequoia: implications for response to current and future concentrations of atmospheric ozone." *Tree Physiology*, Vol. 14, pp: 659-668.

Hurtt, G. C., S. Frolking, M. G. Fearon, B. Moore, E. Shevliakovas, S. Malyshev, S. W. Pacala and R. A. Houghton. 2006. "The underpinnings of land-use history: three centuries of global gridded land-use transitions, wood-harvest activity, and resulting secondary lands." *Global Change Biology*, Vol. 12, pp: 1208-1229.

International Energy Outlook. 2007. Chapter 3: Petroleum and Other Liquid Fuels, pp: 29-38.

IPCC (Intergovernmental Panel on Climate Change). 1996. *Climate Change 1995: Impacts, Adaptations, and Mitigation of Climate Change: Scientific-Technical Analyses*, R. T. Watson, M. C. Zinyowera, and R. H. Moss, eds., Contribution of Working Group II to the Second Assessment Report of the Intergovernmental Panel on Climate Change, Cambridge University Press, Cambridge, U. K.

IPCC (Intergovernmental Panel on Climate Change). 2001. *Climate Change 2001: the Scientific Basis.* Cambridge University Press, New York.

IPCC (Intergovernmental Panel on Climate Change). 2007. *Climate Change 2007: The Physical Science Basis.* Contribution of Working Group I to the Fourth Assessment Report of the Intergovernmental Panel on Climate Change.

Jacoby, H. D., R. S. Eckaus, A. D. Ellerman, R. G. Prinn, D. M. Reiner and Z. Yang. 1997. "CO_2 emissions limits: economic adjustments and the distribution of burdens". *The Energy Journal*, Vol. 18 (3), pp: 31-58. *MIT Joint Program on the Science and Policy of Global Change, Report 9, 1997.* Cambridge, Massachusetts.

Jensen, L. S., Mueller, T., Tate, K. R., Riss, D. J., Magid, J. and Nielsen, N. E. 1996. "Soil surface CO_2 flux as an index of soil respiration in situ: a comparison of two chamber methods." *Soil Biology and Biochemistry*, Vol. 28, pp: 1297-1306.

Kicklighter, D. W., A. Bondeau, A. L. Schloss, J. Kaduk, A. D. McGuire, and the participations of the Potsdam NPP Model Intercomparison. 1999. "Comparing global models of terrestrial net primary productivity (NPP): global pattern and differentiation by major biomes." Global *Change Bio.*, 5 (1), pp: 16-24.

Korner, Ch., and F. I. Woodward. 1987. "The dynamics of leaf extension in plants with diverse altitudinal ranges." Oecologia, Vol. 72, pp: 279-283.

Lee, H. L., T. W. Hertel, B. Sohngen, and N. Ramankutty. 2005. "Towards An Integrated Land Use Database for Assessing the Potential for Greenhouse Gas Mitigation." GTAP Technical Paper No. 25. Center for Global Trade Analysis, Department of Agricultural Economics, Purdue University.

Mauzerall, D. L., and X. Wang. 2001. "Protecting agricultural crops from the effects of tropospheric ozone exposure: reconciling science and standard setting in the United States, Europe, and Asia." *Annual Review of Energy Environment*, Vol, 26, pp: 237-268.

McFarland, J. R., J. M. Reilly, and H. J. Herzog. 2004. "Representing energy technologies in top-down economic models using bottom-up information." *Energy Economics*, Vol. 26, pp: 685-707.

Melillo J. M., A. D. McGuire, D. W. Kicklighter, B. Moore III, C. J. Vorosmarty, and A. L. Schloss. 1993. "Global climate change and terrestrial net primary production." *Nature,* Vol. 363, pp: 234-240.

Melillo J. M., R. A. Houghton, D. W. Kicklighter, A. D. McGuire. 1996. "Tropical deforestation and the global carbon budget." *Annual Review of Energy and the Environment*, Vol. 21, pp: 293-310.

McFarland, J., J. Reilly, and H. J. Herzog. 2004. "Representing energy technologies in top-down economic models using bottom-up information." *Energy Economics*, Vol. 26, pp: 685-707.

McGuire, A. D., S. Sitch, J. S. Clein, R. Dargaville, G. Esser, J. Foley, M. Heimann, F. Joos, J. Kaplan, D. W. Kicklighter, R. A. Meier, J. M. Melillo, B. M. III, I. C. Prentice, N. Ramankutty, T. Reichenau, A. Schloss, H. Tian, L. J. Williams, and U. Wittenberg. 2001. "Carbon balance of the terrestrial biosphere in the twentieth century: analysis of CO_2, climate and land-use effects with four process-based ecosystem models." *Global Biogeochemical Cycles*, Vol. 15, pp: 183-206.

McLaughlin, S. B., and D. J. Downing. 1995. "Interactive effects of ambient ozone and climate measured on growth of mature forest trees." *Nature*, Vol. 374, pp: 252-254.

Mendelsohn, R., W. D. Nordhaus, and D. Shaw. 1994. "The impact of global warming on agriculture: a Richardian analysis." *American Economic Review,* Vol. 84 (4), pp: 753-771.

Moreira, J. R. 2004. "Global biomass energy potential." Paper presented at the Expert Workshop on Greenhouse Gas Emissions and Abrupt Climate Change, Paris, France, September 30th to October 1st, 2004.

Paltsev, S., J. Reilly, H. Jacoby, R. Eckaus, J. McFarland, M. Sarofim, M. Asadoorian, and M. Babiker. "The MIT Emissions Prediction and Policy Analysis (EPPA) Model: Version 4." *MIT Joint Program on the Science and Policy of Global Change Report 125, 2005.* Cambridge, Massachusetts.

Paltsev, S., H. Jacoby, J. Reilly, L. Viguier, and M. Babiker. 2004. "Modeling the transport sector: the role of existing fuel taxes". *Energy and Environment*, R. Loulou, J. - P. Waaub and G. Zaccour (eds.), Springer: New York, pp: 221-238.

Paltsev, S., J. Reilly, H. Jacoby, A. Gurgel, G. Metcalf, A. Sokolov, and J. Holak. 2007. "Assessment of U.S. Cap-and-Trade Proposals." *MIT Joint Program on the Science and Policy of Global Change, Report 146, 2007.* Cambridge, Massachusetts.

Parry, M. L., C. Rosenzweig, A. Iglesias, M. Livermore, and G. Fischer. 2004. "Effects of climate change on global food production under SRES emissions and socio-economic scenarios." *Global Environmental Change*, Vol. 14, pp: 53-67.

Percy, K., M. Nosal, W. Heilman, T. Dann, J. Sober, and D. Karnosky. 2006. *The North American ozone air quality standard: efficacy and performance with two northern hardwood forest tree species.* Letzte Aktualisierung.

Prinn, R. G., H. D. Jacoby, A. Sokolov, C. Wang, X. Xiao, Z. Yang, R. S. Eckaus, P. A. Stone, A. D. Ellerman, J. Melillo, J. Fitzmaurice, D. Kicklighter, G. Holian, and Y. Liu. 1999. "Integrated global system model for climate policy assessment: feedbacks and sensitivity studies." *Climate Change*, 41, pp: 469-546.

Raich, J. W., E. B. Rastetter, J. M. Melillo, D. W. Kicklighter, P. A. Steudler, B. J. Peterson, A. L. Grace, B. Moore III, C. J. Vorosmarty. 1991. "Potential net primary productivity in South America: application of a global model." *Ecological Application*, 1, pp: 399-429.

Rebbeck, J., and K. F. Jensen. 1993. "Ozone effects on grafted mature and juvenile red spruce: photosynthesis, stomatal conductance, and chlorophyll concentration." *Canadian Journal for Research*, Vol. 23, pp: 450-456.

Reich, P. B. 1987. "Quantifying plant response to ozone: a unifying theory." Tree Physiology, Vol. 3, pp: 63-91.

Reich, P. B., and R. G. Amundson. 1985. "Ambient levels of ozone reduce net photosynthesis in tree and crop species." *Science*, Vol. 230, pp: 566-570.

Reilly, J. and N. Hohmann. 1993. "Climate change and agriculture: the role of international trade." *American Economic Review: Papers and Proceedings*, Vol. 83, pp: 306-312.

Reilly, J, M. Mayer, and J. Harnisch. 2002. "The Kyoto Protocol and Non-CO2 Greenhouse Gases and Carbon Sinks." *Environmental Modeling and Assessment*, Vol. 7(4), pp: 217-229 (see also MIT Joint Program on the Science and Policy of Global Change, Report 58).

Reilly, J., F. Tubiello, B. McCarl, D. Abler, R. Darwin, K. Fuglie, S. Hollinger, C. Izaurralde, S. Jagtap, J. Jones, L. Mearns, D. Ojima, E. Paul, K. Paustian, S. Riha, N. Rosenberg, C. Rosenzweig. 2003. "U.S. agriculture and climate change: new results." Climate Change, Vol. 57, pp: 43-69.

Reilly, J., M. Sarofim, S. Paltsev, R. Prinn. 2005. "The role of non-CO2 greenhouse gases in climate policy: analysis using the MIT IGSM." *Energy Journal*, in press (see also MIT Joint Program on the Science and Policy of Global Change, Report 114).

Reilly, J. 2005. Approach and progress on integrating land-use change in the MIT IGSM. EMF 22 Working Group Meeting, Stanford University, May 25-27, 2005.

Reilly, J., S. Paltsev, B. Felzer, X. Wang, D. Kicklighter, J. Melillo, R. Prinn, M. Sarofim, A. Sokolov, and C. Wang. 2007. "Global economic effects of changes in crops, pasture, and forests due to changing climate, carbon dioxide, and ozone." *Energy Policy*, Vol. 35, pp: 5370-5383.

Reiner, D. M. and H. D. Jacoby. 1997. Annex I Differentiation Proposals: Immplications for Welfare, Equity and Policy. Joint Program Report No. 27. MIT, Cambridge, Massachusetts.

Rosenzweig, C., and M. L. Parry. 1994. "Potential impacts of climate change on world food supply." *Nature,* Vol. 367, pp: 133-138.

Rozema, J., H. Lambers, S. C. van de Geijn, and M. L. Cambridge, eds. 1993. *CO2 and Biosphere.* Kluwer Academic Publishers, Dordrecht, Netherlands.

Schimel, D. S., VEMAP Participants, and B. H. Braswell. 1997. "Continental scale variability in ecosystem processes: models, data and the role of disturbance." *Ecol. Mon.*, 67, pp: 251-271.

Sokolov, A. P., C. A. Schlosser, S. Dutkiewicz, S. Paltsev, D. W. Kicklighter, H. D. Jacoby, R. G. Prinn, C. E. Forest, J. Reilly, C. Wang, B. Felzer, M. C. Sarofim, J. Scott, P. H. Stone, J. M. Melillo, and J. Cohen. 2005. "The MIT Integrated Global System Model (IGSM) Version 2: Model Description and Baseline Evaluation." *MIT Joint Program on the Science and Policy of Global Change, Report 124, 2005.* Cambridge, Massachusetts.

Tjoelker, M. G., J. C. Volin, J. Oleksyn, and P. B. Reich. 1995. "Interaction of ozone pollution and light effects on photosynthesis in a forest canopy experiment." *Plant, Cell and Environment*, Vol. 18, pp: 895-905.

Tobey, J., J. Reilly, and S. Kane. 1992. "Economic implications of global climate change for world agriculture." *Journal of Agricultural and Resource Economics*, Vol. 17, pp: 195-204.

United Nations Framework Convention on Climate Change (UNFCCC), 2007. *Status of Ratification.*

Von, Kuhlmann, R., M. Lawrence, P. Crutzen, and P. Rasch. 2003. "A model for studies of tropospheric ozone and non-methane hydrocarbons: model description and ozone results." *Journal of Geophysical Research*, Vol. 108, doi: 10.1029/2002JD002893.

Vörösmarty, C. J., B. Moore, A. L. Grace, M. P. Gildea, J. M. Melillo, B. J. Peterson, E. B. Rastetter, P. A. Steudler. 1989. "Continental scale models of water balance and fluvial transport: an application to South America." *Global Biogeochemical Cycles*, Vol. 3, pp: 241-265.

Webster, M., C. Forest, J. Reilly, M. Babiker, D. Kicklighter, M. Mayer, R. Prinn, M. Sarofim, A. Sokolov, P. Stone, and C. Wang. 2003. "Uncertainty Analysis of Climate Change and Policy Response." *Climatic Change*, Vol. 61(3), pp: 295-320.

Wolfe, D. W., and J. D. Erickson. 1993. "Carbon dioxide effects on plants: uncertainties and implications for modeling crop response to climate change." *Agricultural Dimensions of Global Climate Change*. H. M. Kaiser and T. E. Drennen (eds.), pp: 153-178.

Xiao, X., J. M. Melillo, D. W. Kicklighter, Y. Pan, A. D. McGuire, and J. Helfrich. 1998. "Net primary production of terrestrial ecosystems in China and its equilibrium responses to changes in climate and atmospheric CO_2 concentration." *Act Phytoecologica Sinica*, 22 (2), pp: 97-118.

Yang, D. W., S. Kanae, T. Oki, T. Koike, and K. Musiake. 2003. "Global potential soil erosion with reference to land use and climate changes". *Hydrological Processes*, Vol. 17 (14), pp: 2913-2928.

You, L. and S. Wood. 2006. "An entropy approach to spatial disaggregation of agricultural production." Agricultural Systems, Vol. 90 (1-3), pp: 329-347.

3369-26